1-1-2017

Fast Curing Phenol Formaldehyde and Isocyanate Based Hybrid Resin for Forest Products Application

Xiaomei Liu

Fast curing phenol formaldehyde and isocyanate based hybrid resin for forest products application

By

Xiaomei Liu

A Dissertation
Submitted to the Faculty of
Mississippi State University
in Partial Fulfillment of the Requirements
for the Degree of Doctor of Philosophy
in Forest Resources
in the Department of Sustainable Bioproducts

Mississippi State, Mississippi

August 2017

Fast curing phenol formaldehyde and isocyanate based hybrid resin for forest products application

By

Xiaomei Liu

Approved:

_____

Hui Wan
(Major Professor)

_____

Janice DuBien
(Minor Professor)

_____

Rubin Shmulsky
(Committee Member)

_____

Jilei Zhang
(Committee Member)

_____

Abdolhamid Borazjani
(Committee Member)

_____

Abdolhamid Borazjani
(Graduate Coordinator)

_____

George M. Hopper
Dean
College of Forest Resources

Name: Xiaomei Liu

Date of Degree: August 11, 2017

Institution: Mississippi State University

Major Field: Forest Resources

Major Professor: Hui Wan

Title of Study: Fast curing phenol formaldehyde and isocyanate based hybrid resin for forest products application

Pages in Study: 124

Candidate for Degree of Doctor of Philosophy

The objective of this study is to develop a fast curing phenolic formaldehyde (PF) and polymeric diphenyl methane isocyanate (MDI) based hybrid resin system for wood products applications. Various formulas of PF resins were synthesized with different formaldehyde to phenol ratio, sodium hydroxide to phenol and isocyanate group (-NCO) to hydroxyl group (-OH) molar ratios. The shear bonding strength property was used to evaluate and optimize the formulations by appropriate sample preparation. The optimized resins were characterized by rheometer, Fourier transform infrared spectroscopy (FTIR) and other methods.

In order to eliminate the influence of hydroxyl groups from water in the PF resin, a frozen dried method was applied to remove the water while keeping PF resin in liquid state. Acetone was used to disperse the hybrid co-polymer to improve the mobility of the mixture of frozen dried PF resins and MDI. An unexpected phenomenon was observed when the two resins were mixed in acetone and a sharp reaction occurred. This led to an assumption that acetone promoted the curing of hybrid resin. The effect of acetone on the

curing behavior of hybrid resin was studied by differential scanning calorimetry (DSC), confocal laser scanning microscope (CLSM) and other techniques.

It was confirmed that acetone promoted the curing of the co-polymer system. The gel time of hybrid resin with acetone decreases sharply compared to that of pure phenolic resin and original hybrid resin. Acetone also helped the hybrid resin to have better penetration behavior by improving the mobility and this also resulted in less variation of the strength distribution.

Finally, lap shear samples were prepared at room temperature curing commercial polyurethane (PU), phenol-resorcinol-formaldehyde resin (PRF) and laboratory made hybrid resins based on PF and MDI to compare the shear strength of different resins under different application conditions. The strength reduction of frozen dried PF with acetone/MDI is the lowest in humidity, temperature and humidity-temperature conditions. With just humidity condition, its shear strength reduction is significantly lower than that of any other resins including the solid wood control.

DEDICATION

I would like to dedicate this research to my parents, Jiebin Liu and Youying Song. Their selfless love, support and encouragement made me get out of a rural village where almost all my childhood friends can only finish middle school; however I have had the best education in both China and the United States.

I would also like to dedicate this research to my son, Daniel Robert Magee. His smile and love support me and give me strength to go through these days from the moment he was born.

In addition, I would like to dedicate this research to my husband, Kelly Christopher Magee, my father in-law Robert Edward Magee, my mother in-law Anna Mae Magee. Without their support, it is impossible for me to finish my degree. I will never forget that my mother in-law once after taking care of my nephew and niece, drove two hours and arrived at 9:30 pm at night to take care of my son for the next day because both my husband and I had meetings in the early morning.

I love them all forever.

ACKNOWLEDGEMENTS

I would like to express the deepest appreciation to my advisor, Dr.Wan, for his endless guidance and support throughout the whole research.

I am also very grateful to Dr. Rubin Shmulsky, Dr.Hamid Borazjani, Dr.Jilei Zhang and Dr. Jan Dubien, who have served as my committee members, for their help in reviewing the proposal, detailing the experiment procedures and analyzing the data. They spared no effort to direct this research and make it go much smoother than I expected.

A big thank you to Yawei Cao, who spent lot of time on helping me to cut the samples, to George Miller, David Butler, Franklin Quin, Dr.Dan Seale, I-Wei Chu, Amanda Lawrence, Rooban Venkatesh K G Thirumalai, Ming Liu, Guangmei Cao, Zhengwei Xiong for helping me with experiments.

At last, I would like to thank Mississippi State University and the department of Sustainable Bioproducts for providing the chance to study and explore more about forest products. And also, I appreciate the help from Central South University of Forestry and Technology for their help of running some of the test.

Thank you all very much.

TABLE OF CONTENTS

LIST OF TABLES

LIST OF FIGURES

CHAPTER I

INTRODUCTION

1.1 Research summary

Forest and the forest products industry are a source of economic growth and employment, with the value of global forest products traded internationally reaching $270 billion (Patterson and Coelho 2009). As a contrast, forest resources are declining due to human activities and climate change. According to the forest products industry technology roadmap, the first research and development (R&D) priority for wood composites is energy-efficient technologies such as moisture-activated or non-heat activated adhesives or reduced materials drying time (U.S. Department of Energy 2006). This issue mostly concerns wood adhesive which is the most critical factor for wood composite manufacturing. Environment friendly, cost effective and durable wood adhesive has been a popular research topic for decades.

Phenol formaldehyde (PF) resin is the most cost efficient and desirable thermosetting adhesive for exterior application with good heat and chemical resistant properties (Pizzi and Muttka 2011). Polymeric MDI (PMDI) which has high moisture tolerance, fast cure rate, and high resin efficiency is another thermosetting resin that is widely used. Much research in the past has been conducted to combine these two resins using the hybrid concept to get a better comprehensive resin system. Most of the research focused on the fundamental investigation of the chemical reaction between these two

resins. The performance of this hybrid resin system for exterior use especially in rapid change environments has not been well researched. During the wood composite application process, the resin's performance can be significantly affected by the surrounding environment where temperature and relative humidity (RH) play an important role. A good performance of this hybrid resin concept under such conditions could generate the necessity of related research. The evaluation and comparison of its performance with other commercial resins or adhesives will provide further information for its future development.

In this study, three main factors: formaldehyde to phenol (F/P), sodium hydroxide to phenol (S/P) and isocyanate group to hydroxyl group (-NCO/-OH) molar ratios were studied in a series of experiments to determine the best formula to prepare high performance hybrid resins. The shear strength of southern pine wood blocks was used to evaluate and optimize the formulas for bonding wood. Various techniques including Fourier transform infrared spectroscopy (FTIR), thermos gravimetric analysis (TGA/DTG), rheometer, X-Ray Diffraction (XRD), three-dimensional (3D) X-ray microscope and other techniques were applied to characterize the properties of the hybrid resin and especially, to find out how the molecular weights of phenolic resin can affect the properties of the hybrid system.

To eliminate the moisture in PF resin which may distract the reaction between hydroxyl group (-OH) in PF resin and isocyanate group (-NCO) in MDI, frozen-dried technology was utilized. In order to get homogeneously mixed hybrid resin, frozen-dried phenolic resin was dispersed into acetone. While adding MDI into the solution of acetone and PF resin with designed amount, the mixture began to react immediately. This

phenomenon is strong evidence that indicates adding acetone may have promoted the reaction of PF and MDI resin. To confirm this, the effect of adding acetone on the curing behavior of hybrid resin was studied using rheometer, differential scanning calorimetry (DSC), atomic-force microscopy (AFM), confocal laser scanning microscope techniques.

Then lap shear samples were prepared using room temperature curing commercial polyurethane (PU), phenol-resorcinol-formaldehyde resin (PRF) and laboratory made hybrid resins based on PF and MDI. The shear strength of these samples were tested and compared after the treatment with different humidity and temperature conditions to compare those resins' resistance to rapid change environment.

1.2 References

Patterson, T. M., & Coelho, D. L. (2009). Ecosystem services: Foundations, opportunities, and challenges for the forest products sector. Forest Ecology and Management, 257(8), 1637-1646.

Forest Products Industry Technology Roadmap; Agenda 2020 Technology Alliance, U.S. Department of Energy, Office of Energy Efficiency and Renewable Energy, Industrial Technologies Program,: Washington DC, 2006., p 32.

Pizzi, A., & Mittal, K. L. (Eds.). (2011). Wood adhesives. CRC Press.

CHAPTER II

LITERATURE REVIEW

2.1 Phenolic formaldehyde resin

Phenol formaldehyde resin (PF) is synthetic polymer obtained by the reaction of phenol with formaldehyde. There are two types of phenolic resins, novolacs and resoles. Novolac type of PF resin, mainly comprised of excess of phenols was first patented in 1909 (Baekeland 1909). Resole type of PF resin which is comprised of more formaldehyde is the first synthetic polymer material (Gardziella et al. 2013) with primary usage as wood composite binders, which has many good properties including heat resistance, excellent mechanics and corrosion resistance (Trick et al. 1995). It is continuously being developed into more and more applications and the resin chemistry and technology have been well described and summarized by Hultzsch (Hultzsch 1950), Martin (Martin 1956) and Megson (Megson 1958). In this research, the resoles type of PF resin is the subject to study for.

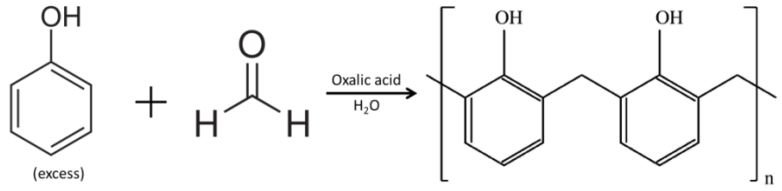

Figure 2.1 Formation of a novolac type phenolic resin

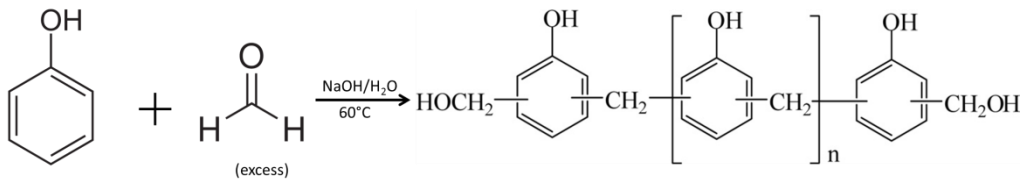

Figure 2.2 Formation of a resol type phenolic resin

The resole type of PF resin is mainly the products of the reaction between phenol and formaldehyde, which is catalyzed by alkali to provide a thermosetting polymer.

Owing to its superior physical and chemical properties, phenolic resins can be modified to suit specific applications by altering the catalysts used during the manufacturing. According to Zion Research (Zion Research 2015), the global phenolic resins market was valued at approximate USD 10.0 billion in 2014 and is expected to reach approximately USD 14.0 billion by 2020, growing at a compound annual growth rate (CAGR) of around 5.5% between 2015 and 2020. In terms of volume, the global phenolic resins market stood at approximately 4.7 million tons in 2014.

2.2 Isocyanate resin

Diisocyanates (also commonly known as isocyanates) are highly reactive and versatile chemicals with widespread commercial and consumer use (California EPA 2011). Over 90% of the diisocyanates' market is dominated by two diisocyanates: MDI and toluene diisocyanate (TDI) (Allorpt et al. 2003).

The principal raw materials for polyurethane are crude oil and natural gas. The diisocyanates having the greatest commercial importance originate from the aromatic content (benzene and toluene), while the polyols come almost exclusively from the

aliphatic content. Some renewable materials are also used as raw material sources for polyols (Boustead 2005).

The typical synthesis process of MDI from principal raw material to final product is shown in Figure 2.3 (Boustead 2005).

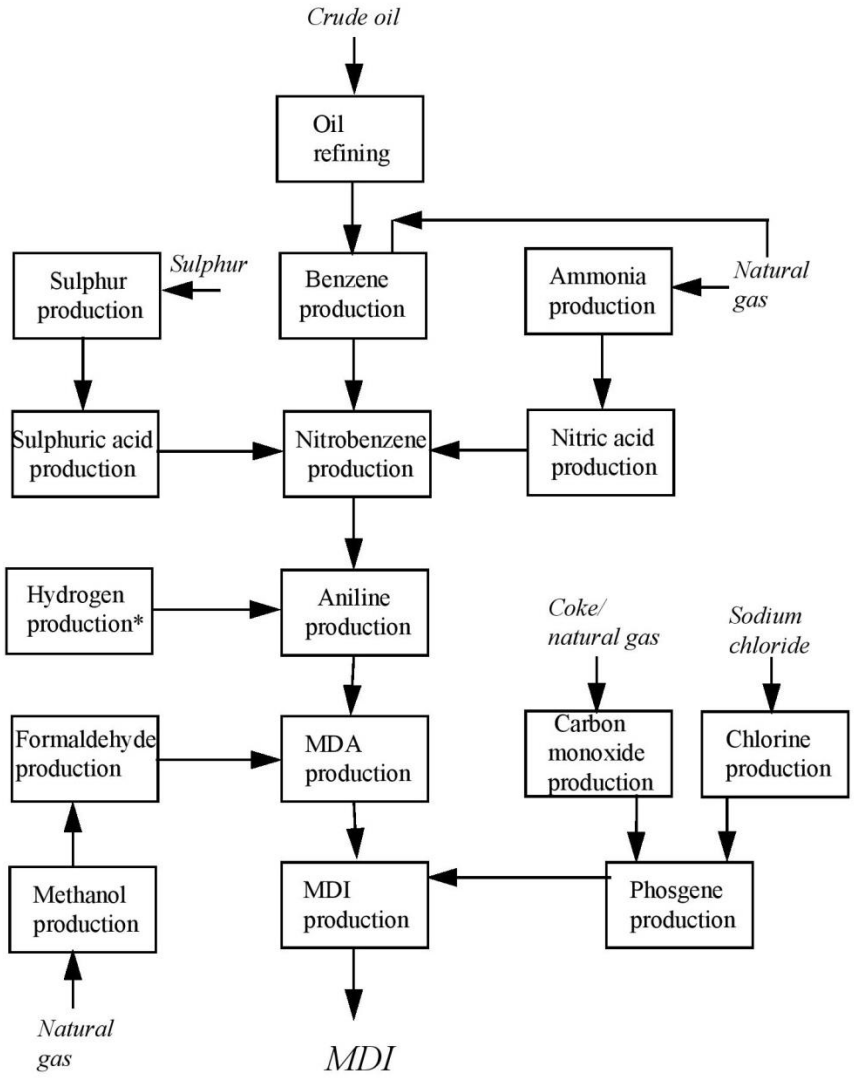

Figure 2.3 MDI manufacturing process

The commercial form of MDI is a yellow to brown toxic mixture which contains 25-80% monomeric 4,4'-MDI as well as oligomers containing 3-6 rings and other minor isomers. Monomeric 4,4'-MDI is a white to pale yellow solid at room temperature, with a molecular weight of 250. It has a boiling point of >300 °C at 101.3 kPa, a melting point of 39–43 °C, and a vapor pressure of <1 mPa at 20°C (Sekizawa 2000). Polymeric MDI (PMDI) is a technical grade MDI which contains 30-80% w/w 4,4'-methylene diphenyl isocyanate; the rest consists of MDI oligomers and MDI homologues (MAK value documentation 2000).

MDI is used to make rigid and flexible foam, foundry resin sand binders, and heat insulating material (Sekizawa 2000). The 2006 Inventory Update Reporting (IUR) database indicates that MDI chemicals are used in the following consumer/commercial categories: adhesives and sealants; paints and coatings; transportation products; rubber and plastic products; and lubricants, greases and fuel additives (California EPA 2010).

A growing literature exists on the use, and copolymerization, of MDI with a variety of other resins to yield thermosetting wood adhesives of excellent performances (Pizzi 1994). Those approaches can not only result in a lower cost than MDI while keeping its excellent performance but also decrease the toxicity of MDI. This research is more important especially in plywood industry, where MDI cannot be directly used due to its low viscosity and high mobility.

In this research, the isocyanate resin refers polymeric MDI (PMDI) which is highly reactive to hydroxyl groups (Wang et al. 2002). There has been much argument about whether or not there is bonding between the isocyanate group and wood cellulose, hemicellulose and lignin components of wood based on urethane linkages due to the fact

that there is active hydrogen existing in hydroxyl group (Langenberg et al. 2010). Many researches have been conducted to investigate the potential reaction of forming urethane linkages of isocyanate groups and hydroxyl groups from wood.

2.3 PF/MDI hybrid polymer system

Hybrid polymer usually means a system which contains two or more monomers with each providing one specific function in the system. Among different hybrid polymer systems, the organic/inorganic hybrid materials have been extensively studied recently because of combining the balanced properties of organic polymers (e.g. flexibility, ductility, di electric) and inorganic materials (e.g. high thermal stability, strength, hardness, UV absorbance and high refractive index) (Chen et al 2006). Even acquiring some special or novel properties due to their special micro structures thus can be potentially used in many fields such as electrical, optical, structural, photoelectrical, nonlinear optical materials, plastics, rubbers, fibers, coatings, inks, etc.

Contrary to pure solid state inorganic materials that often require a high temperature treatment for their processing, hybrid materials show a more polymer-like handling, either because of their large organic content or because of the formation of crosslinked inorganic networks from small molecular precursors just like in polymerization reactions (Eder, 2010; Liu, et al. 2014). Light scattering in homogeneous hybrid material can be avoided and therefore optical transparency of the resulting hybrid materials and nanocomposites can be achieved.

Usually, common hybrid material consist of two compounds in which one is inorganic and the other one is organic. But according to the properties they can obtain after synthesis, normally, hybrid materials can also combine two organic compounds

together. And in this research, the hybrid concept which has been utilized for decades from 1970's of using PF and MDI was discussed to recover more information for future use and further research.

As mentioned above, PF/MDI hybrid resin also has been attempted to be applied for wood composites manufacturing since the 1970's (Deppe 1977; Hse, C. Y. 1980 US Patent 4209433) and it has been reported successfully for plywood application (Pizzi et al.1993; Pizzi, A et al. 1995 US Patent 5407980). This hybrid resin has been described in various patents (Dunnavant et al. 1986 US Patent 4602069; Carpenter et al. 1991 US Patent 5001190) which it is typically cured and applied in an organic solvent (Rosthauser et al. 2001 US Patent 6214265). A thermochemical study of –NCO and –OH reactions were conducted in 1962 in which the heat reactions of hydroxyl groups from normal, iso-, and secondary-butyl alcohols with phenyl isocyanate using differential calorimeter (Lovering and Laidler 1962). The result shows that the effect of changing the hydroxyl groups from normal to iso- to secondary-butyl is concerned; a decrease in stability of the resulting urethane will be expected.

For many decades, researchers showed great interest in improving the toughness of phenolic resins; in those studies, different types of polymers were blended with phenolic resin to accomplish this goal. Among these polymers, isocyanate resin has the highest potential to react with PF resins and it is also another important binder in woodworking industry and has been used as a wood adhesive for more than 30 years because of its remarkable comprehensive properties (Pizzi and Walton 1992). This PF/MDI co-polymer system has shown very strong bonds, faster pressing time, and greater tolerance to higher moisture content than traditional PF resins (Shafizadeh et al.

1999). Phenolic resin contains a high amount of hydroxyl groups which can interact with other polymers. MDI, which contains many isocyanate groups (-N=C=O), can easily react with a hydroxyl group. This reaction between the two compounds was well described (Vandenabeele et al. 2001; Draye and Tondeur 1999). The reaction between MDI and PF resin is shown in Figure 2.4 (Blank et al.1999).

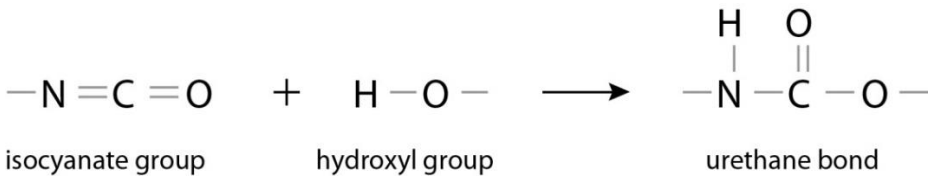

Figure 2.4 Chemical reaction of MDI with PF via forming urethane bond

2.4 Overview of resin fast curing research

2.4.1 Fast curing research of PF resins

Thermosetting resins play an important role in forest product industry today because of their high flexibility ion tailoring desired ultimate properties (Yousefi et al. 1997). In resin formulations, different types of additives including promoting agents, fillers and inorganic and organic catalysts are introduced into the cure system. There is also extensive research on fast curing modification of phenol-formaldehyde resin and hybrid resin based on PF and isocyanate resins.

The curing of PF resin requires relatively high temperature, higher pressure and longer time which results in low production efficiency, large energy and equipment cost which limit its extensive application. Developing fast, low temperature curing phenolic resin has an important significance in its practical production and application. In recent

years, researchers pay more attention to catalyst, synthesis process and curing accelerator while conducting fast curing research PF and PF based adhesives.

For the catalyst approach, strong base catalyst, alkali metal oxide catalyst and composite catalyst gain more attention.

KOH was used as catalyst to synthesize a resole phenolic resin with high hydroxymethyl content (Shang et al. 2001). The hydroxymethyl content, bromide content and intrinsic viscosity were measured and the influence of conditions to reaction was studied by calculation of the conversion of formaldehyde. The results showed that both the hydroxymethyl content and intrinsic viscosity was affected by the reaction conditions. Along with the increase of reaction temperature, the amount of formaldehyde, the amount of the catalyst and the time for reaction, the content of hydroxymethyl in the resin increased first and then decreased with the presence of maximum value. Among those conditions, the reaction temperature and the amount of catalyst had greater effect on the intrinsic viscosity of the resin.

$Ba(OH)_2$ was also studied as a catalyst for the synthesis of high ortho phenolic resin (Wang et al. 2010). Prepolymers were synthesized under the controlled conditions of 85-90 °C and molar ratio of formaldehyde to phenol and catalyst of 1.00:1.80:0.03. The curing time of barium PF resin was reduced by 30 % compared with that of ordinary PF resin. The product was characterized by FTIR which showed that the phenolic ring was linked via methylene, and the para-substituted was much higher than the ortho-substituted. This indicated the reaction mechanism of fast curing of the barium PF resin and the hot pressing time of plywood made by Ba-PF can be sharply reduced. Another approach using $Ba(OH)_2$ (Zhang et al. 2009) as a catalyst was conducted to study the

effect of the raw materials (phenol, formaldehyde and $Ba(OH)_2$) on the curing time of barium phenolic resin. According to this research, when the molar ratio of $Ba(OH)_2$ to phenol is 0.03 and formaldehyde to phenol is 1.8, the phenolic resin has shortest curing time and fastest curing speed. The curing temperature needed using this formula is lower than ordinary phenolic resin. It was explained that the high ortho character made it cure faster.

Alkali metal oxides like CaO were used as catalysts to reduce the free aldehyde content and reduce the curing time. Wu (Wu et al. 2010) confirms that the content of catalyst can significantly reduce the free aldehyde content by maximizing the methylol content and benefit the curing process. Similar research was conducted by Fu (Fu te al. 2004) which shows that when the molar ratio of phenol to formaldehyde and catalyst to phenol is 1.2 and 0.02, respectively, the reaction time can be reduced to 3 hours under 70 °C.

Composite catalyst is also widely used for promoting the curing process of resins. Zhao et al. (Zhao et al. 2000; Shi et al. 2000) used composite catalyst containing divalent metal ions and monovalent metal ions to make fast curing phenolic resin with low toxicity. By adding 5%-10% this composite catalyst, the pressing temperature and time of this resin can be close to urea-formaldehyde resin with an improved bonding strength. A composite catalyst with $Ba(OH)_2$ and NaOH also achieved the purpose of low free formaldehyde and high ortho-hydroxyl methyl content of phenolic resins (Xie et al. 2012).

For a synthesis process approach, a two-step base catalyzed synthesis was adapted to promote the methylation reaction on the phenol benzene rings (Li et al. 2003). This

method can effectively improve the degree of hydroxyl methylation of the phenolic resin to accelerate the condensation of the reaction. With the increasing the molar ratio of formaldehyde to phenol, the curing time and temperature were both reduced and the curing condition of the resin was improved. Another method was proposed to add amino resin and other additives to make a poly-condensed co-polymer adhesive (Xu 1995). After optimization, the resulting multicomponent poly-condensation is not only cured fast but also has low cost of raw materials.

For the curing accelerator approach, acid or alkali and organic esters curing accelerators were found effectively to speed up the curing process of resins. Alkaline earth metal magnesium oxide or hydrogen oxides were prepared for the condensation reaction of phenolic resin (Zhang et al. 2006). The results show that pH value has different influences on magnesium based phenolic resin and sodium hydroxide based phenolic resins. For magnesium based phenolic resin, a suitable acidity modifier can make the resin cure faster so that to reduce the polymerization time significantly. After adding a small amount of ammonium chloride, both the curing time and the free formaldehyde content were significantly reduced. When the amount of it continues increasing and is higher than 1.2%, the content of free formaldehyde continues reduced while there is very little effect on the reduction in curing time. Carbonate is another accelerator which was studied to promote the curing of phenolic resin (Park et al. 1999, 2000, 2002). By thermal analysis, it confirms that the propylene carbonate, potassium carbonate and sodium carbonate can improve the curing rate of phenolic resin in which propylene carbonate improved the most. The gel time was shortened as the amount of carbonate increased at 120 °C. The effect of other organics like methyl formate, alkene

ester, gamma-butyrolactone and triacetyl glyceride on the accelerating the curing process of phenolic resin was also studied (Corner et al. 2002, 1996). Through the introduction of these accelerators into O-hydroxymethylphenol and p-hydroxymethylphenol standard reactants at 20 °C, the result showed that the organic accelerators greatly increased the reaction rate and the reaction process and was similar with the curing process of phenolic resin.

2.4.2 Fast curing research of MDI resin

MDI resin's fast curing research is based on the catalyzing isocyanate group for polyurethane formation which is a relatively stable state and structure. Those catalysts are either nucleophilic or electrophilic. Another kind of catalysts is used to promote the structure transition by stereo chemical orientation. These catalysts include weak acid salts, tertiary amine bases and organometallic catalysts. Metals such as Sn, Zn, or Fe salts can promote the reaction rate (Haupt 2013). During the formation of urethane bond, electrophilic reactive hydroxyls will bond with the nucleophilic isocyanate nitrogen atom. The catalysts accentuate this basic electronic mechanism through a coordinate complex between the catalyst, isocyanate and reactive hydroxyl groups (Szycher 1999).

The mechanism of promoting the curing behavior is consistent with accelerating the reaction between isocyanate group and hydroxyl group which will be talked about in the next section in this literature review.

2.4.3 Fast curing research of PF/MDI co-polymers

PF and MDI resins are now economically suitable adhesive options for the mass production for exterior grade forest products (Riedlinger 2008). Given the widespread use

of the individual systems, a potentially synergistic adhesive combining both PF and MDI is not novel. As a co-polymer system, PF/MDI can benefit from both materials good properties. MDI itself was investigated as an accelerator to promote the curing process of synthetic PF resins through gel time tests (Stephanou and Pizzi, 1993). On the basis of several combinations of MDI and PF resins for particleboard application, exterior grade production was obtained with 25% MDI resin mixture. The pressing time was shorter than using methylolated bagassc lignin (MBL) resols and methylolated kraft softwood lignin (MLK) resols. It also confirms the urethane-forming, cross-linking mechanism of MDI and synthetic PF resins. Same researchers also reported using organic esters such as triacetin (glycerol triacetate), propylene carbonate, vinyl acetate and methyl formate to accelerate the curing of PF/MDI mixtures (Stephanou and Pizzi, 1993). The ester species causing the additional cross-linking mechanism appeared. The acceleration mechanisms of MDI and ester were shown not to depend on each other, and thus involved cross-linking through different reactive groups of the resin. The 46% of MDI in PF/MDI resin mixture showed much shorter pressing times for exterior grade particleboard application than those used with traditional synthetic PF resins. But the accelerating effect relying only on esters appeared to have longer pressing time than MDI and ester combinations. However, the amount of ester accelerator used is generally high, between 5-15% of total resin solids. In general, the amount of catalyst for promoting the curing process of PF/MDI co-polymer is relatively small, between 0.5-1% of total resin solids and low cost (Johns 1982). The reaction between isocyanate groups and hydroxyl groups is a case of urethane bridge formation although in water it is possible to use urethane formation

catalysts which are routinely used in non-water-based systems (Ho, C.U.S. Patent 5798409).

As mentioned in the last section, the catalysis of the isocyanate-hydroxyl reaction has been studied by many researchers (Squiller and Rosthauser 1987) which confirmed that the reaction of aliphatic isocyanates with hydroxyl groups can be catalyzed by many metal carboxylates and organo tin compounds. T-Amine catatlysis of the reaction of aromatic isocyanates with hydroxyl groups has been practiced for some time and is common for the preparation of flexible polyurethane foams (Bechara and Carroll 1980). Tin compounds, especially dibutyltin dilaurate are widely used in coating as catalysts for the isocyanate/hydroxyl reaction (Blank and Hessell 1999).

Other catalysts which have been widely reported for isocyanate and hydroxyl groups' reaction is metal catalysts although they display highest activity in this reaction. Those metal containing compounds in roughly descending catalytic activity are: Bi, Pb, Sn, triethylenediamine, strong bases, Ti, Fe, Sb, U, Cd, Co, Th, Al, Hg, Zn, Ni, trialkylamines, Ce, Mo, V, Cu, Mn, Zr, trialkyl phosphines (Britain and Gemeinhardt 1960).

Several years after Britain and Geneinhardt's research, the catalysis of the reaction of n-butyl alcohol with isocyanates, using organometallic derivatives of lead, tin, and mercury, has been investigated (Abbate and Uirich 1969). The mechanism of these chemicals of promoting the reaction of isocyanate and hydroxyl groups occurs via a template-type mechanism whereby the catalyst acts to complex both reactants in a catalyst phase allowing the reaction to occur with greater facility. By measuring the disappearance of the isocyanate absorption in the infrared, it has been confirmed that

within the same series of catalysts, RnMOAc, the catalytic effect decreases in the order RHg > R_3Sn > R_3Pb; and in all cases R = aryl > R = alkyl. The electronic effects of substituents on the aryl moiety are not pronounced.

A systematic study of acid organocatalysts for the polyaddition reaction diisocyanate in solution has been performed (Sardon et al. 2013). Among organic acids evaluated, sulfonic acids were found the most effective for urethane formations even when compared with conventional tin-based catalysts (dibutyltin dilaurate). Sulfonic acids gave polyurethanes with higher molecular weights than was observed using traditional catalyst systems. Ternary adducts in the presence of acid and engender both electrophilic isocyanate activation and nucleophilic alcohol activation through hydrogen bonding.

Isocyanate and hydroxyl groups' reaction has also been catalyzed by bifunctional catalysis (Briody and Narinesingh 1971). Bifunctional catalysis is a term used when two catalytic groups present within the same molecule act on a substrate (Katsamberis and Pappas 1990). By recording the catalytic rate constant, it was confirmed that benzoic acid and 2-pyrinone can worked as bifunctional catalysts for the urethane bond forming by promoting the proton transfer between oxygen and nitro gen atoms.

In summary, the reaction between isocyanate and hydroxyl group can be catalyzed by a varieties of chemical from inorganic to organic and from metal compounds to relative stable substances. There is a possibility that more common chemicals which are used daily in labs can serve as catalysts to promote the curing of PF/MDI hybrid resin.

2.5 Thermoset resins characterization techniques

2.5.1 Gel permeation chromatography (GPC)

Gel permeation chromatography (GPC) is one of the most powerful techniques for characterizing the polydispersity of polymeric materials that entails the chromatographic fractionation of macromolecules according to molecular size (Moore 1964). A versatile commercial apparatus (Cantow et al. 1967) has been used successfully in numerous laboratories on various problems of molecular weight distributions.

The technique was developed using cross-linked polydextran gels with different pore sizes (Flodin et al. 1962). When such gels swelled in water, they formed a three-dimensional network that acts as a molecular sieve. When an aqueous solution of macromolecules is allowed to move through a column containing the gel, a chromatographic separation takes place. Molecules of low molecular weight or molecules having a small hydrodynamic radius are able to penetrate into the gel particle pores but large molecules are excluded from the pores and pass directly through the column. As a result, the largest molecules elute first and the smallest last (Gellerstedt 1992).

In this research, gel chromatography of the PF resin was revealed for comparison the properties the resins with different molecular weights using a gel permeation chromatography instrument (OMNISEC, Malvern Company, Worcestershire, UK.)

2.5.2 Fourier transforms infrared spectroscopy (FTIR)

Fourier transform infrared spectroscopy is a technique which is used to obtain an infrared spectrum of absorption or emission of a solid, liquid or gas (Griffiths and Haseth 2007). An FTIR spectrometer simultaneously collects high spectral resolution data over

a wide spectral range. This confers a significant advantage over a dispersive spectrometer which measures intensity over a narrow range of wavelengths at a time.

Infrared spectroscopy has been widely used for characterization of organic compounds and thermosetting resin curing (Gonzalez et al. 2012; Enns and Gillham 1983). Theoretically, the principle of kinetic building consists in following the evolution of a reactive vibration band of the resin versus cure treatments, time and temperature. This evolution is related to a reference vibration band, whose intensity does not vary during the curing process. This methodology is well known as the internal reference method, and is currently used (Bartolomeo and Vernet 2001).

In this research, both qualitative and quantitative information of chemical groups especially isocyanate groups and hydroxyl groups were obtained by this techniques using Spectrum Two IR spectrometer (PerkinElmer, Waltham, MA, US) which needs a simple sample preparation process.

2.5.3 Differential scanning calorimetry (DSC)

The nomenclature committee of the International Confederation for Thermal Analysis (ICTA) has defined DSC as a technique in which the difference in energy inputs into a substance and a reference material is measured as a function of temperature whilst the substance and reference material are subjected to a controlled temperature program (Barton 1985). As the most commonly used thermal technique, DSC is widely used to study polymer's thermal transitions including glass transition, crystalline and melting transition. The power of this technique was first described by Watson et al. (Watson et al. 1964).

By measuring the heat flow of the sample as a function of temperature, DSC technique has been extensively used to study the cure kinetics of various thermosetting polymers (Montserra and Malek 1993; Montserrat 1993; Roşu et al. 2002; Reddy et al. 1990).

In this research, DSC was used to measure different curing mechanism parameters including energy of activation, reaction order and pre-exponential factor to utilize the variation in peak exotherm temperature with heating rate, thus to build a related curing process model and predict the suitable curing parameters like temperature and pressing time.

2.5.4 Thermal gravimetric analysis (TGA)

Thermogravimetric analysis (TGA) measures weight/mass change (loss or gain) and the rate of weight change as a function of temperature, time and atmosphere. Measurements are used primarily to determine the composition of materials and to predict their thermal stability. The technique can characterize materials that exhibit weight loss or gain due to sorption/desorption of volatiles, decomposition, oxidation and reduction (Prime et al. 2009).

As proved to be one of the best methods for the study of kinetics of curing behavior, TGA techniques has been extensively used at low heating rates and temperatures up to 900 °C (Saddawi et al. 2009). It is especially useful for the study of polymeric materials, including thermoplastics, thermosets, elastomers, composites, films, fibers, coatings and paints. TGA measurements provide valuable information that can be used to select materials for certain end-use applications, predict product performance and improve product quality (Seymour and Carraher 2000). It also

provides complimentary and supplementary characterization information to DSC technique.

In this research, the TGA was performed on a SDT Q600 (V20.9 Build 20) (TA instrument, New Castle, DE, US) instrument to provide the thermal stability property comparison of different resin samples.

2.5.5 X-ray diffraction (XRD)

X-ray powder diffraction (XRD) is a rapid analytical technique primarily used for phase identification of a crystalline or crystalline like material and can provide information on unit cell dimensions. The analyzed material is finely ground, homogenized, and average bulk composition is determined (Klug & Alexander 1954).

X-ray diffraction is based on constructive interference of monochromatic X-rays and a crystalline sample. These X-rays are generated by a cathode ray tube, filtered to produce monochromatic radiation, collimated to concentrate, and directed toward the sample (Whittig & Allardice 1986). The interaction of the incident rays with the sample produces constructive interference (and a diffracted ray) when conditions satisfy Bragg's Law ($n\lambda=2d \sin \theta$) (Jauncey 1924). This law relates the wavelength of electromagnetic radiation to the diffraction angle and the lattice spacing in a crystalline sample. These diffracted X-rays are then detected, processed and counted. By scanning the sample through a range of 2θ angles, all possible diffraction directions of the lattice should be attained due to the random orientation of the powdered material. Conversion of the diffraction peaks to d-spacing allows identification of the mineral because each mineral has a set of unique d-spacing. Typically, this is achieved by comparison of d-spacing with standard reference patterns (Higgins & Schlenkert 1988).

In this research, although there is no evidence of crystal formed in PF/MDI co-polymer structure, the powder diffraction file exhibited broad peaks at 2θ angles can provide some description of their cross-linking behavior.

2.5.6 Rheometer analysis

The modern rheometers allow the accurate measurement of a complex material's response to an applied force (stress) or deformation (strain) (Grillet & Wyatt 2012). At the beginning, rheometers were categorized as stress controlled (applies a force and measures the resulting deformation) or strain controlled (applies a deformation and measure the resulting fore) (Artavia & Macosko 1994).

One main application of rheometer technique is to reveal the polymer gel rheology. Polymer gels are crosslinked networks of polymers which behave as viscoelastic solids which are found in many applications of resins (Creton 2003). A wide variety of physical properties can be revealed by manipulating the gel's microstructure. The strength of a gel, which is characterized by the equilibrium modulus, is generally proportional to the density of crosslinks with stiffer gels having a higher density of crosslinks (Friedman et al. 1981).

Thermosetting resin's curing process involves transformation of low-molecular weight monomers from the liquid to the solid state as a result of the formation of a polymer network by the chemical reaction of the reactive groups of the system (Babayevsky and Gillham 1973). The liquid to solid transition of polymerization process is marked by the gel point which can divide the process into two stages (Winter et al. 1986). At the first stage, the polymer system is soluble and fusible in which the polymer chains grow and branch. However, the occurring of network of polymer chains only

appears at the second stage which is after the gel time. Then, the system begins to lose solubility and become solid. Thus, the gel time is an important parameter to be considered as it determines at which point the polymer becomes physically unprocessable (Laza et al. 2005).

In this research, the rheological measurements were performed using an AR-1500 rheometer (TA Instruments, Delaware, US) with geometry of serrated parallel plates (B40 mm) and gap of 800 mm, which was adopted based on preliminary results.

2.5.7 Confocal laser scanning microscopy (CLSM)

Confocal laser scanning microscopy (CLSM) is very useful for routine imaging of fluorescently labeled biological specimens, was introduced in the late 1980s (White and Amos 1987). The immediately clear digital images are a major advantage of the CLSM. The main application of the CLSM is to collect single optical sections from fixed and immunofluorescent specimens in single, double, triple and multiple wavelength modes (Paddock 1999). Now it is also widely used to scan the interior of relatively thick histological sections (Knobler et al. 1978). By observing multiple layers of samples, CLSM technique can provide 3-D visualization images of large thick sections which are particularly useful when attempting to view entire wood plants cells (Knebel 1991). More importantly, this formation of 3-D images using CLSM does not require complex mechanical sectioning of the specimen.

In this research, the CLSM technique was applied to capture the distribution behavior and penetration depth of different resins on wood surface for comparison purpose using a confocal laser scanning microscope (CLSM; TCS-NT, Leica, Heidelberg, Germany).

2.5.8 Atomic-force microscopy (AFM)

Since its invention, the atomic force microscope (AFM) has been used to image a wide range of samples, including wood adhesives. The images including 3D adhesion force distribution images can be obtained by the mechanical interactions between AFM tip and the sample's surface (Moy et al. 1994). It is an amazing technique that makes getting images showing the arrangement of individual atoms in a selected area in a sample comes true. It occupies totally different principles with other microscopes because it does not form an image by focusing light or electrons onto the surface of samples. An AFM physically touches the sample's surface with a sharp probe and builds up a map of the height of the sample's surface and thus it makes it possible to look at the sample from any conceivable angle with simple analysis software (Eaton & West 2010).

In this research, AFM technique was used to obtain the 3D adhesion force distribution the surface morphology and roughness information of different resins using the PeakForce QNM mode using a Dimension Icon AFM (Bruker, USA).

2.6 Objectives and significances

The objectives of this study are to:

1) Developing a hybrid polymer system based on PF and MDI for wood products manufacturing.

2) Evaluating the morphology, thermogravimetric and functional groups' information of hybrid resin by using various characterization techniques,

3) Exploring the possibility of using acetone to pursue fast curing ability of hybrid resin.

4) Comparing the performance of common commercial cold-setting resins with laboratory made optimized hybrid resins to provide some information for its future application in rapid environment change circumstances.

According to preious research, PF resin has low cost, good thermal resistance property and MDI resin has faster curing behavior, higher resin efficiency and high moisture tolerance ability. By using a hybrid concept to combine those two resins strength, it is possible to achieve a better overall performance.

Meanwhile, the isocyanate groups from MDI can react with hydroxyl groups not only from PF resin, but also from wood substrate itself which can form a closely connected structure between wood and resins. This may make this hybrid resin have better humidity or temperature change resistance.

From the preliminary experiment, it has been confirmed that acetone can promote the reaction between PF resin and isocyanate resin which has not been reported by any other researchers. This may lead to a fast curing method for the hybrid resin used for wood products manufacturing.

2.7 References

Baekeland, L. H. (1909). U.S. Patent No. 942,699. Washington, DC: U.S. Patent and Trademark Office.

Gardziella, A., Pilato, L. A., & Knop, A. (2013). Phenolic resins: chemistry, applications, standardization, safety and ecology. Springer Science & Business Media.

Trick, K. A., & Saliba, T. E. (1995). Mechanisms of the pyrolysis of phenolic resin in a carbon/phenolic composite. Carbon, 33(11), 1509-1515.

Hultzsch, K. (1950). Chemieder Phenolharze.

Martin, R. W. (1956). Chemistry of phenolic resins.

Megson, N. J. L. (1958). Phenolic resin chemistry.

Zion research. (2015). Phenolic Resins (Resols, Novolac and Others) Market for Wood-adhesives, Molding Compounds, Laminates, Insulation and Other Applications: Global Industry Perspective, Comprehensive Analysis, and Forecast, 2014 – 2020.

California EPA (2011). Office of Environmental Health Hazard Assessment (OEHHA). Air Toxics Hot Spots Program – Proposed Revised Reference Exposure Levels For Toluene Diisocyanate And Methylene Diphenyl Diisocyanate.

Allport, D. C., Gilbert, D. S., & Outterside, S. M. (Eds.). (2003). MDI and TDI: safety, health and the environment: a source book and practical guide. John Wiley & Sons.

Boustead, I. (2005). Eco-profiles of the European Plastics Industry: Diphenylmethane Diisocyanate (MDI). PlasticsEurope (March 2005).

Sekizawa, J. (2000). Diphenylmethane diisocyanate (MDI), Concise international chemical assessment document 27. WHO Library Cataloguing-in-Publication Data, Geneva.

MAK Value Documentation. (2000). 4, 4'-Methylene diphenyl isocyanate (MDI) and "Polymeric MDI" (PMDI). The MAK Collection for Occupational Health and Safety. 132-133.

Pizzi, A. (1994). Advanced wood adhesives technology. CRC Press.

Wang, H., Sun, X., & Seib, P. (2002). Mechanical properties of poly (lactic acid) and wheat starch blends with methylenediphenyl diisocyanate. Journal of applied polymer science, 84(6), 1257-1262.

Langenberg, K. V., Warden, P., Adam, C., & Milner, H. R. The durability of isocyanate-based adhesives under service in Australian conditions. The results from a 3 year exposure study and accelerated testing regime (Literature Review), PNB034-0506, Forest & Wood Products Australia, 2010.

Chen, Y., Zhou, S., Gu, G., & Wu, L. (2006). Microstructure and properties of polyester-based polyurethane/titania hybrid films prepared by sol–gel process. Polymer, 47(5), 1640-1648.

Eder, D. (2010). Carbon nanotube− inorganic hybrids. Chemical reviews, 110(3), 1348-1385.

Liu, T., Fan, W., & Zhang, C. (2014). Carbon Nanotube-Based Hybrid Materials and Their Polymer Composites. Polymer Nanotube Nanocomposites: Synthesis, Properties, and Applications, Second Edition, 239-277.

Deppe, H. J. (1977). Technical progress in using isocyanate as an adhesive in particleboard manufacture. In Proceedings Washington State University Symposium on Particleboard.

Hse, C. Y. (1980). U.S. Patent No. 4,209,433. Washington, DC: U.S. Patent and Trademark Office.

Pizzi, A., Valenzuela, J., & Westermeyer, C. (1993). Non-emulsifiable, water-based, mixed diisocyanate adhesive systems for exterior plywood. Part II. Theory application and industrial results. Holzforschung-International Journal of the Biology, Chemistry, Physics and Technology of Wood, 47(1), 68-71.

Pizzi, A., Von Leyser, E., & Westermeyer, C. (1995). U.S. Patent No. 5,407,980. Washington, DC: U.S. Patent and Trademark Office.

Dunnavant, W. R., Gardikes, J. J., & Langer, H. J. (1986). U.S. Patent No. 4,602,069. Washington, DC: U.S. Patent and Trademark Office.

Carpenter, W. G., & Henry, C. M. (1991). U.S. Patent No. 5,001,190. Washington, DC: U.S. Patent and Trademark Office.

Rosthauser, J. W., & Detlefsen, W. D. (2001). U.S. Patent No. 6,214,265. Washington, DC: U.S. Patent and Trademark Office.

Lovering, E. G., & Laidler, K. J. (1962). Thermochemical studies of some alcohol–isocyanate reactions. Canadian Journal of Chemistry, 40(1), 26-30.

Pizzi, A., & Walton, T. (1992). Non-emulsifiable, water-based, mixed diisocyanate adhesive systems for exterior plywood-part I. Novel reaction mechanisms and their chemical evidence.

Shafizadeh, J. E., Guionnet, S., Tillman, M. S., & Seferis, J. C. (1999). Synthesis and characterization of phenolic resole resins for composite applications. Journal of applied polymer science, 73(4), 505-514.

Vandenabeele-Trambouze, O., Mion, L., Garrelly, L., & Commeyras, A. (2001). Reactivity of organic isocyanates with nucleophilic compounds: amines; alcohols; thiols; oximes; and phenols in dilute organic solutions. Advances in Environmental Research, 6(1), 45-55.

Draye, A. C., & Tondeur, J. J. (1999). Kinetic study of organotin-catalyzed alcohol–isocyanate reactions: Part 1: Inhibition by carboxylic acids in toluene. Journal of Molecular Catalysis A: Chemical, 138(2), 135-144.

Blank, W. J., He, Z. A., & Hessell, E. T. (1999). Catalysis of the isocyanate-hydroxyl reaction by non-tin catalysts. Progress in Organic Coatings, 35(1), 19-29.

Yousefi, A., Lafleur, P. G., & Gauvin, R. (1997). Kinetic studies of thermoset cure reactions: a review. Polymer Composites, 18(2), 157-168.

Shang, Y.H., Tan, X.M., Li, Y. (2001). Synthesis of resole phenol-formaldehyde resin containing large number of hydromethyl groups. Adhesion, 22.5, 7-10.

Wang, J., Zhang, Y.F. (2010). Fast-curing phenol formaldehyde resin used for plywood. Journal of Northeast Forestry University, 38(12), 75-76.

Zhang, Y.F., He, L.J., Han, R.L. (2009). Study of fast-curing phenol formaldehyde resin sued for wooden formwork. Journal of Building Materials, 12(6), 752-756.

Wu, J.E., Liu, Z.L. (2010). Synthesis of high methylene content and low free formaldehyde phenolic resin. Journal of Materials Research and Application, 4(4), 473-479.

Fu, C.L., L, L. (2004). Synthesis of phenol formaldehyde resin with high hydroxyl methylene content and low free formaldehyde. Journal of Thermosetting Resin, 19(5), 17-19.

Zhao, L.W., Wang, C.P., Liu, Y. (2000). Preparation and application of fast-curing phenol formaldehyde resin. China Forest Products Industry, 27(4), 17-21.

Shi, J.Y., Yao, D.D., Le, L., Gao, Y., Liu, G.Y. (2000). Study on low toxic fast-curing phenolic resin for plywood application. Journal of Beihua University, 1(3), 259-263.

Xie, J.J., Zeng, N., Li, N., Xiao, M., Rao, X.B., Wu, Y.Q. (2012). Preparation of phenol-formaldehyde adhesive for high-ortho methylol group content and its properties. Natural Science Journal of Xiangtan University. 34(2), 66-69.

Li, G., Zhang, S.M., Hao, L.G. (2003). Synthesis of water-soluble phenolic resin by two-step alkaline catalytic method. Journal of China adhesion, 19(1), 18-21.

Xu, S.H. (1995). Study of fast-curing phenolic adhesive. China Forest Products Industry, 22(6), 16-19.

Zhang, Y.Y., Zhang, Y.F., He, L.J. (2006). Influence of pH value on curing rate of phenol formaldehyde resol resins. Journal of North-east Forestry University, 34(6), 80-81.

Natural Science Journal of Xiangtan University. 34(2), 66-69.

Park, B. D., Riedl, B., Hsu, E. W., & Shields, J. (1999). Differential scanning calorimetry of phenol–formaldehyde resins cure-accelerated by carbonates. Polymer, 40(7), 1689-1699.

Park, B. D., Riedl, B., & So, W. T. (2002). Effect of synthesis parameters on thermal behavior of phenol–formaldehyde resol resin. Journal of applied polymer science, 83(7), 1415-1424.

Park, B. D., & Riedl, B. (2000). 13C-NMR study on cure-accelerated phenol-formaldehyde resins with carbonates. Journal of applied polymer science, 77(6), 1284-1293.

Conner, A. H., Lorenz, L. F., & Hirth, K. C. (2002). Accelerated cure of phenol–formaldehyde resins: studies with model compounds. Journal of applied polymer science, 86(13), 3256-3263.

Conner, A. H., River, B. H., & Lorenz, L. F. (1986). Carbohydrate Modfied Phenol-Formaldehyde Resins. Journal of wood chemistry and technology, 6(4), 591-613.

Haupt, R. A. (2013). Structural Determination of Copolymers from the Cross-catalyzed Reactions of Phenol-formaldehyde and Polymeric Methylenediphenyl Diisocyanate.

Szycher, M. (1999). Basic concepts in polyurethane chemistry and technology. Szycher's handbook of polyurethanes.

Riedlinger, D. A. (2008). Characterization of PF Resol/Isocyanate Hybrid Adhesives (Doctoral dissertation, Virginia Polytechnic Institute and State University).

Stephanou, A., & Pizzi, A. (1993). Rapid curing lignin-based exterior wood adhesives. Part I. diisocyanates reaction mechanisms and application to panel products. Holzforschung-International Journal of the Biology, Chemistry, Physics and Technology of Wood, 47(5), 439-445.

Stephanou, A., & Pizzi, A. (1993). Rapid-curing lignin-based exterior wood adhesives. Part II: Esters acceleration mechanism and application to panel products. Holzforschung-International Journal of the Biology, Chemistry, Physics and Technology of Wood, 47(6), 501-506.

Johns, W. E. (1982). Isocyanates as wood binders—a review. The Journal of Adhesion, 15(1), 59-67.

Ho, C. T. (1998). U.S. Patent No. 5,798,409. Washington, DC: U.S. Patent and Trademark Office.

Squiller, E. P., & Rosthauser, J. W. (1987, February). Catalysis in aliphatic isocyanate-alcohol reactions. In Water-Borne and Higher Solids Coatings Symposium, New Orleans Feb (Vol. 460).

Bechara, I. S., & Carroll, F. P. (1980). Unusual Catalysts For Flexible Urethane Foams. Journal of Cellular Plastics, 16(2), 89-101.

Britain, J. W., & Gemeinhardt, P. G. (1960). Catalysis of the isocyanate-hydroxyl reaction. Journal of Applied Polymer Science, 4(11), 207-211.

Abbate, F. W., & Ulrich, H. (1969). Urethanes. I. Organometallic catalysis of the reaction of alcohols with isocyanates. Journal of applied polymer science, 13(9), 1929-1936.

Sardon, H., Engler, A. C., Chan, J. M., García, J. M., Coady, D. J., Pascual, A., ... & Hedrick, J. L. (2013). Organic acid-catalyzed polyurethane formation via a dual-activated mechanism: unexpected preference of N-activation over O-activation of isocyanates. Journal of the American Chemical Society, 135(43), 16235-16241.

Briody, J. M., & Narinesingh, D. (1971). Bifunctional catalysis by amides and ureas in the reaction of amines with phenylisocyanate. Tetrahedron letters, 12(44), 4143-4146.

Katsamberis, D., & Pappas, S. P. (1990). Catalysis of isocyanate—alcohol and blocked-isocyanate—alcohol reactions by amidines. Journal of Applied Polymer Science, 41(9-10), 2059-2065.

Moore, J. C. (1964). Gel permeation chromatography. I. A new method for molecular weight distribution of high polymers. Journal of Polymer Science Part A: General Papers, 2(2), 835-843.

Cantow, M. J., Porter, R. S., & Johnson, J. F. (1967). Effect of temperature and polymer type on gel permeation chromatography. Journal of Polymer Science Part A-1: Polymer Chemistry, 5(5), 987-991.

Flodin, P., & Killander, J. (1962). Fractionation of human-serum proteins by gel filtration. Biochimica et biophysica acta, 63(3), 403-410.

Gellerstedt, G. (1992). Gel permeation chromatography. In Methods in lignin chemistry (pp. 487-497). Springer Berlin Heidelberg.

Griffiths, P. R., & De Haseth, J. A. (2007). Fourier transform infrared spectrometry (Vol. 171). John Wiley & Sons.

González, M. G., Baselga, J., & Cabanelas, J. C. (2012). Applications of FTIR on epoxy resins-identification, monitoring the curing process, phase separation and water uptake (pp. 275-298). INTECH Open Access Publisher.

Enns, J. B., & Gillham, J. K. (1983). Time–temperature–transformation (TTT) cure diagram: Modeling the cure behavior of thermosets. Journal of Applied Polymer Science, 28(8), 2567-2591.

Bartolomeo, P., Chailan, J. F., & Vernet, J. L. (2001). Curing of cyanate ester resin: a novel approach based on FTIR spectroscopy and comparison with other techniques. European Polymer Journal, 37(4), 659-670.

Barton, J. M. (1985). The application of differential scanning calorimetry (DSC) to the study of epoxy resin curing reactions. In Epoxy resins and composites I (pp. 111-154). Springer Berlin Heidelberg.

Watson, E., O'neill, M. J., Justin, J., & Brenner, N. (1964). A Differential Scanning Calorimeter for Quantitative Differential Thermal Analysis. Analytical Chemistry, 36(7), 1233-1238.

Montserrat, S., & Málek, J. (1993). A kinetic analysis of the curing reaction of an epoxy resin. Thermochimica acta, 228, 47-60.

Montserrat, S. (1993). Calorimetric measurement of the maximum glass transition temperature in a thermosetting resin. Journal of Thermal Analysis and Calorimetry, 40(2), 553-563.

Roşu, D., Caşcaval, C. N., Mustată, F., & Ciobanu, C. (2002). Cure kinetics of epoxy resins studied by non-isothermal DSC data. Thermochimica Acta, 383(1), 119-127.

Reddy, P. V., Thiagarajan, R., Ratra, M. C., & Gowda, N. M. (1990). Transition metal chelates as accelerators for epoxy resin systems—studies with cobalt (III) acetylacetonate. Journal of Applied Polymer Science, 41(1-2), 319-328.

Prime, R. B., Bair, H. E., Vyazovkin, S., Gallagher, P. K., & Riga, A. (2009). Thermogravimetric analysis (TGA). Thermal analysis of polymers: Fundamentals and applications, 241-317.

Saddawi, A., Jones, J. M., Williams, A., & Wojtowicz, M. A. (2009). Kinetics of the thermal decomposition of biomass. Energy & Fuels, 24(2), 1274-1282.

Seymour, R. B., & Carraher, C. E. (2000). Polymer chemistry (Vol. 181). Marcel Dekker.

Klug, H. P., & Alexander, L. E. (1954). X-ray diffraction procedures.

Whittig, L. D., & Allardice, W. R. (1986). X-ray diffraction techniques. Methods of Soil Analysis: Part 1—Physical and Mineralogical Methods, (methodsofsoilan1), 331-362.

Jauncey, G. E. M. (1924). The scattering of x-rays and Bragg's law. Proceedings of the National Academy of Sciences, 10(2), 57-60.

Higgins, J. B., & Schlenkert, J. L. (1988). A new family of mesoporous molecular sieves prepared with liquid crystal templates. Nature, 331, 698-699.

Grillet, A. M., Gloe, L. M., & Wyatt, N. B. (2012). Polymer gel rheology and adhesion. INTECH Open Access Publisher.

Artavia, L. D., & Macosko, C. W. (1994). Polyurethane flexible foam formation. In Low density cellular plastics (pp. 22-55). Springer Netherlands.

Creton, C. (2003). Pressure-sensitive adhesives: an introductory course. MRS bulletin, 28(06), 434-439.

Friedman-Kien, A. E., Laubenstein, L., Marmor, M., Hymes, K., Green, J., Ragaz, A., ... & Weintraub, M. (1981). Kaposis sarcoma and Pneumocystis pneumonia among homosexual men--New York City and California. MMWR. Morbidity and mortality weekly report, 30(25), 305-8.

Babayevsky, P. G., & Gillham, J. K. (1973). Epoxy thermosetting systems: dynamic mechanical analysis of the reactions of aromatic diamines with the diglycidyl ether of bisphenol A. Journal of Applied Polymer Science, 17(7), 2067-2088.

Winter, H. H., & Chambon, F. (1986). Analysis of linear viscoelasticity of a crosslinking polymer at the gel point. Journal of rheology, 30(2), 367-382.

Laza, J. M., Vilas, J. L., Mijangos, F., Rodriguez, M., & Leon, L. M. (2005). Analysis of the crosslinking process of epoxy–phenolic mixtures by thermal scanning rheometry. Journal of applied polymer science, 98(2), 818-824.

White, J. G., & Amos, W. B. (1987). Confocal microscopy comes of age.

Paddock, S. W. (1999). Confocal laser scanning microscopy. Biotechniques, 27, 992-1007.

Knobler, R. L., Stempak, J. G., & Laurencin, M. (1978). Preparation and analysis of serial sections in electron microscopy. Principles and techniques of electron microscopy. Biological applications, 8, 113-155.

Knebel, W., & Schnepf, E. (1991). Confocal laser scanning microscopy of fluorescently stained wood cells: a new method for three-dimensional imaging of xylem elements. Trees, 5(1), 1-4.

Moy, V. T., Florin, E. L., & Gaub, H. E. (1994). Adhesive forces between ligand and receptor measured by AFM. Colloids and Surfaces A: Physicochemical and Engineering Aspects, 93, 343-348.

Eaton, P., & West, P. (2010). Atomic force microscopy. Oxford University Press.

CHAPTER III

SYNTHESIS AND CHARACTERIZATION OF PHENOLIC FORMALDEHYDE AND ISOCYANATE RESIN BASED HYBRID POLYMER

3.1 Introduction

As the first commercial synthetic polymeric material, phenolic resin is widely divided into novolac and resol with different formaldehyde / phenol (F/P) molar ratio (Lee et al. 2003). PF resol resins are made by the reacting of phenol and formaldehyde in the presence of base catalyst with the F/P ratios range of 1.8-2.5 for wood adhesives application (Aierbe et al. 2000). This high F/P molar ratio makes the polymerization reaction be well controlled by monitoring the alkaline pH. Another important factor that can affect this reaction is the base catalyst which is usually sodium hydroxide. The sodium hydroxide / Phenol ratio (S/P) is between 0.2 and 0.6 depending on adhesive applications and it decides the extent of advancements of PF resins (Gardziella et al. 2013). Meanwhile, it has the viscosity-reducing effect as it increases ionization of phenolic hydroxyl groups of PF resins (Lee et al. 2007). For a determined time and temperature controlling, the F/P and S/P molar ratios can determine the property of PF resins.

Phenolic resin (PF) which contains numerous hydroxyl groups (-OH) can interact with isocyanate resin (MDI), which contains many isocyanate groups (-N=C=O) as indicated before. For this hybrid polymer system, the molar ratio of -NCO/-OH can

determine the extent of the reaction so that it affects the performance of phenolic isocyanate hybrid polymer system.

In this chapter, F/P, S/P and NCO/OH molar ratio were chosen as main factors to determine the best formula to prepare high performance hybrid resins. Meanwhile, the morphology and structure of the co-polymer system composed of isocyanate and phenolic resin with different molecular weights has also been investigated. Although this type of co-polymer system has shown very strong bonds, faster pressing time, and greater tolerance to higher moisture content of bonded wood than the traditional PF resins (Shafizadeh et al. 1999), very few reports have discussed the characterization of their reaction mechanism. As intermolecular interactions play a key role in the polymer compatibility (Lenghaus et al. 2000), different molecular weights of phenolic resins should display different properties when they react with the isocyanate group of isocyanate resin (Poljanšek et al. 2014). The objective of this chapter was to explore the characterization of the reaction mechanism of PF/MDI resin co-polymer system, and to study the impact of phenolic resin molecular weights on the properties of the system. It was expected that this study will provide the basis for improving adhesive properties for wood composite products.

3.2 Materials and methods

3.2.1 Materials

Phenol, a 99% aqueous solution (USP), was obtained from Fisher Scientific Co., Ltd (Hampton, NH). Paraformaldehyde, a 96% extra pure powder was purchased from Fisher Scientific Co., Ltd (Hampton, NH). Isocyanate, a polymeric MDI with 33% -NCO functional group, was obtained from BASF Polyurethanes (Wyandotte, MI). It was a dark

yellow liquid with a viscosity of 226 mPa·s at 25°C. Sodium hydroxide, 97% pure pellets, was purchased from Fisher Scientific Co., Ltd.

Southern pine veneer with dimensions of 305 mm (length) × 305 mm (width) × 3 mm (thickness) was used in this study. The southern pine lumber was bought from East Mississippi Lumber Company (Starkville, MS).

In this study two layers of southern pine veneer (12% moisture content) were pressed by a laboratory hot press (Hydraulic Press Co., Clifton, NJ) in both vertical and parallel to the grain. The designed amount of PF and MDI resins were mixed using laboratory blender (Stir-Pak General Laboratory Mixer, Cole-Parmer, Vernon Hills, IL) with 500 rpm. The adhesive were applied evenly on both sides of the veneer glue line with a resin loading of 330 g/m^2. The press time, pressure and temperature were 4 min, 1.38 MPa and 180°C, respectively. After pressing the plywood panels were conditioned at 20 °C and 60% relative humidity environment for one week before testing.

3.2.2 Methods

3.2.2.1 Synthesis of PF resin

The hybrid resin was prepared under laboratory conditions using MDI and PF resins made above with different molar ratios of –NCO/-OH group which is shown in Table 3.1. To prepare the hybrid resin, PF resins were first placed in a 200 ml beaker and then MDI was put inside with calculated amount. After being stirred evenly using laboratory blender (Stir-Pak General Laboratory Mixer, Cole-Parmer, Vernon Hills, IL) with 500 rpm, the mixture hybrid resin was set for 15 mins before applying on the surface of wood samples.

Table 3.1 Factors and levels for determination –NCO/-OH molar ratio

Factors	Levels		
	-1	0	-1
-NCO/-OH	1	1.25	1.5

3.2.2.2 Statistical design and calculation

A Box-Wilson Central Composite Design (CCD), commonly called a central composite design, contains an imbedded factorial or fractional factorial design with center points that is augmented with a group of 'star points' allowing estimation of curvature.

Table 3.2 Factors and levels determination for CCD

Factors	Levels				
	-1.4	-1	0	1	1.4
F/P	1.72	1.8	2.0	2.2	2.28
S/P	0.12	0.2	0.4	0.6	0.68

Note: according to CCD, 1.414=21/2, which 2 is the number of factors so that +1.4 and -1.4 level was determined.

Means and standard deviations of the tested data obtained were calculated using one-way analysis of variance (ANOVA). Duncan’s multiple range tests and multilinear regression tests with SAS® 9.4 software (Cary, NC) were used to determine the differences among different formulas. The results were evaluated using a 95% confidence interval, which reflects a significance level of 0.05 ($P<0.05$). Six replicates for each formula were tested.

Table 3.3 Central composite design experiment run

Formula code	coded level A	coded level B
1	-1	-1
2	-1	1
3	0	-1.41
4	0	1.41
5	1	-1
6	1	1
7	-1.41	0
8	0	0
9	1.41	0
10	0	0
11	0	0
12	0	0

Note: according to CCD, $1.414=2^{1/2}$, which 2 is the number of factors so that +1.4 and -1.4 level was determined.

3.2.2.3 Hydroxyl group value

The hydroxyl group value was determined by the standard esterification method using phthalic anhydride (ASTM E222-10 2010). Polyol (1g) and the pthalation reagent (25mL) were heated at 100 °C for 15 min, cooled to room temperature, pyridine (50 mL) was added, followed by water (10 mL), and then titrated with 0.5 M NaOH to its equivalence point. The phthlation reagent was a solution of phthalic anhyrdride (41.43 g) and imidazole (6.43 g) in pyridine (250 mL). Where S and B1 are the milliliters at the equivalence point of the sample and blank (no polyol), respectively; N is normality of NaOH; and W is the weight of the sample; OHV is the hydroxyl value in milligrams KOH per gram of sample (D'Souza et al. 2014).

$$OHV_{PA} = (B_1 - S)(56.1)(N)/W \quad (3.1)$$

When this experiment was processed, it was hard to see the end of the titration because the color change of the equivalence point can be covered by the natural color of PF resin. Instead of using phenolphthalein as indicator, a pHs-3E digital pH meter (Yoke Instrument, Shanghai, China) was used to indicate the end of the titration when the Ph reaches 7.0.

3.2.2.4 Shear bonding strength testing

The samples were cut to 110×25×7 mm^3 and were conditioned to 8% moisture content (ϕ = 65 ± 3% and t = 20 ± 2 °C). The shear bond strength (SBS) was represented by tensile-shear strength using a lap joint test according to EN 205 (EN 205 2003) which was determined with an Instron 5960 dual column testing system (Instron, USA). The constant loading speed was set to 5+0.5 mm/min such that the time was between 30 s to 50 s before the sample reached failure. Maximum loading force was directly recorded by the testing system.

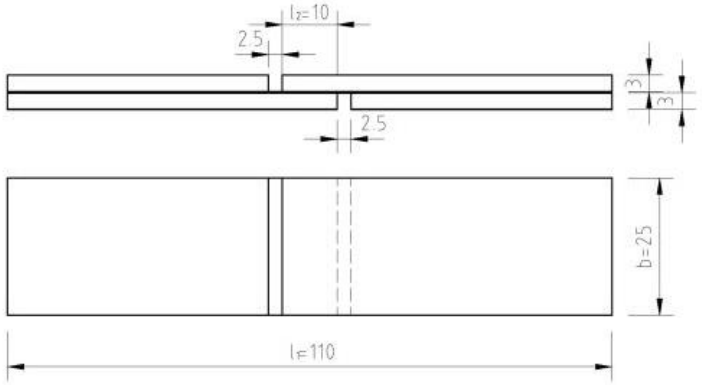

Figure 3.1 Dimensions of shear bonding strength testing samples

Note: l_1-sample length (mm), l_2- shear area length (mm), b-shear area width (mm), h-share area thickness (mm).

The tensile-shear strength was calculated according to EN 205 (2003) and the following equation:

$$\tau = \frac{F_{max}}{l_2 b} \quad (3.2)$$

Where τ is the tensile-shear strength parallel to the fibers (MPa), F_{max} is the maximum loading force recorded at the breaking point (N), l_2 is the length of the shear area (mm), and b is the width of the shear area/sample (mm).

For the wet bonding strength, samples were soaked in water at 20 ± 1°C for 24h before the test and were tested within 30 mins upon removal from the water (ASTM D1037).

3.2.2.5 Viscosity analysis

Adhesive viscosity was measured on an AR1500 rheometer with steady-state flow (1–500 s^{-1}) and a stainless steel, cone-and-plate geometry (40 mm, 2°, 50 μm gap, 25°C). Three replicates were collected per adhesive type, and used to prepare average flow curves (Paris et al. 2014). The resin began to gel, and became unworkable within 5-10 min, and thus three separate batches were prepared for viscosity determination (Paris et al. 2014).

3.2.2.6 FTIR analysis

The FTIR spectra of samples were measured with a Spectrum Two IR spectrometer (PerkinElmer, Waltham, MA, US) in the wavenumber range of 500 to 4000 cm-1 and 10 scans. The samples were prepared after oven drying the samples at 50°C for 24 h and were then ground to a powder.

3.2.2.7 TGA analysis

The TG/DTG experiment was performed on a SDT Q600 (V20.9 Build 20) (TA instrument, New Castle, DE, US) instrument. The sample was put into an aluminum crucible and was heated with nitrogen at the rate of 10 °C/min, from room temperature to 1,000 °C.

3.2.2.8 X-Ray diffraction (XRD)

The X-ray diffraction analysis was performed on Ultima III Lab X-ray diffraction (Rigaku, Woodlands, TX, US) system. The wide-angle X-ray diffraction was used to study the d-spacing of the samples. The X-ray diffraction patterns were recorded using CuKα radiation (λ=0.15418 nm). The X-ray scanning was operated under 40 kV and 44 mA, and the data collection was recorded in the range of 2θ=5 to 90° with the speed of 1°/min. The pulverized samples were loaded on a zero background slide. Results were compared to the international center for diffraction data - powder diffraction file (ICDD PDF) database.

3.2.2.9 3D X-ray microscope analysis

The samples' particle size and distribution was produced using Zeiss Xradia Versa 520 X-ray system (Pleasanton, CA. USA) with 3D dataset. The accelerating voltage and tube current were chosen based on the X-ray absorption coefficients of the samples. The transmission images from all scans were reconstructed using a commercial software package. The details of the testing parameters are shown in Table 3.4.

Table 3.4 X-ray microscope scanning parameters

Voxel size (μm)	FOV (mm)	Energy (kV/w)	Total scan time (hrs)
2	2*2	40/3	2
0.4	0.4*0.4	40/3	13

3.3 Results and Discussion

3.3.1 Optimization of synthesis parameters

3.3.1.1 F/P ratio and S/P ratio optimization

Table 3.5 ANOVA for the difference among formulas with grain in a parallel direction

Source	d.f.	Sum of squares	Mean squares	F	P
Formula	8	36.7953	4.5994	15.12	<0.0001
Error	45	13.6849	0.3041		
Total	53	50.4802			

Table 3.6 ANOVA for shear strength comparison among formulas with grain in a perpendicular direction

Source	d.f.	Sum of squares	Mean squares	F	P
Formula	8	17.1757	2.1470	8.76	<0.0001
Error	45	11.0295	0.2451		
Total	53	28.2052			

Table 3.7 Mean comparison of shear strength (MPa) for different formulas with grain in parallel and perpendicular directions

Formula	Direction to the grain	
	Parallel	Perpendicular
1	2.17 C	1.57 BC
2	1.62 DCE	1.23 DCE
3	1.96 C	1.46 DC
4	1.24 DE	0.97 DE
5	3.18 AB	2.40 A
6	0.99 E	0.73 E
7	1.68 DC	1.29 DCE
8	3.52 A	2.34 A
9	2.84 B	2.13 AB

According to this result, among 9 different formulas, formula 8 (F/P=2.0, S/P=0.4) and formula 5 (F/P=2.2, S/P=0.2) are significantly stronger than other formulas. However, formula 9 (F/P=2.28, S/P=0.4) has no significant difference with formula 5. This shows that suitable formaldehyde to phenol ratio and sodium amount are very necessary to prepare PF resin with higher bonding strength.

So for the next step, all formulas in including 5(F/P=2.2, S/P=0.2), 8(F/P=2.0, S/P=0.4), and 9(F/P=2.28, S/P=0.4) were chosen to determine the best –NCO to –OH ratio.

Table 3.8 RSREG procedure for shear strength comparison of hybrid resins with different F/P and S/P molar ratios

Residual	DF	Sum of Squares	Mean Square	F Value	Pr > F
Lack of Fit	3	3.438189	1.146063	3.77	0.0170
Pure Error	45	13.684895	0.304109		
Total Error	48	17.123084	0.356731		
Linear	2	13.681398	0.2710	19.18	<.0001
Quadratic	2	15.601042	0.3091	21.87	<.0001
Cross product	1	4.074680	0.0807	11.42	0.0014
Total Model	5	33.357120	0.6608	18.70	<.0001

Table 3.9 Interaction analysis for shear strength comparison of hybrid resins with different F/P and S/P molar ratios

Parameter	DF	Estimate	Standard Error	t Value	Pr > |t|	Parameter Estimate from Coded Data
Intercept	1	3.518482	0.243735	14.44	<.0001	3.518482
FP	1	0.251915	0.086643	2.91	0.0055	0.352681
SP	1	-0.473758	0.086643	-5.47	<.0001	-0.663262
FP*FP	1	-0.618243	0.144619	-4.27	<.0001	-1.211756
SP*FP	1	-0.412042	0.121917	-3.38	0.0014	-0.807602
SP*SP	1	-0.956168	0.144619	-6.61	<.0001	-1.874090

From the analysis of variance, it shows that the lack of fit for the model is highly significant. The factors of F/P and S/P ratio are both significant. The canonical analysis indicates that the stationary point of the predicted response surface is a maximum and indicates the unique optimum of this experiment locates at the coded F/P=0.220 and S/P=-0.224. According to the experimental design, the actual F/P ratio was 2.04 and the actual S/P ratio was 0.44 which are very close to the result of the T test for determining the best formula. According to the T test, the best formula is No.8 with F to P ratio of 2.0 and S to P ratio of 0.4.

These indicate that moderate F/P ratio and S/P ratio are suitable for PF resin cooking. And the best formula for PF resin cooking is F/P ratio of 2.04 and S/P ratio of 0.44. This procedure also gives the prediction of stationary values which is 3.63 MPa which is higher than current highest shear bonding strength of 3.52 MPa when the best F/P and S/P ratio are used. Alternatively, a contour plot of the predicted response surface confirms this conclusion.

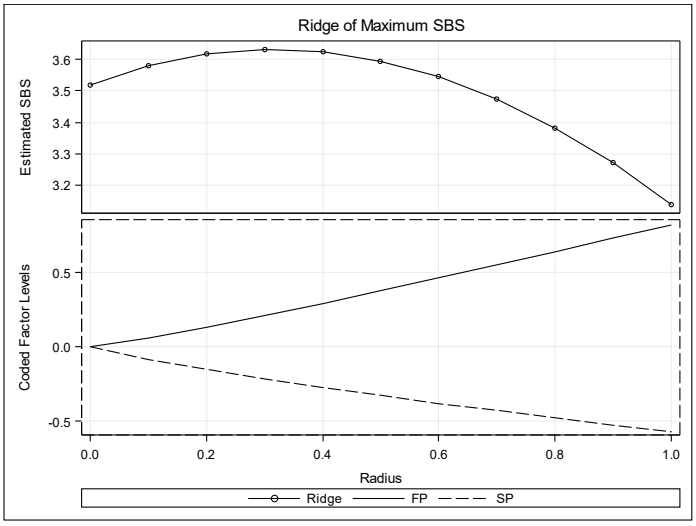

Figure 3.2 Ridge of the maximum shear bonding strength (SBS) with different F/P and S/P ratios

Table 3.10 Prediction of stationary values of F/P and S/P ratios

Factor	Critical Value	
	Coded	Uncoded
FP	0.220311	0.308436
SP	-0.224425	-0.314195
Predicted value at stationary point: 3.631758		

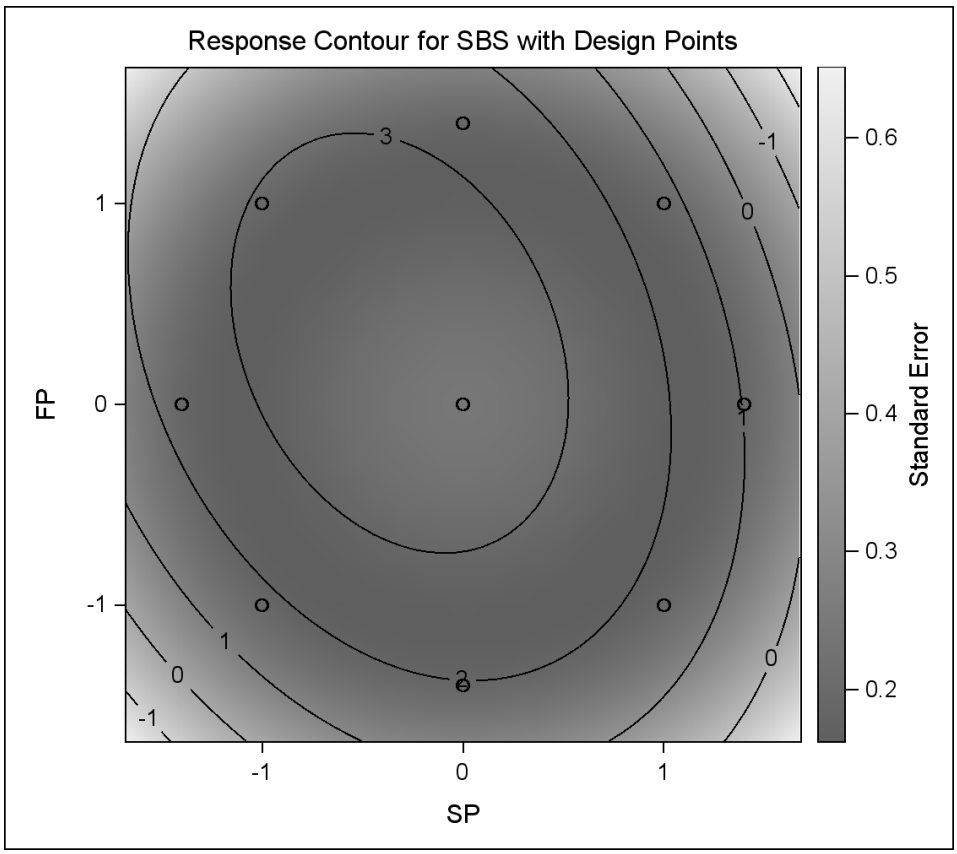

Figure 3.3 Contour plot of the predicted response surface of maximum shear bonding strength with different F/P and S/P molar ratios

3.3.1.2 –NCO/-OH molar ratio

There are two sources of hydroxyl groups in phenolic resin. The main part is direct from the functional group in resin itself and the remained is from water or moisture in phenolic resin. Both existences are important for the reaction between the hydroxyl group and the isocyanate group which was well described by former researches (Pizzi et al. 1992; Zhuang et al. 1993; Riedlinger 2008). The ratio of the group of hydroxyl and isocyanate significantly affected the reaction which resulted in the urethane linkages (Zheng 2002).

Table 3.11 Hydroxyl group value of PF resins with different formulas

Samples	1	2	3	4	5	6	7	8	9
-OH (mg KOH/g)	242	215	251	249	278	293	266	253	282

Table 3.12 ANOVA for shear strength comparison among formulas with different –OH/-NCO ratios

Source	DF	Sum of Squares	Mean Square	F Value	Pr > F
Model	8	43.77007167	5.47125896	18.52	<.0001
Error	45	13.29729433	0.29549543		
Corrected Total	53	57.06736600			

Table 3.13 Mean comparisons of shear bonding strength (MPa) of formulas with different –NCO/-OH ratios

Formula code	Testing condition	
	Dry	Wet
522	2.20 C	-
554	3.62 A	2.94 B
532	1.91 C	-
822	3.80 A	2.92 B
854	4.15 A	3.69 A
832	2.01 C	-
922	1.99C	-
954	2.85 B	-
932	1.58 C	-

According to Table 3.13, there is no significant difference between resin type 854 (PF resin formula 8 with –NCO to –OH ratio of 1.25), 822 (PF resin formula 8 with –NCO to –OH ratio of 1), and 554 (PF resin formula 5 with –NCO to –OH ratio of 1.25).

Wet shear bonding strength testing was conducted to finalize the best formula determination.

3.3.2 General properties of optimized hybrid resin

The data in Table 3.14 show that the general properties of different optimized hybrid resins. The viscosities are slightly different, which is because of the different –NCO and –OH group ratios. With higher –NCO/-OH ratio, the cross-linking between

these two functional groups was more complex and the network made the viscosity higher.

Table 3.14 General properties of optimized hybrid resin

Resin code	Nonvolatile solid content (%)	Viscosity (MPa·s)	Dry bonding strength (MPa)	Wet bonding strength (MPa)
854	62.0	1023	4.15	3.69
554	64.5	987	3.62	2.94
822	68.6	1230	3.80	2.92

Note: 854: PF resin formula 8 with –NCO to –OH ratio of 1.25;
822: PF resin formula 8 with –NCO to –OH ratio of 1;
554: PF resin formula 5 with –NCO to –OH ratio of 1.25.

Table 3.15 Number Average Molecular Weight (Mn) and Weight Average Molecular Weight (Mw) of PF Resins of Different Molecular Weights

PF resin samples	Number Average Molecular Weight (Mn)	Weight Average Molecular Weight (Mw)	PDI
A	277.74	488.29	1.76
M	327.09	734.87	2.25
W	504.84	974.64	1.93

According to the optimization analysis above especially the bond strength which is the most important property of a resin, formula NO.8 ((F/P=2.0, S/P=0.4)) with –NCO to –OH ratio of 1.25 was chosen for further study and characterization.

The molecular weights of the optimized resin were measured with gel permeation chromatography (GPC) (OMNISEC, Malvern Company, Worcestershire, UK.). The measured molecular weights are listed in Table 3.15.

3.3.3 FTIR analysis result

The FTIR analysis performed in the optimized polymer system with PF resin with molecular weight of M is shown in Figure 3.4. The characteristic band of the aromatic ring was observed at 1633 cm^{-1} to 1513 cm^{-1} region. The band detected in the 885 cm^{-1} was attributed to CH out-of-plane (isolated H) stretching. The remarkable difference between the co-polymer system and the PF resin were the band features of the isocyanate group observed at 2259 cm^{-1}. This indicated that there were –NCO groups present in the co-polymer system in such optimized hybrid resin.

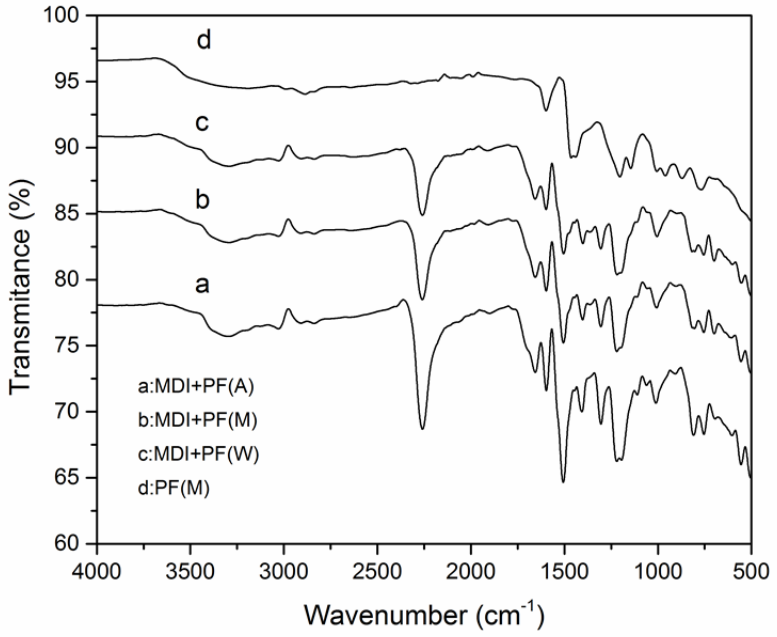

Figure 3.4 FTIR spectra for hybrid resin with different molecular weights

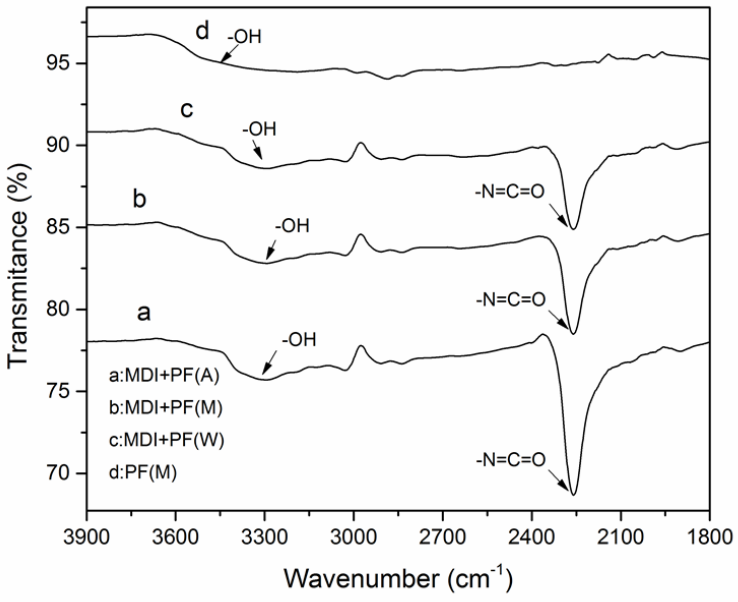

Figure 3.5 FTIR spectra indicating –OH and –NCO groups in hybrid resin

Figure 3.5 displays the difference in the reaction of –OH and –NCO groups in PF/MDI co-polymers with different molecular weight resins. There are some residual isocyanate compounds left; it gave us a perspective to compare co-polymers between PF resins with different molecular weights. It was obvious that there are variable –NCO groups left in the resin when using different molecular weights of PF resins. The peak intensity of the –NCO groups in lower-molecular weight PF resins is much stronger than that of higher-molecular weight PF resins. This indicates that the higher-molecular weight PF resins can promote the reaction of MDI and PF resins and the reaction between higher-molecular weight PF resins and MDI is much more completely. The relationship between this reaction and the bonding strength needs to be further studied.

3.3.4 TGA/DSC analysis result

Thermogravimetric analysis under an inert environment can provide insight into the composition through differences in the thermal stability of chemical bonds (Wandler and Frazier 1996; D'Pa et al. 2014). The thermal stabilities of co-polymer systems with different molecular weights of phenolic resins can be followed from Figures 3.6 to 3.11. It is obvious from the TG curve (Figure 3.6) and DTG curve (Figure 3.7) that the co-polymer decompositions occurred at various temperature ranges.

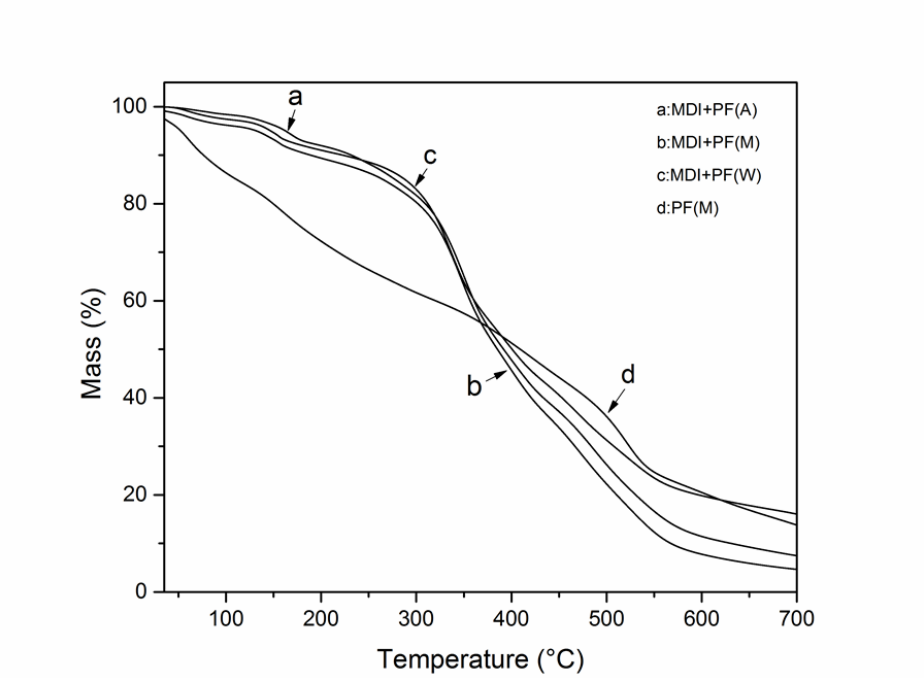

Figure 3.6 TG curves of hybrid resin with different molecular weights

There are two stages for the decomposition of PF/MDI co-polymer, while there is only one stage in the decomposition of PF resins. The initial decomposition rate of co-polymer is relatively slow. In the second decomposition stage, as the molecular weights of the PF resin increases, the mass loss rate becomes slower while the total weight loss rate decreases. The higher the molecular weight of PF resin, the better thermal property it showed.

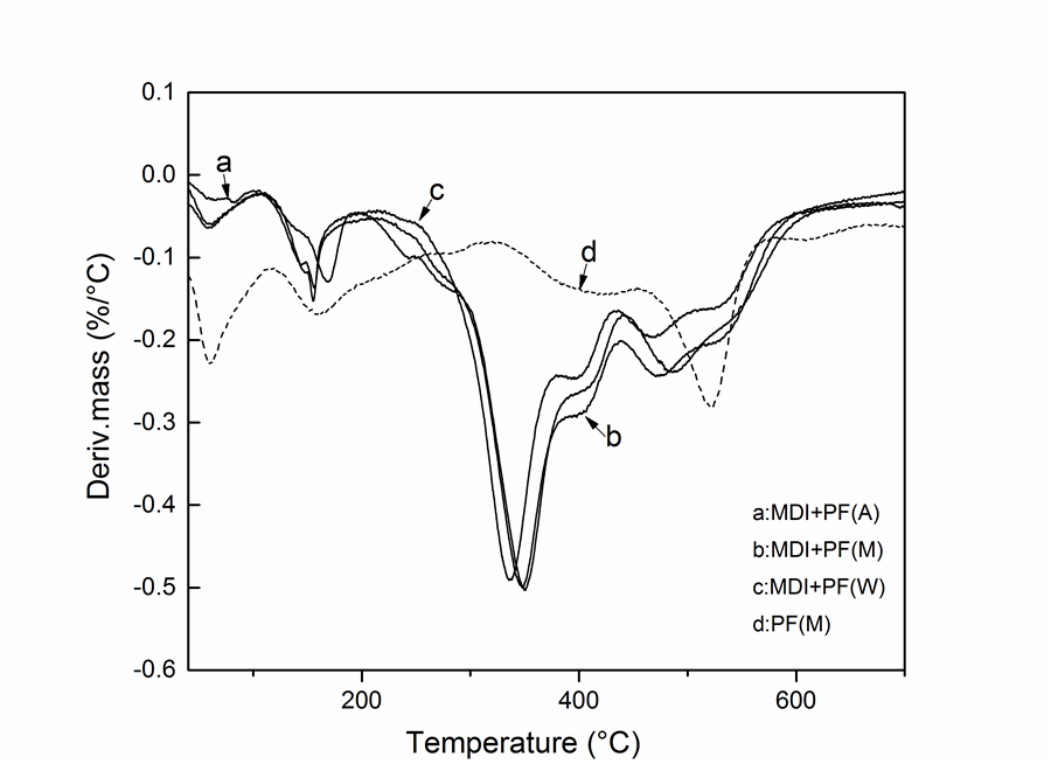

Figure 3.7 DTG curves of hybrid resins with different molecular weights

The first stage represents the decomposition of MDI involving the breakage of urethane bonds, while the second stage denotes the ester decomposition. Under 320 °C, the higher the molecular weights of PF resins, the slower the decomposition rates of the co-polymer system (Figure 3.7).

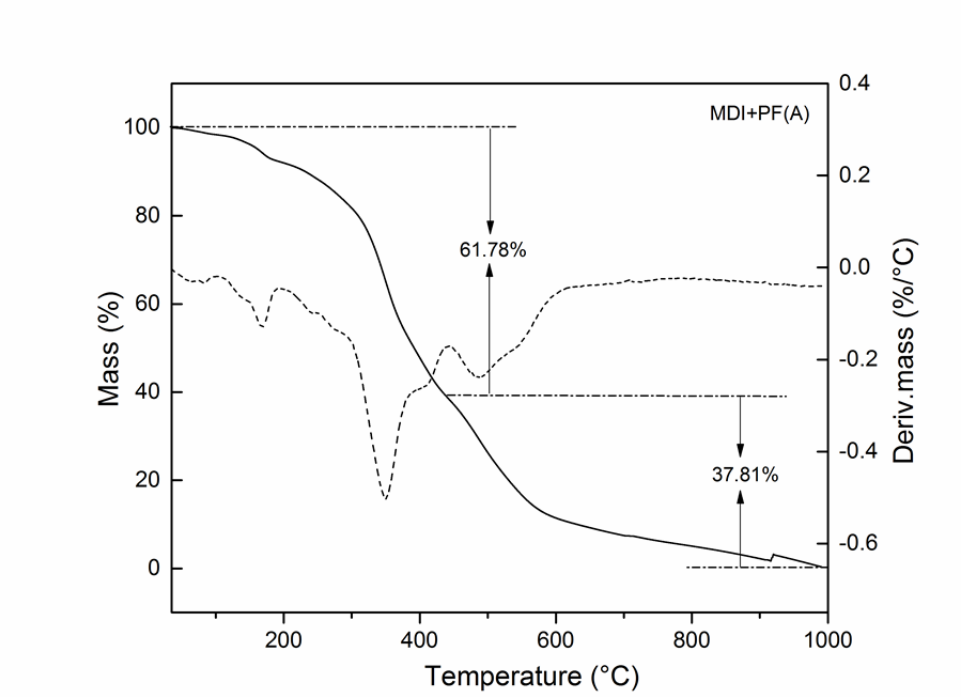

Figure 3.8 TG/DTG curves of hybrid resin with molecular weight of A

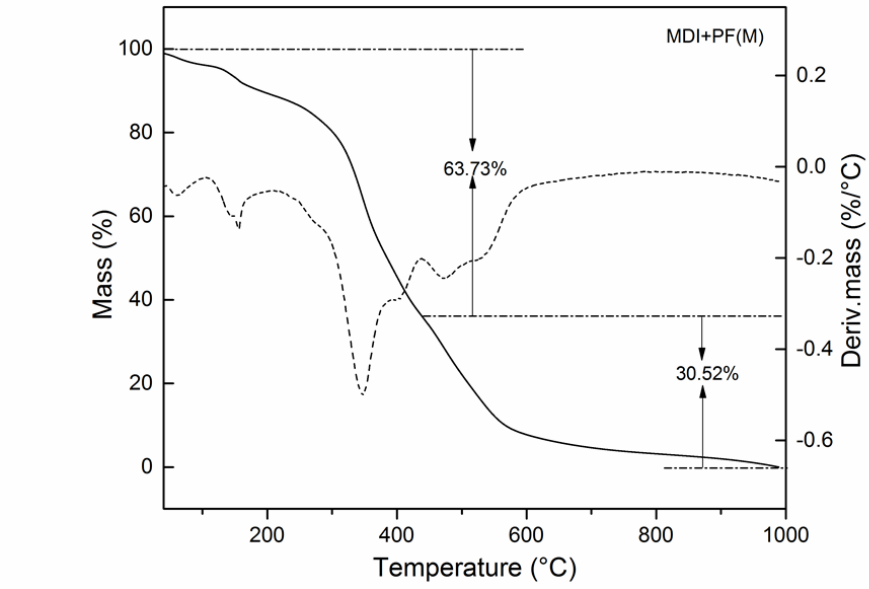

Figure 3.9 TG/DTG curves of hybrid resin with molecular weight of M

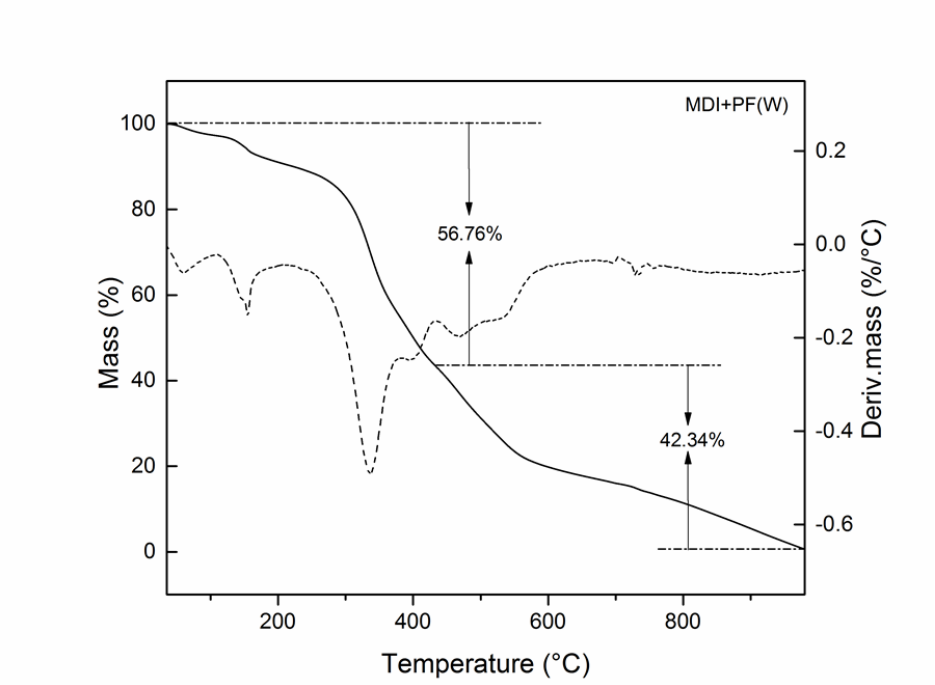

Figure 3.10 TG/DTG curves of hybrid resin with molecular weight of W

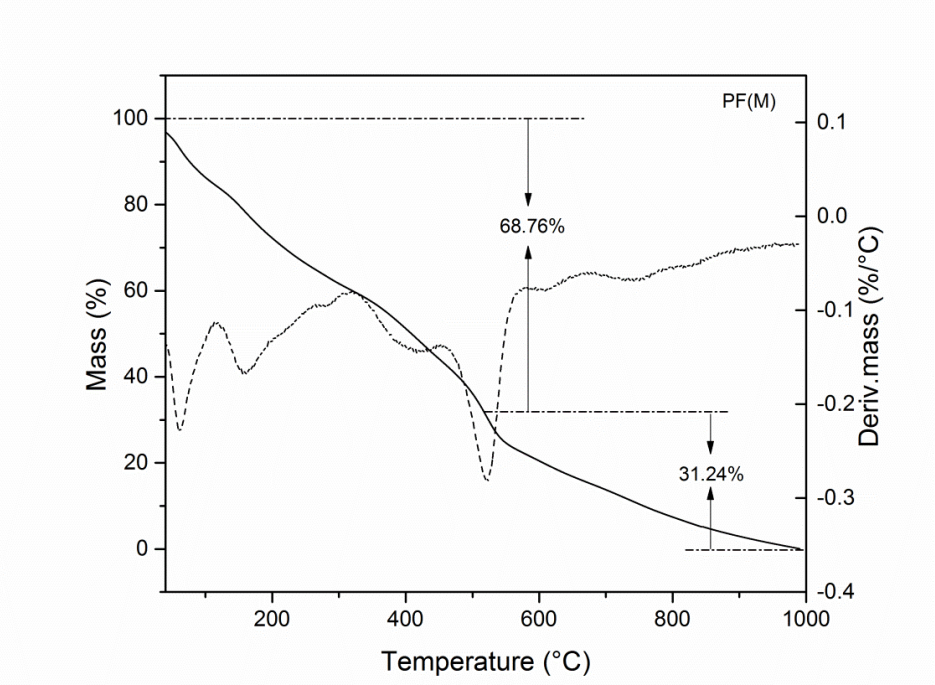

Figure 3.11 TG/DTG curves of PF resins with molecular weight of M

Figures 3.8 to 3.11 show the TG/DTG curves of co-polymer systems with different molecular weights of phenolic resins, and the control group of PF resins with molecular weight of M. In organic polymer systems, the total mass loss ratios of all the samples were approximately 100%. However, the first stage had lower mass loss ratio than phenolic resins' with molecular weight of M. This indicated that the co-polymer had better thermal properties under the temperature of 500 °C. Among all the three samples of co-polymers, during the first stage, the mass loss ratio of the sample of MDI/PF resins with the molecular weight of W was 56.76% which was significantly lower than that of the phenolic resin with molecular weight of A (61.78%) and M (68.76%). Generally, the co-polymer system of isocyanate resin with higher molecular weight of phenolic resin showed better thermal property.

3.3.5 XRD analysis result

The X-ray diffraction techniques examine the long-range order produced as a consequence of very short range interactions. Figure 3.12 shows the X-ray diffraction patterns of MDI/PF co-polymers with different molecular weights. The powder diffraction file exhibited broad peaks at 2θ angles around 18°, 21°, 30.3°, and 34.4°, indicating some degree of crosslinking. These peaks were assigned to the scattering from MDI/PF co-polymer system with different molecular weights. The degree of order in these materials was established in relation to the molecular weights of phenolic resins.

The evidence of crosslinking behavior of the co-polymer system was mainly from peaks at 2θ 30.3° and 34.4°. When compared with the X-ray diffraction patterns of phenolic resins in Figure 3.13, the co-polymers showed clear evidence of crosslinking. From Figure 3.12, it is very distinctive that with the increase of the molecular weight of

phenolic resins, the co-polymer systems are more crosslinked, with the most intense peaks located at 2θ, 20°, 30.3°, and 34.4°. Through changes in the molecular weights of phenolic resins A to W, the characteristic peaks became smaller, indicating a decrease in crosslinking of the sample. The characteristic peaks disappeared completely in the samples without MDI. These results showed that the degree of crosslinking has some relationship with the molecular weights of phenolic resins. The variation of this can be explained by the extent of reaction between hydroxyl and isocyanate groups.

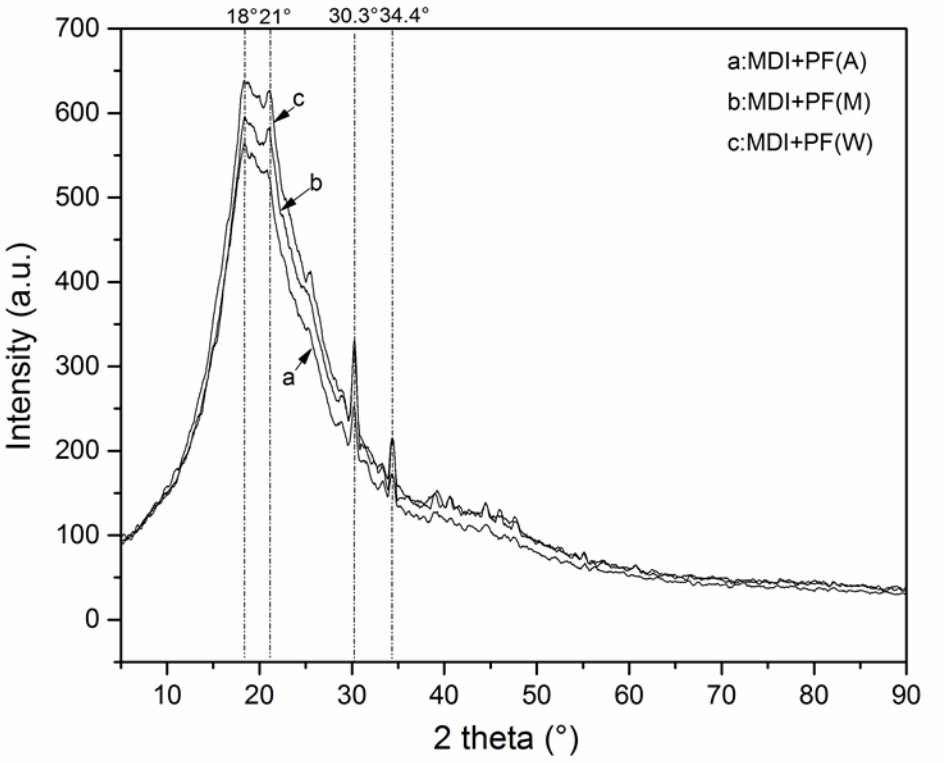

Figure 3.12 XRD patterns of hybrid resins with different molecular weights

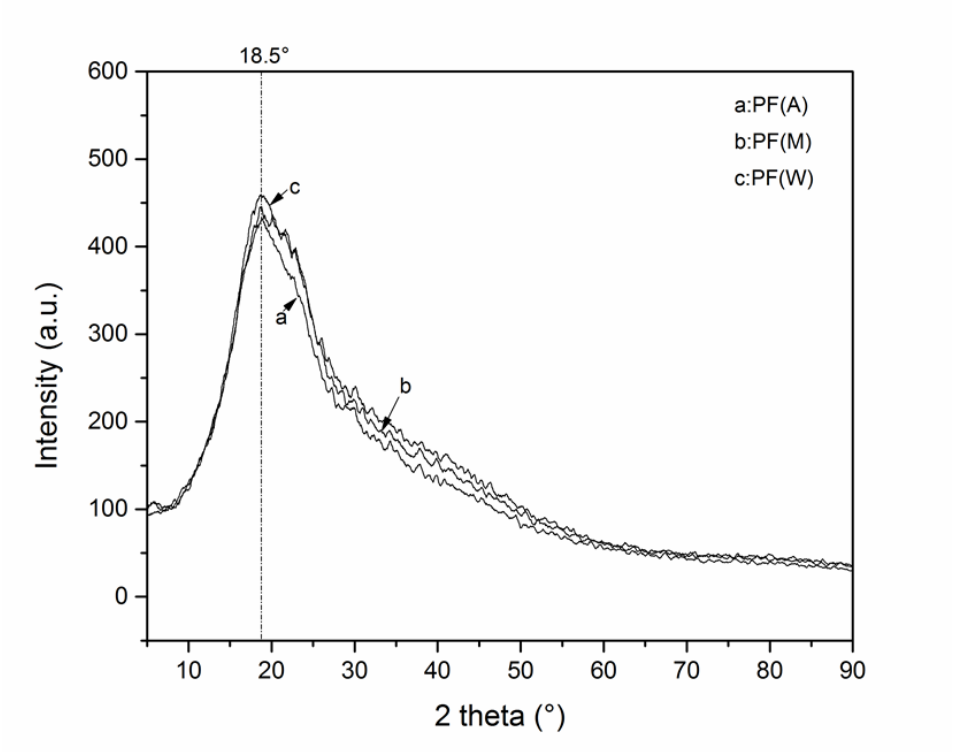

Figure 3.13 XRD patterns of PF resins with different molecular weights

As the molecular weight of W-resin indicated better thermal property and can promote the reaction between isocyanate resin and the phenolic resins effectively. The XRD technique was used to characterize this property in order to get more detailed information. In a crystal structure, d-spacing is defined as the distance between adjacent planes. Although it has not been confirmed that the co-polymer system in this study is crystal or not, but we can still use the same technique and calculation method to get the general average size of the particle which can be named d'-spacing.

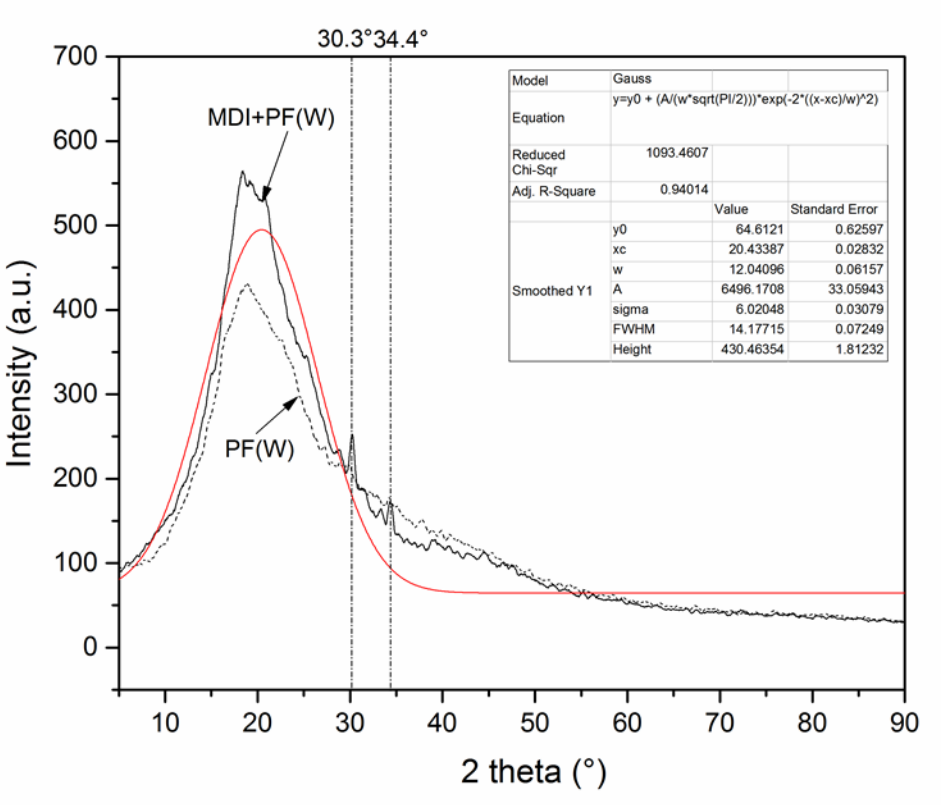

Figure 3.14 Gauss fitting of XRD patterns of hybrid and PF resins with the molecular weight of W

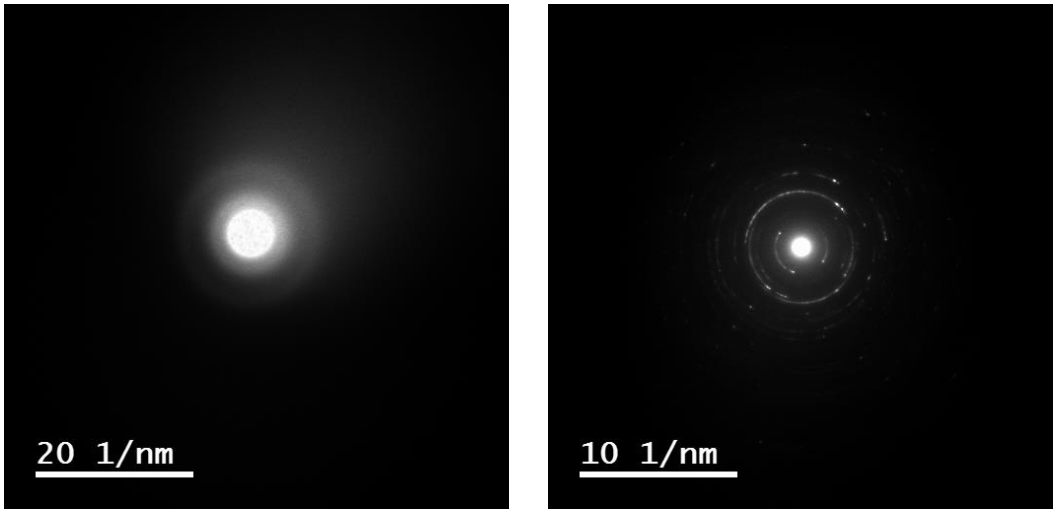

Figure 3.15 TEM images of pure PF resin and hybrid resin

The peaks at 2θ of 30.3 º and 34.4 º can be confirmed in TEM test.

From the Fig. 3.14 above, with the function of Gauss fitting, the full-width at half-maximum (FWHM) of the peaks at 2θ was 14.18. Using the equation of λ=CuKα=1.540 Å, the average particle size of the co-polymer system with the molecular weight of W was 0.57 nm as calculated (The standard reference for FWHM of 0.1 degree was used in this calculation).

The d'-spacing's corresponding to the large peak(s) in the respective curves was calculated from Bragg's equation:

$$2d\sin\theta = \lambda \qquad (3.3)$$

Where 2θ is the X-ray scattering angle and λ represents the incident wavelength used.

The d'-spacing of diffraction peaks found in co-polymer system are shown in Table 3.16.

Table 3.16 Summary of X-Ray scattering peaks and corresponding d'-spacing of hybrid resin

2θ (º)	2sinθ	d'-spacing (nm)
18	0.3129	4.90
21	0.3645	4.23
30.3	0.5227	2.95
34.4	0.5914	2.61

3.3.6 X-ray microscope analysis result

To better illustrate the difference of the co-polymer system using lower and higher molecular weight of phenolic resin, X-ray microscope technique was introduced. ZEISS Xradia 520 Versa 3D X-ray microscope is a new way which unlocks new degrees of flexibility for scientific discovery. Building on industry-best resolution and contrast, Xradia 520 Versa expands the boundaries of non-destructive imaging for breakthrough flexibility and discernment critical to wide variety of research.

Here, the lowest and the highest molecular weight of PF resin were used to mix with MDI for comparison. From Figure 3.16 and Figure 3.17, the particle distribution of hybrid resin with different molecular weights is different. The distribution for low molecular weight is more even but without obvious big molecules. However, for high molecular weight, the molecules due to cross-linking between PF and MDI are obviously bigger which can potentially improve the strength of it but it may also cause some problems when it is tried to be used for forest products. Further research or modification need to be conducted.

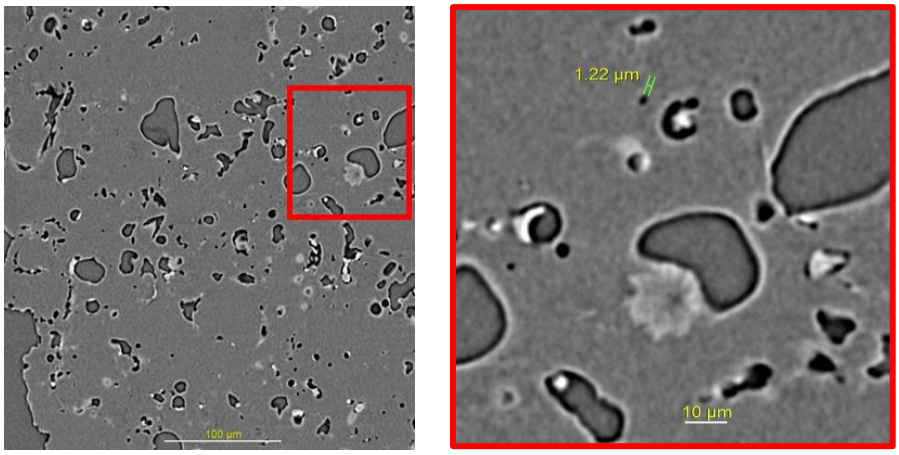

Figure 3.16 Particles distribution of hybrid resin with the molecular weight of A

Figure 3.17 Particles distribution of hybrid resin with the molecular weight of W

It shows much clearer in Figure 3.18 which is the rendering of scanned area of hybrid resins with the molecular weight of A and W. For low molecular weight, isolated particles are presented. For hybrid resins with high molecular weight of PF resin, clear intertwined structures present.

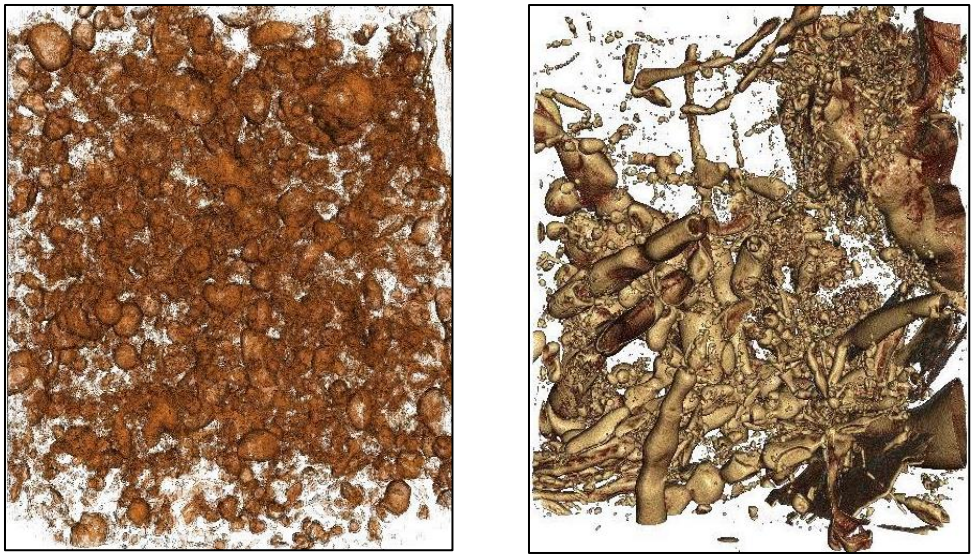

Figure 3.18 3D rendering of scanned area of hybrid resins with the molecular weight of A (left) and W (right)

3.4 Conclusions

All the three factors: F/P, S/P and –NCO/-OH ratios affect the strength of PF resin and hybrid resin significantly. Considering both dry shear strength and wet shear strength, the formula NO.8 ((F/P=2.0, S/P=0.4)) with –NCO to –OH ratio of 1.25 was chosen for further study and characterization.

Lower molecular weight of the PF-resins led to more –NCO residual groups in the copolymer system. Higher molecular weights of PF resins could promote the reaction of MDI and PF resins. The reaction between isocyanate and phenolic resin with the molecular weight of W appeared to be more thorough.

In the decomposition stage of hybrid resin, the breakage of urethane bonds occurred and the decomposition rates were found to be much slower than those of phenolic resins. The co-polymer systems had significantly better thermal properties than

PF resins' below 500 °C. The co-polymer of isocyanate resin with the highest molecular weight of phenolic resin showed the best thermal property.

The co-polymer systems were a kind of amorphous material. The powder diffraction exhibited broad peaks at 2θ angles around 30.3° and 34.4°, indicating crosslinking behavior.

An increase in molecular weight of phenolic resins indicated more crosslinking in the co-polymer system. The average particle size of the co-polymer system with molecular weight of W was 0.57 nm.

This kind of hybrid polymer system has the potential to improve the thermal resistance and mechanical properties. The relationship between these properties and the molecular weights of phenolic resins needs further study.

3.5 References

Lee, Y. K., Kim, D. J., Kim, H. J., Hwang, T. S., Rafailovich, M., & Sokolov, J. (2003). Activation energy and curing behavior of resol-and novolac-type phenolic resins by differential scanning calorimetry and thermogravimetric analysis. Journal of applied polymer science, 89(10), 2589-2596.

Aierbe, G. A., Echeverrıa, J. M., Martin, M. D., Etxeberria, A. M., & Mondragon, I. (2000). Influence of the initial formaldehyde to phenol molar ratio (F/P) on the formation of a phenolic resol resin catalyzed with amine. Polymer, 41(18), 6797-6802.

Gardziella, A., Pilato, L. A., & Knop, A. (2013). Phenolic resins: chemistry, applications, standardization, safety and ecology. Springer Science & Business Media.

Lee, S. M., & Kim, M. G. (2007). Effects of urea and curing catalysts added to the strand board core‐layer binder phenol–formaldehyde resin. Journal of applied polymer science, 105(3), 1144-1155.

Shafizadeh, J. E., Guionnet, S., Tillman, M. S., and Seferis, J. C. (1999). "Synthesis and characterization of phenolic resole resins for composite applications," Journal of Applied Polymer Science 73(4), 505-514.

Lenghaus, K., Qiao, G. G., and Solomon, D. H. (2000). "Model studies of the curing of resole phenol-formaldehyde resins Part 1. The behaviour of ortho quinone methide in a curing resin," Polymer 41(6), 1973-1979. DOI: 10.1016/S0032-3861(99)00375-4.

Poljanšek, I., Fabjan, E., Moderc, D., and Kukanja, D. (2014). "The effect of free isocyanate content on properties of one component urethane adhesive," International Journal of Adhesion and Adhesives 51, 87-94. DOI:10.1016/j.ijadhadh.2014.02.012

ASTM D1037-12 Standard Test Methods for Evaluating Properties of Wood-Base Fiber and Particle Panel Materials, ASTM International, West Conshohocken, PA, 2012

ASTM E222-10 Standard Test Methods for Hydroxyl Groups Using Acetic Anhydride Acetylation, ASTM International, West Conshohocken, PA, 2010

D'Souza, J., Camargo, R., and Yan, N. (2014). "Polyurethane foams made from liquefied bark‐based polyols," Journal of Applied Polymer Science, 131(16).

EN, B. (2003). 205, Adhesives. Wood adhesives for non-structural applications. Determination of tensile shear strength of lap joints. British Standards Institution.ASTM

Paris, J. L., & Kamke, F. A. (2014). Quantitative wood–adhesive penetration with X-ray computed tomography. International Journal of Adhesion and Adhesives, 61, 71-80.

Pizzi, A., & Walton, T. (1992). Non-emulsifiable, water-based, mixed diisocyanate adhesive systems for exterior plywood-part I. Novel reaction mechanisms and their chemical evidence.

Zhuang, J. M., & Steiner, P. R. (1993). Thermal reactions of diisocyanate (MDI) with phenols and benzylalcohols: DSC study and synthesis of MDI adducts. Holzforschung-International Journal of the Biology, Chemistry, Physics and Technology of Wood, 47(5), 425-434.

Riedlinger, D. A. (2008). Characterization of PF Resol/Isocyanate Hybrid Adhesives (Doctoral dissertation, Virginia Polytechnic Institute and State University).

Zheng, J. (2002). Studies of PF resole/isocyanate hybrid adhesives (Doctoral dissertation, Virginia Polytechnic Institute and State University).

Paris, J. L. (2014). Wood-adhesive bondline analyses with micro X-ray computed tomography.

Wandler, S. L., and Frazier, C. E. (1996). “The effects of cure temperature and time on the isocyanate-wood adhesive bondline by 15 N CP/MAS NMR,” International journal of adhesion and adhesives, 16(3), 179-186.

CHAPTER IV

THE EFFECT OF ACETONE ON CURING BEHAVIOR OF HYBRID RESIN BASED ON PHENOL FORMALDEHYDE AND ISOCYANATE RESIN

4.1 Introduction

When acetone was introduced into hybrid resin system to disperse frozen-dried phenolic resin so that it can react with MDI, it was found that adding MDI into the solution of acetone and PF resin with specified amount, the mixture began to react immediately. This unusual phenomenon is strong evidence indicating that acetone may have promoted the reaction of PF and MDI resin. During the process, the reaction of acetone and phenol can be ignored because this reaction needs strong acid catalysts or ion exchange resin catalyst (Zakoshansky et al. 1993; Alamdari et al. 2010; Baohe et al. 2013).

There is very limited research about using acetone to promote the co-polymerization of PF and MDI even this reaction is typically cured and applied in an organic solvent as mentioned in literature review (Rosthauser et al. 2001 US Patent 6214265). In this part of study, the effect of acetone on the curing behavior of hybrid resin system was studied using differential scanning calorimetry (DSC), and rheometer. DSC is among one of the most popular and reliable methods to study the kinetics of cure reactions in both isothermal and no isothermal modes (Kamal et al. 1973; Cuadrado et al. 1983; Liu et al. 1995). Those studies were based on the assumption that the rate of heat

generation is proportional to the rate of the cure reactions (Kamal et al. 1984; Kama et al. 1980). Thermal analysis using DSC is a powerful techniques to make time-temperature predictions and thus to serve to optimize the curing process variables of polymers (Khanna et al. 1987).

Meanwhile, confocal laser scanning microscope (CLSM) and technique was used to characterize the distribution of resins in wood and atomic force microscope (AFM) technique was applied to compare the toughness and image surface area difference of different resins.

4.2 Materials and Methods

4.2.1 Materials

Phenol, a 99% aqueous solution (USP), was obtained from Fisher Scientific Co., Ltd (Hampton, NH). Paraformaldehyde, a 96% extra pure powder was purchased from Fisher Scientific Co., Ltd (Hampton, NH). Isocyanate, a polymeric MDI with 33% -NCO functional group, was obtained from BASF Polyurethanes (Wyandotte, MI). It was a dark yellow liquid with a viscosity of 226 mPa·s at 25°C. Sodium hydroxide, 97% pure pellets, was purchased from Fisher Scientific Co., Ltd. Acetone, >= 99.5% liquid, was purchased from Fisher Scientific Co., Ltd.

PF resin (formula NO.8 ((F/P=2.0, S/P=0.4)) with –NCO to –OH ratio of 1.25) was dried in speed vacuum drier (model LYPH-LOCK 6, LABCONCO) with -50 °C. The frozen dried hybrid resin with and without acetone were blended for a few minutes for homogenization and then they were ready to be measured. In this part of study, hybrid resin refers to PF and MDI co-polymer system without acetone. Hybrid resin with

acetone refers that acetone was mixed with frozen-dried PF resin first and then evenly mixed with MDI.

4.2.2 Methods

4.2.2.1 DSC analysis

Thermal characterization was performed on a SDT Q600 (V20.9 Build 20) (TA instrument Inc, New Castle, DE, US) instrument. First, the curing process was studied using isothermal scans on 5 mg samples of hybrid resin with different amount of acetone by in the modulated DSC (MDSC) mode (Abdalla et al. 2008). Cured samples were ramped from room temperature to the desired isothermal temperature (250 °C) at a rate of 10 °C/min and then held isothermally. The initiation temperature (T_0), the peak temperature (T_p), the termination temperature (T_i) and the heat of reaction (ΔH) were recorded for calculation. Secondly, 5 mg of hybrid resin samples with optimized amount of acetone were heated at rates of 5°C/min, 10°C/min, 15°C/mins and 20°C/mins. The data was baseline corrected and by determining the instrument time constant and the heat transfer rate using an indium melting peak (Flammersheim et al. 1991).

All the DSC scans were conducted using hermetically sealed aluminum sample pans and pure nitrogen was used as the carrier gas with a flow rate of 100 mL/min to maintain the inert atmosphere for the samples. Exothermic peaks are represented by upward peaks in the DSC thermos grams. The kinetic analysis was done using TA advantage specialty library package provided by TA instruments.

4.2.2.2 Rheological analysis

The rheological measurements were performed using an AR-1500 rheometer (TA Instruments, Delaware, US) with geometry of serrated parallel plates (B40 mm) and gap of 800 mm, which was adopted based on preliminary results. Samples of 2.0 mL were introduced in the rheometer and left at rest for 5 min before measurements. All the samples were tested in duplicate and a new sample was used for each replicate.

This technique was designed and developed for monitoring the viscoelastic state of a wide range of materials and particularly the changes in the rheological properties with temperature or time (Laza et al. 2005). The oscillatory motion of the probe is progressively damped by viscous drag, which allows for the monitoring of viscoelastic properties, such as viscosity and its components, the storage modulus (G'), the loss modulus (G''), and the loss tangent ($\tan \delta$), during the curing process. The oscillation frequency is 2 Hz, and readings are obtained every second (Laza et al. 1999).

Although according to the exploring test result from Figure 4.1, the gel temperature for PF resin is around 123 °C, in all the cases, the cure temperature was set between 75 to 100 °C. If the experiments were carried out below 75 °C, the curing process of the phenolic resin was too slow to be measured. If the curing temperature is above 100 °C, the water condensed during the curing reaction will be boiled and this will make it difficult to monitor the viscoelastic properties during the curing process.

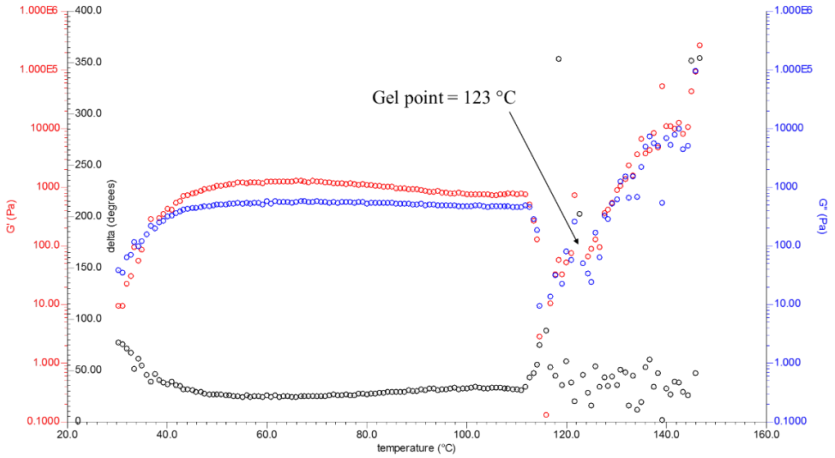

Figure 4.1 G', G'', and tan δ versus cure temperature for pure phenolic resin

Table 4.1 Sample curing conditions for rheological analysis

Samples	T (°C)
Pure PF	70, 80, 90, 100
Hybrid resin	70, 80, 90, 100
Frozen-dried hybrid resin	70, 80, 90, 100
Frozen-dried hybrid resin in acetone	70, 80, 90, 100

4.2.2.3 Confocal laser scanning microscope

Samples were observed using a confocal laser scanning microscope (CLSM; TCS-NT, Leica, Heidelberg, Germany) in combined florescence and transmission mode. Excitation light had a maximum wavelength of 543 nm, and fluorescence was detected using a 525/50 nm bandpass filter. Transmitted light was detected without filters. Images were recorded with a lateral resolution of 1024*1024 pixels and 1000*1000 um, and analyzed using Leica Confocal Software (LCS Lite version 2.61, Leica)

4.2.2.4 AFM analysis

AFM was performed with the PeakForce QNM mode using a Dimension Icon AFM (Bruker, USA).The sample was attached to a glass slide using a double-sided tape, followed by scanning of the surface by a silicon nitride probe (Model RTESP, 5N/m of spring constant) in air at ambient conditions. The images were obtained at a speed of 5 μm/s (1 Hz), force of 0.15 nN, and scan sizes of 1μm with a sampling resolution of 512 points per line.

4.3 Results and Discussion

4.3.1 Optimization of the amount of acetone

As shown in preliminary experiment (the macro level), acetone has emerged to promote the curing process of the hybrid resin system. This promotion can be significantly affected by the amount of acetone used. In this research, different mass ratio of acetone/hybrid resin (0.2:1, 0.4:1, 0.6:1, 0.8:1, and 1:1) of optimized hybrid resin with acetone.

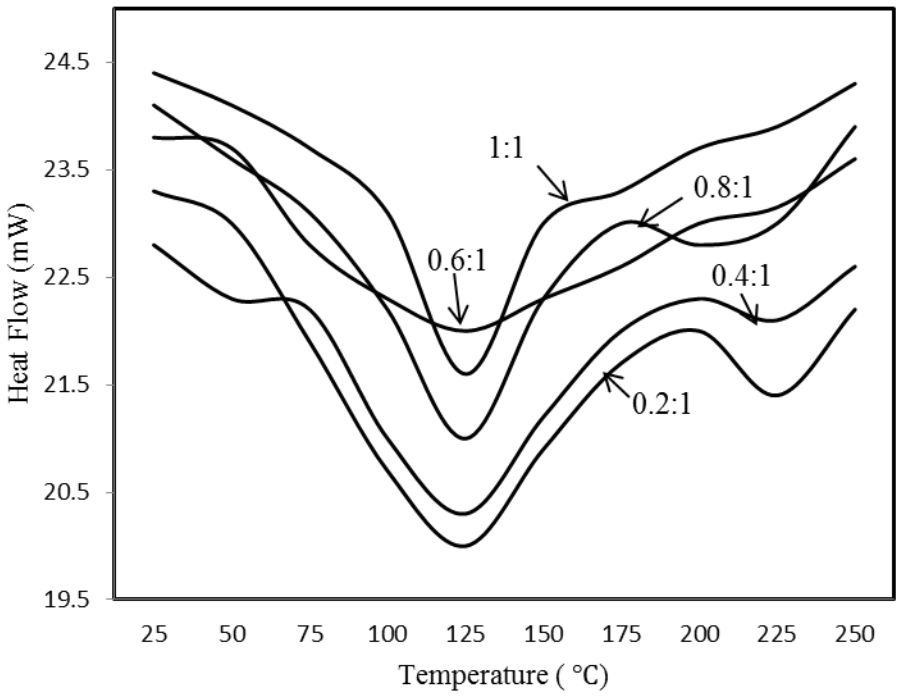

Figure 4.2 DSC curves at the heating rate of 10°C/min

It is obvious that the widths of exothermic peak varied from one to another due to the change of mass ratio of acetone to hybrid resin. From mass ratio of 0.2:1 to 0.6:1, the peak widths increased gradually while they decreased from mass ratio 0.6:1 to 1:1. When the mass ratio of acetone to hybrid resin was 0.6:1, the exothermic peak was the widest which indicated the areas of exothermic peak as well as the heat release of curing process were the largest. In other words, the curing reaction of this system completed the most. When the mass ratio further increased, the width of the peak became narrower. The possible reason is excessive acetone absorbs part reaction heat.

Table 4.2 Main curing parameters at the heating rate of 10°C/min

Mass ratio	0.2:1	0.4:1	0.6:1	0.8:1	1:1
T_0(K)	307.12	309.55	305.21	307.33	310.24
T_p(K)	401.22	428.94	433.35	430.21	419.87
T_i(K)	493.27	495.31	506.23	491.22	482.36
ΔH(Kj/mol)	171.38	176.54	190.22	182.51	168.23

Note: T_0 is the initiation temperature; T_p is the peak temperature; T_i is the termination temperature and ΔH is the heat release of reaction.

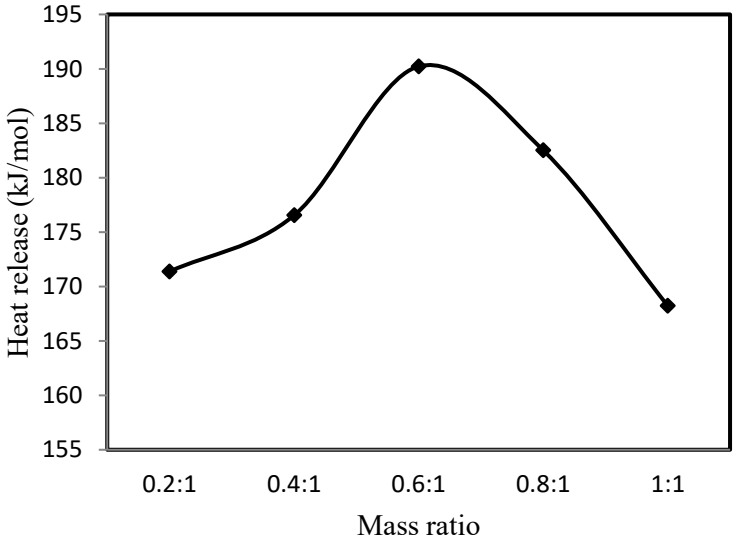

Figure 4.3 The influence of the amount of acetone

Table 4.2 is the main curing parameters of the system with different mass ratios of acetone to hybrid resin at the constant heating rate of 10°C/min. Figure 4.3 is the heat release curve of the system with different mass ratios. It is obvious that with the increase of the amount of acetone, the heat release increased first then decreased. When the mass ratio is 0.6:1, the heat release was the largest and the peak temperature was the highest.

When the mass ratio kept increasing, the heat release of this curing reaction began to decrease.

4.3.2 Analysis of kinetics parameters of curing reaction

Isothermal curing studies are ideal for determining the kinetic parameters for the curing reaction. The curing kinetics of resins can be categorized as n-th order reaction which was originally described by Borchardt and Daniels (Borchardt and Daniels 1957). And then was subsequently refined for solids (Swarin and Wims 1977). The activation energy (Ea) can determine if it is easy or not for this reaction to happen. Only when the curing system obtains energy which is larger than the activation energy, the reaction happens. The reaction order (n) is a macroscopic representation of the complexity of the curing reaction.

In order to obtain reaction kinetics parameters of curing behaviors of hybrid resin with acetone, the Kissinger and Crane equations were used to analyze the DSC curves for mixture after being tested with DSC.

Since the mass ratio 0.6:1 of acetone to hybrid resin showed the best curing behavior. In this experiment, samples with the mass ratio of 0.6:1 at rates of 5°C/min, 10°C/min, 15°C/mins and 20°C/mins were heated from room temperature to 250°C. By recording the peaking temperature and the activation energy, the reaction order can be determined using Kissinger equation (Kissinger 1957).

$$\ln\left(\frac{\beta}{{T_p}^2}\right) = \ln\left(\frac{AR}{E_a}\right) - \frac{E_a}{R}\frac{1}{T_p} \qquad (4.1)$$

Where: β is the heating rate (deg. min^{-1} or °C $\cdot min^{-1}$);

T_p is the exothermic peak temperature (K);

A is the pre-exponential factor ($K^{-m}\cdot min^{-1}$)

E_a is the energy of activation ($kJ\cdot mol^{-1}$);

R is the universal gas constant (8.31434 $kJ\cdot mol^{-1}$ K^{-1}).

Among those parameters, β, T_p can be recorded from experiment. R is constant. So only A and E_a are unknown which can be calculated from experimental data.

According to equation (1), if $\ln\left(\frac{\beta}{T_p{}^2}\right)$ is dependent variable and $\frac{1}{T_p}$ is independent variable, the slope will be $-\frac{E_a}{R}$ and the intercept will be $\ln\left(\frac{AR}{E_a}\right)$.

Table 4.3 The influence of heating rate on curing behavior of the acetone/hybrid polymer system

Heating rate (°C /min)	Tp (K)	$1/Tp\times10^3$	lnβ	$Ln(\beta/Tp^2)$	Ea kJ/mol	n	A /Km·min
5	412.27	2.426	1.609	-10.433	25.28	0.77	$5.95*10^4$
10	433.35	2.308	2.303	-9.841	25.28	0.77	$5.95*10^4$
15	467.32	2.140	2.708	-9.586	25.28	0.77	$5.95*10^4$
20	475.38	2.104	2.996	-9.332	25.28	0.77	$5.95*10^4$

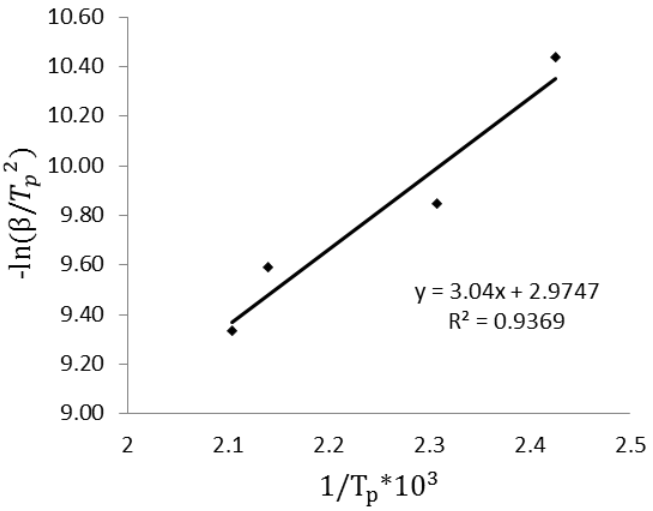

Figure 4.4 The relationship between ln (β/T_p^2) and $1/T_P$

$$\ln(\beta/T_p^{\,2}) = 2.9747 - 3040/T_p \quad (4.2)$$

$$-\frac{E_a}{R} = -3040$$

$$\ln\left(\frac{AR}{E_a}\right) = 2.9747$$

R = 8.31434 kJ/mol·K

According to the equation above, Ea=25.28 KJ/mol, A=5.95*10^4/K^m·min.

The curing reaction of the adhesive is a complex multistage chemical reaction process involving the crosslinking polymerization of each branch and functional group. The reaction order can be calculated according to the Crane equation (Crane 1973):

$$\frac{d(ln\beta)}{d(\frac{1}{T_p})} = -(\frac{E_a}{nR} + 2T_P) \quad (4.3)$$

When $Ea/nR >> 2T_p$, this equation can be simplified into:

$$\frac{d(ln\beta)}{d(\frac{1}{T_p})} = -\frac{E_a}{nR} \quad (4.4)$$

Here n is reaction order. The value of n can be obtained from the plot of lnβ versus $1/T_p$.

Figure 4.5 shows the plot of lnβ versus $1 / T_p$ for the exothermic peak in the cured resin samples. It also shows the good linear correlation. The reaction order (n) was obtained from the slope of the curve.

$$\frac{E_a}{nR} = 3927.7$$

$$\frac{E_a}{R} = 3040$$

And the value of reaction order n is calculated to equal to 0.77.

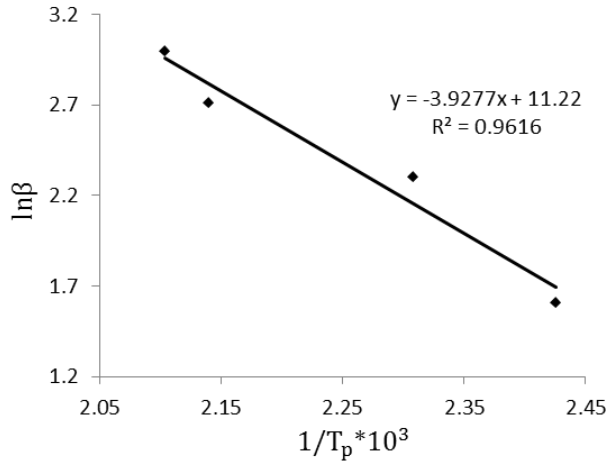

Figure 4.5 The relationship between lnβ and 1/Tp

The curing reaction kinetics model is always used to visually understand the curing conditions.

In the isothermal curing process, according to the chemical reaction rate equation:

$$\frac{d_a}{d_t} = K(1-\alpha)^n \qquad (4.5)$$

Here: $\mathrm{K} = \mathrm{Aexp}(\frac{-E_a}{RT})$

Through integral calculation:

$$\alpha(\mathrm{t}) = 1 - \left[\mathrm{Aexp}\left(\frac{-E_a}{RT}\right)(\mathrm{n}-1)\mathrm{t}+1\right]^{\frac{1}{1-n}} \quad (4.6)$$

Ea, n and A were all calculated above, R is the constant, so the curing reaction kinetics model of frozen-dried hybrid resin with acetone is:

$$\alpha(\mathrm{t}) = 1 - \left[1 - 1.37 * 10^4 \exp\left(\frac{-3.04}{T}\right)\mathrm{t}\right]^{4.35} \quad (4.7)$$

It can be seen that the curing reaction conversion rate is both related to temperature and curing time, the higher the temperature, the longer the time, the greater the degree of curing (conversion rate).

4.3.3 The application of curing reaction mechanism

The curing temperatures of hybrid resin with acetone differed with different temperature increasing rates (heating rate) which made it hard to determine the actual curing temperature. While in real manufacturing condition, the curing of resin always undergoes at a constant temperature which can be considered with a heating rate of 0°C/min. To determine the best range of curing temperature, the parameters obtained from the experiment or calculated can be used (with the best acetone amount which was the mass ratio of acetone/hybrid resin 0.6:1).

Table 4.4 The initiation temperature (T_0), the peak temperature (T_p) and the termination temperature (T_i) at different heating rates

Rate / T	5 °C/min	10 °C/min	15 °C/min	20 °C/min
T_0(K)	285.12	305.21	324.86	347.33
T_p(K)	412.27	433.35	467.32	495.38
T_i(K)	447.13	506.23	538.29	562.30

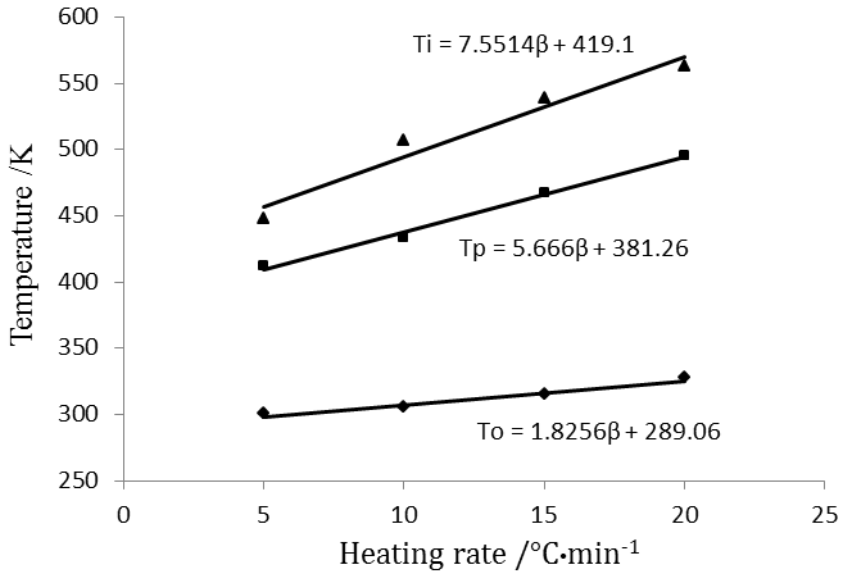

Figure 4.6 The relationship between temperature and heating rate

The intercepts (when the heating rate is 0°C/min) of these three trend lines are 289.06 K (15.85°C), 381.26 (108.11°C) and 419.10 K (145.95°C), respectively. Those key points are corresponded with the initiation temperature (T_0), the peak temperature (T_p) and the termination temperature (T_i). In other words, the curing of the hybrid resin system with acetone (mass ratio 0.6:1) begins at 15.85°C which is pretty low and can be predicted from the preliminary experiment. The best curing process is from the best

beginning temperature at 15.85°C and the resin is gradually heated to 108.11°C as the major curing period before the temperature is increased to 145.95°C and kept for a period of time to make sure the resin is fully cured.

Although the hybrid resin can be cured at a relatively low temperature, curing at elevated temperatures has the added advantage that it actually increases the end mechanical properties of the material, and many resin systems will not reach their ultimate mechanical properties unless the resin is given this 'postcure'. The postcure involves increasing the laminate temperature after the initial low temperature cure, which increases the amount of cross-linking of the molecules that can take place. To some degree this postcure will occur naturally at warm room temperatures, but higher properties and shorter postcure times will be obtained if elevated temperatures are used. Curing reaction conversion rate (α) can also be determined by the following equation:

$$\alpha = \frac{\Delta H_0 - \Delta H_t}{\Delta H_0}$$

ΔH_t is the rest heat release after curing for t time;

ΔH_0 is the heat release when the curing process completes.

As analyzed above, when the mass ration of acetone and hybrid resin is 0.6:1, the system has the largest heat release, in which ΔH_0 is 190.22 KJ/mol.

Table 4.5 Curing reaction conversion rate at different temperature with different times

Time (min)		2		4		6		8	
		ΔH_t (KJ/mol)	α	ΔH_t (KJ/mol)	α	ΔH_t (KJ/mol)	α	ΔH_t (KJ/mol)	α
T (°C)	23 °C	148.7	22	135.8	29	116.3	39	106.5	44
	108°C	35.8	82	21.7	89	9.2	96	7.5	96

Table 4.5 shows different curing conversion rate at different temperature with different time of acetone and frozen dried hybrid resin with the mass ratio of 0.6:1. It is obvious that under room temperature (23 °C), the curing process is too slow. While at the optimized temperature (108°C), it only needs 6-8 mins to complete the curing reaction. Considering comparing the shear strength of this hybrid resin and commercial PRF and PU resin which are cured at room temperature, it has been found out that it needs 16 hours for the hybrid resin to have 96.2% conversion rate under room temperature (Table 4.6). So in the following experiment, when making compress shear testing samples, 16 hour were chosen to be the pressing time.

Table 4.6 Curing reaction conversion rate of optimized frozen dried hybrid resin with/without acetone at room temperature with different times

Time (h)		4	8	12	16	20	24
Rate (%)	With acetone	77.5	82.3	88.7	96.2	96.5	96.8
	Without acetone	26.2	29.8	39.7	51.2	65.9	69.8

4.3.4 Gel time comparison and analysis

Figure 4.7 shows a typical rheometer scanning of phenolic resin. Three different regions are apparent. In the first region, the G' curve is parallel to the time axis, which corresponds to the region where the modulus is below the sensitivity of the instrument. In the second region, this modulus increases exponentially with time, and the t_g is reached. Finally, in the third region, although some dispersion of data is obtained, the modulus appears to level off, which indicates that the resin has been cured. The change in dynamic-mechanical properties of a curing system is directly proportional to the extent of the reaction and then some kinetic parameters such as t_g can be determined.

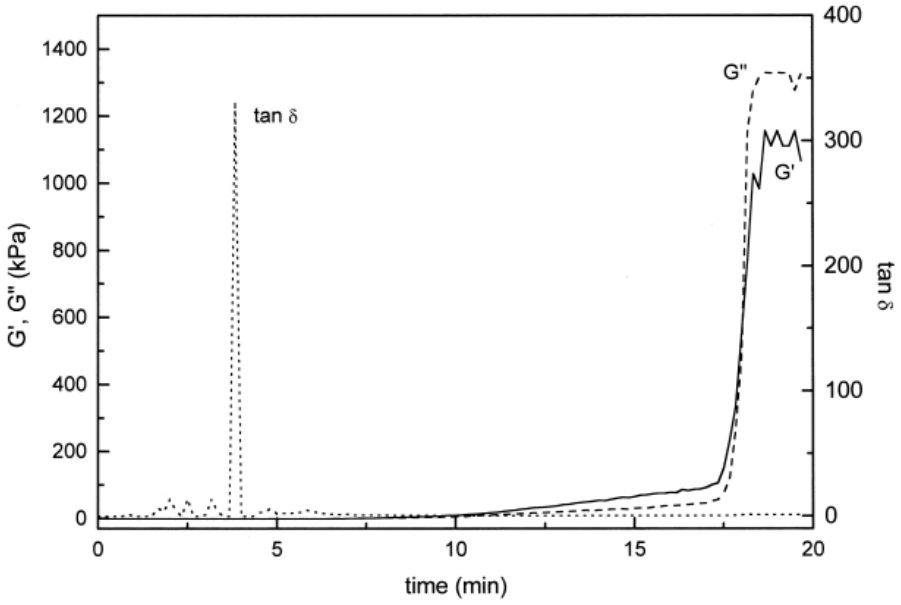

Figure 4.7 G′ , G″ , and tan δ versus cure time for a typical phenolic resin system

Table 4.7 T_g's (min) comparison for PF and hybrid resins

Resin	T (°C)	Tg 1	Tg 2	Tg 3	Tg 4
Pure PF	70	1052.1	1232.0	1298.5	1274.6
	80	425.3	512.0	534.8	550.2
	90	195.0	201.2	225.0	228.6
	100	87.9	93.6	104.9	112.3
Hybrid resin	70	953.2	1120.1	1132.5	1173.8
	80	399.8	476.3	485.3	526.4
	90	167.4	172.4	186.7	201.7
	100	76.3	82.1	86.4	90.8
Frozen-dried hybrid resin	70	885.3	937.5	940.2	-
	80	352.2	389.1	431.5	-
	90	141.7	163.0	170.2	-
	100	62.5	70.2	73.1	-
Frozen-dried hybrid resin in acetone	70	530.2	545.3	553.7	-
	80	214.8	213.6	230.2	-
	90	99.7	102.1	103.5	-
	100	35.0	44.2	48.7	-

tg1= criterion of the maximum peak in tan η; tg2 = criterion of G'= G''; tg3 = criterion of the tangent line to the G' curve; tg4 = criterion of viscosity for η' = 1000 Pa.s.

There are several criteria which are used to determine the t g (Chambon and Winter 1985, 1987; Tung et al. 1982; Harran et al. 1985; Gillham 1979):

1. Maximum peak in tan d: based on the point where there was a maximum difference between the elastic and the viscous behavior of the system.

2. Tangent line to the G' curve: The tg was taken at the point corresponding to the intercept between the base line (G' = 0) and the tangent drawn at G' when G' reached a value close to 100 kPa.

3. The crossover between the G' and G'' curves: At this point, the loss energy was equal to the energy stored.

4. Viscosity: At this point, the real dynamic viscosity (η') reached several determined values (1000, 2000, and 5000 Pa.s).

From Table 4.7, from all the criterions, it shows that the T_g's of each resin decreased when the cure temperature increased. It can be explained that with the increasing of the temperature, the groups for reaction as well as the chains in polymers became more active and can be cured faster. But the gel time for hybrid polymer was much shorter than that of pure PF resin because of the decreasing of the mobility of the resin due to the cross-linking reaction between hydroxyl groups and isocyanate groups. After frozen dried, the phenolic resin reacted with isocyanate resin with less moisture which further decreased the mobility. However, when acetone was introduced into frozen dried hybrid resin system, although it increased the fluidity of the hybrid resin system at the beginning, as described in the preliminary experiment as well as the DSC analysis, acetone promoted the reaction between phenolic resin and isocyanate resin. The gel time

of hybrid resin with acetone decreased sharper than those of pure phenolic resin and original hybrid resin.

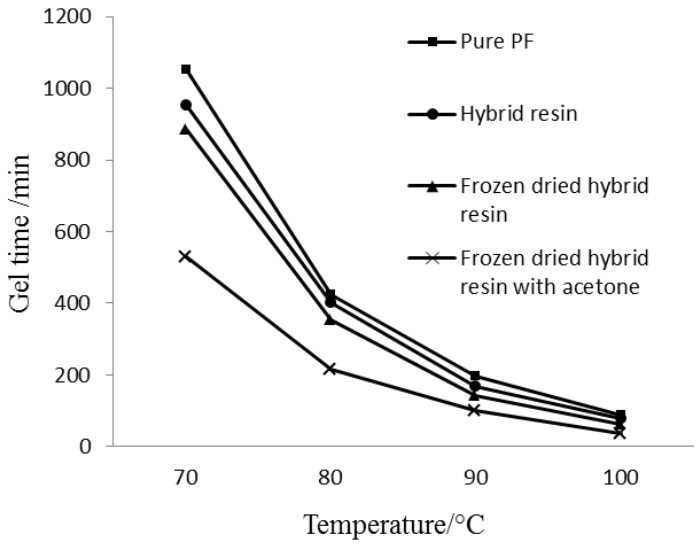

Figure 4.8 Gel time comparison of different resins at different temperature under criterion of the maximum peak in tan η

4.3.5 Confocal laser scanning microscopy analysis

In the confocal microscopic images, the red fluorescence was assigned to solid wood substrate. In contrast, the green fluorescence was due to resins penetration. The calculation of this penetration depth and area was finished using image J, a Java image processing program developed by National Institutes of Health.

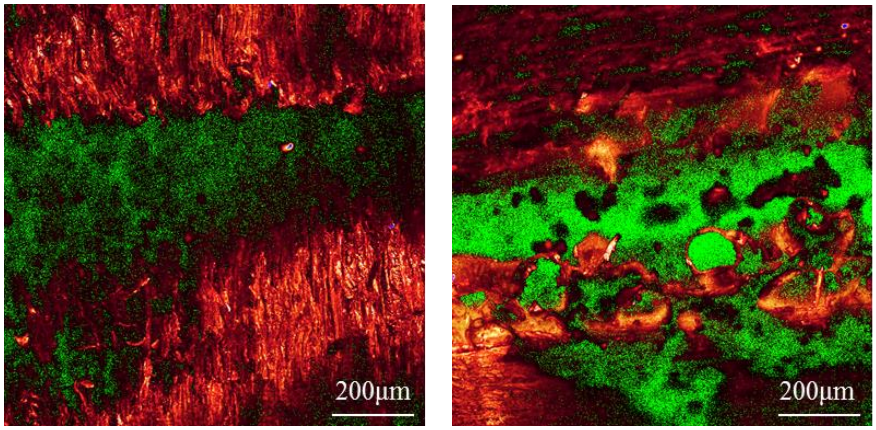

Figure 4.9 Comparison of penetration depth of hybrid resin with (right) and without (left) acetone

It is obvious that the area and depth of penetration with or without acetone are very different. With the help of the digital measuring ruler, a feature present in the CLSM image recorder software, the average penetration depth of hybrid resin without acetone is around 300 µm along the glue line. However, 23% area expands the resin to the wood porous with an average 425 µm depth. The resin was concentrated between wood substrates. But for the hybrid resin with acetone, the glue line is much wider than the one without acetone with an average of 677µm penetration depth. There are some intertwined structure between resins and wood materials. The resin was well distributed as can be seen from the section view of the glue line. In other words, the existence of acetone makes the resin go freely into wood interspace and it may also let the rest of the –NCO group to react with the hydroxyl group in wood and this needs further exploration.

4.3.6 Adhesion force measurements by AFM

Atomic interaction force and the morphology of different sample surfaces were determined at different locations using atomic force microscopy technique. The images were generated for the additional morphology and surface roughness of different resins.

For pure phenolic resin, the surface was furnished with small needle shaped resin bars. This is an indicator that PF resin was more brittle than that of hybrid resin which was consistent with the nature of PF resin (Amran et al. 2015). In other words, hybrid resin improved the toughness of phenolic resin. However, after frozen dried, phenolic resin could not be well mixed with isocyanate resin as shown in Figure 4.12. At different locations, the surface presented totally different morphologies. This may severely affect the bonding quality when the resin is used for forest products application. However, after dissolving the frozen dried phenolic resin into acetone and then mixing it with isocyanate resin, the surface of the resin system was much more uniform and may provide less variation in bonding quality when used for forest products application.

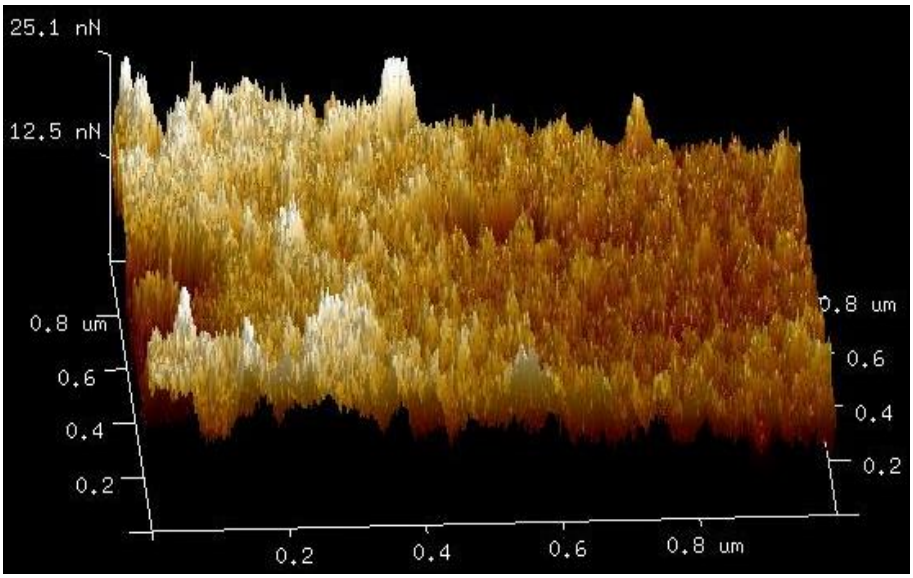

Figure 4.10 3D adhesion force distribution image of pure PF resin

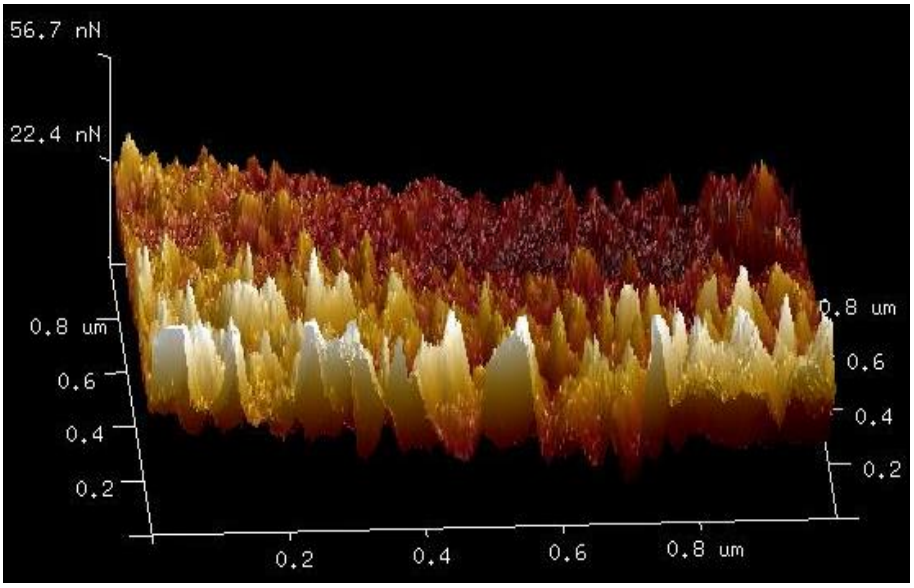

Figure 4.11 3D adhesion force distribution image of hybrid resin

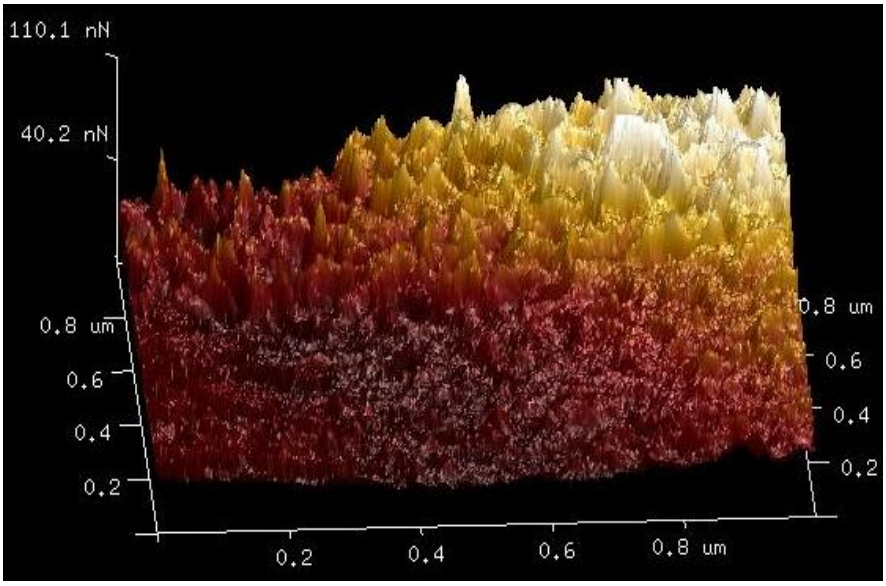

Figure 4.12 3D adhesion force distribution image of frozen-dried hybrid resin

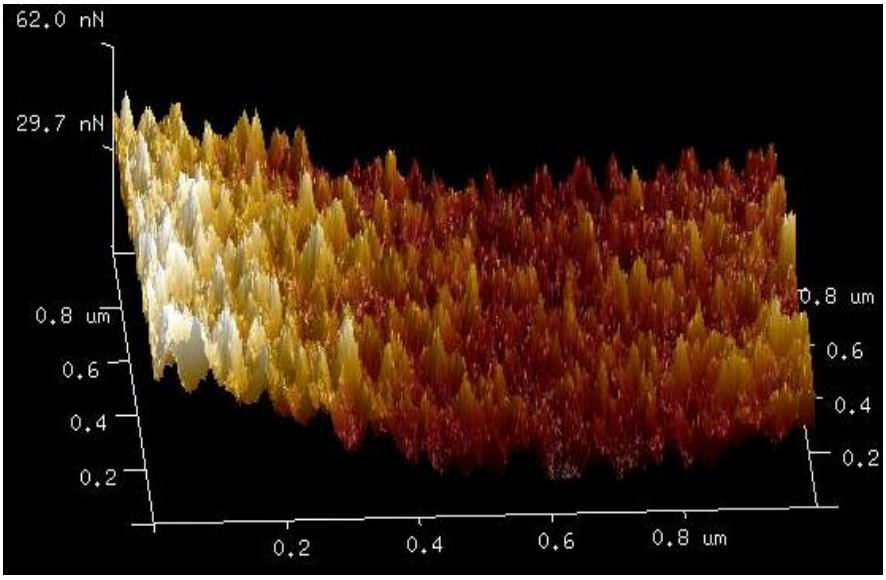

Figure 4.13 3D adhesion force distribution image of frozen-dried hybrid resin with acetone

The "Roughness" concept generates a wide variety of statistics on surfaces, including classical roughness values, peak and summit texture data and surface area calculations for the entire image (Peng et al. 2001; Sundararajan et al. 2004). Image Surface area is the three-dimensional area of the analyzed region as the sum of the area of all of the triangles formed by three adjacent data points (Poon et al. 1995). The Image Area Difference represents the difference between the image's three-dimensional Surface area and its two-dimensional, footprint area (Sundararajan et al. 2004). Finally, the image Z range indicates the maximum vertical distance between the highest and lowest data points in the image (Simpson et al.1999).

Table 4.8 Roughness results analysis of different resin samples

Samples	Image raw mean (nN)	Image Z range (nN)	Image surface area difference (%)
PF	13.2	27.0	26.8
Hybrid resin	15.7	78.5	57.0
Frozen-dried hybrid resin	23.6	130	97.3
Frozen-dried hybrid resin with acetone	24.0	67.2	50.4

From the data in Table 4.8, the frozen-dried hybrid resin with acetone has the highest image raw mean. While the image Z ranges of frozen-dried hybrid resin is the highest. Meantime, the frozen-dried hybrid resin has the highest image surface area difference too which indicates that it may reach a higher adhesion strength but may have higher variation at different locations. In other words, the instant reaction between PF and MDI resin make the hybrid resin hard to be distributed evenly. However, after dissolving it into acetone, the image surface area difference is 50.4 % which is significantly lower than 97.3% of frozen-dried hybrid resin. Obviously, acetone can make the resin application process easier. But it needs further study to keep the high adhesion strength and reduce the image surface area difference at the same time.

4.4 Conclusions

From DSC analysis results, the best mass ratio for using acetone to promote the curing process of optimized hybrid resin is 0.6:1 with the largest heat release and the highest peak temperature.

By analysis and calculation of kinetics parameters of the curing reaction, it has been noticed that the energy of activation is 25.28 KJ/mol and the pre-exponential factor is $A=5.95*10^4/ K^m \cdot min$. The reaction order is 0.77. Three temperatures which are important for hybrid resin curing are 289.06 K (15.85°C), 381.26 (108.11°C) and 419.10 K (145.95°C), respectively. It illustrates the best curing technique for the optimized hybrid resin with acetone is from the best beginning temperature at 15.85°C and the resin is gradually heated to 108.11°C as the major curing period before the temperature is increased to 145.95°C and kept for a period of time to make sure the resin is fully cured.

When acetone was introduced into frozen dried hybrid resin system, it can promote the curing reaction between phenolic resin and isocyanate resin. The gel time of hybrid resin with acetone decreases sharply compared to that of pure phenolic resin and original hybrid resin.

For the hybrid resin with acetone, the glue line is much wider than the one without acetone with an average of 677μm penetration depth. It confirms that the existence of acetone helped the frozen dried hybrid resin to apply better on wood substrate surface. From AFM analysis, it shows that hybrid resin can improve the toughness of phenolic resin. And dissolving frozen dried hybrid resin into acetone may help it better applied on wood surface to possibly ensure less variation of the strength.

The image surface area difference of frozen dried hybrid resin with acetone which is 50.4 % is significantly lower than that of frozen-dried hybrid resin which is 97.3%.

4.5 References

Zakoshansky, V. M. (1993). U.S. Patent No. 5,254,751. Washington, DC: U.S. Patent and Trademark Office.

Alamdari, A., Nasab, S. S., & Jahanmiri, A. (2010). Kinetic study of adductive crystallization of bisphenol-A. Chemical Engineering Research and Design, 88(12), 1615-1623.

Baohe, W. A. N. G., Lili, W. A. N. G., Jing, Z. H. U., Shuang, C. H. E. N., & Hao, S. U. N. (2013). Condensation of phenol and acetone on a modified macroreticular ion exchange resin catalyst. Frontiers of Chemical Science and Engineering, 7(2), 218-225.

Rosthauser, J. W., & Detlefsen, W. D. (2001). U.S. Patent No. 6,214,265. Washington, DC: U.S. Patent and Trademark Office.

Kamal, M. R., & Sourour, S. (1973). Kinetics and thermal characterization of thermoset cure. Polymer Engineering & Science, 13(1), 59-64.

Cuadrado, T. R., Borrajo, J., Williams, R. J. J., & Clara, F. M. (1983). On the curing kinetics of unsaturated polyesters with styrene. Journal of Applied Polymer Science, 28(2), 485-499.

Liu, S. B., Yang, J. F., & Yu, T. L. (1995). Curing reaction of saturated aliphatic polyester modified unsaturated polyester resins. Polymer Engineering & Science, 35(23), 1884-1894.

Kamal, M. R., & Ryan, M. E. (1984). Reactive polymer processing: Techniques and trends. Advances in Polymer Technology, 4(3‐4), 323-348.

Kamal, M. R., & Ryan, M. E. (1980). The behavior of thermosetting compounds in injection molding cavities. Polymer Engineering & Science, 20(13), 859-867.

Khanna, Y. P., & Taylor, T. J. (1987). Practical aspects of physicochemical kinetics using thermal techniques. Polymer Engineering & Science, 27(10), 764-771.

Abdalla, M., Dean, D., Robinson, P., & Nyairo, E. (2008). Cure behavior of epoxy/MWCNT nanocomposites: The effect of nanotube surface modification. Polymer, 49(15), 3310-3317.

Flammersheim, H. J., Eckardt, N., & Kunze, W. (1991). The deconvolution of DSC-curves in the experimental time domain. Thermochimica acta, 187, 269-274.

Laza, J. M., Vilas, J. L., Mijangos, F., Rodriguez, M., & Leon, L. M. (2005). Analysis of the crosslinking process of epoxy–phenolic mixtures by thermal scanning rheometry. Journal of applied polymer science, 98(2), 818-824.

Laza, J. M., Julian, C. A., Larrauri, E., Rodriguez, M., & Leon, L. M. (1999). Thermal scanning rheometer analysis of curing kinetic of an epoxy resin: 2. An amine as curing agent. Polymer, 40(1), 35-45.

Borchardt, H. J., & Daniels, F. (1957). The application of differential thermal analysis to the study of reaction kinetics1. Journal of the American Chemical Society, 79(1), 41-46.

Swarin, S. J., & Wims, A. M. (1977). A method for determining reaction kinetics by differential scanning calorimetry. In Analytical Calorimetry (pp. 155-171). Springer US.

Kissinger, H. E. (1957). Reaction kinetics in differential thermal analysis. Analytical chemistry, 29(11), 1702-1706.

Arrhenius, S. (1889). Über die Dissociationswärme und den Einfluss der Temperatur auf den Dissociationsgrad der Elektrolyte. Wilhelm Engelmann.

Crane, L. W., Dynes, P. J., & Kaelble, D. H. (1973). Analysis of curing kinetics in polymer composites. Journal of Polymer Science Part C: Polymer Letters, 11(8), 533-540.

Chambon, F., & Winter, H. H. (1985). Stopping of crosslinking reaction in a PDMS polymer at the gel point. Polymer Bulletin, 13(6), 499-503.

Chambon, F., & Winter, H. H. (1987). Linear viscoelasticity at the gel point of a crosslinking PDMS with imbalanced stoichiometry. Journal of Rheology, 31(8), 683-697.

Tung, C. Y. M., & Dynes, P. J. (1982). Relationship between viscoelastic properties and gelation in thermosetting systems. Journal of Applied Polymer Science, 27(2), 569-574.

Harran, D., & Laudouard, A. (1985). Caractérisation de la gélification d'une résine thermodurcissable par méthode rhéologique. Rheologica acta, 24(6), 596-602.

Kamal, M. R. (1974). Thermoset characterization for moldability analysis. Polymer Engineering & Science, 14(3), 231-239.

Gillham, J. K. (1979). Award address formation and properties of network polymeric materials. Polymer Engineering & Science, 19(10), 676-682.

Amran, U. A., Zakaria, S., Chia, C. H., Jaafar, S. N. S., & Roslan, R. (2015). Mechanical properties and water absorption of glass fibre reinforced bio-phenolic elastomer (BPE) composite. Industrial Crops and Products, 72, 54-59.

Peng, X. L., Barber, Z. H., & Clyne, T. W. (2001). Surface roughness of diamond-like carbon films prepared using various techniques. Surface and Coatings Technology, 138(1), 23-32.

Sundararajan, S., & Bhushan, B. (2001). Static friction and surface roughness studies of surface micromachined electrostatic micromotors using an atomic force/friction force microscope. Journal of Vacuum Science & Technology A: Vacuum, Surfaces, and Films, 19(4), 1777-1785.

Poon, C. Y., & Bhushan, B. (1995). Comparison of surface roughness measurements by stylus profiler, AFM and non-contact optical profiler. Wear, 190(1), 76-88.

Simpson, G. J., Sedin, D. L., & Rowlen, K. L. (1999). Surface roughness by contact versus tapping mode atomic force microscopy. Langmuir, 15(4), 1429-1434.

CHAPTER V

EVALUATION OF HYBRID RESIN IN RAPID CHANGE ENVIRONMENT

5.1 Introduction

During wood composite application process, the resin used for bonding wood composites continuously undergoes polymerization reaction with itself and chemical reaction with wood under various environmental conditions (Wang et al. 1995). The curing and bonding behavior of resins as well as the consequent final performance of these resin bonded wood composites can be significantly affected by the surrounding environment in which temperature and relative humidity (RH) play important roles (Wang et al. 1995). Thus it is necessary to evaluate the performance of hybrid resin after its application in rapid change environment.

Many fundamental studies have been conducted to characterize the reaction behaviors of PF/MDI co-polymer system (Riedinger 2008; Haupt 2013; Zheng 2012). Attempts of using PF/MDI resins as binders have also been reported in forest products manufacturing (Zheng 2012). This co-polymer or hybrid system has been first applied in particleboard manufacturing and then in other applications with a proven result of good mechanical properties of applied products (Deppe 1977; Deppe and Ernst 1971; Hse 1978). PF/MDI system was also applied in plywood for exterior environment application with various viscosity and pot life (Pizzi et al 1995; Batubenga et al 1995). Knowing the fact of isocyanate group reacting with not only hydroxyl group from PF resin but also

moisture from the wood substrate, researchers explored the application of this co-polymer system in difficult-to-bond wood species with high moisture content and achieved strong strength of the final industrial production (Pizzi et al. 1993). Still, there are few studies on the strength change under different temperature, humidity and their combination environment in a relative long time range.

In this study, southern pine wood joints were bonded and were subject to an environment of controlled humidity and temperature for a range of time according to Iwata's research (Iwata and Inagaki 2006). The bonded specimens with hybrid resin (including frozen dried and frozen dried PF resins dispersed with acetone) as well as commercial resins (PRF and PU resins) were tested at room temperature in shear by compression loading according to ASTM 905 (ASTM D905 2013). The purposes are to:

1. Obtain the mean shear strength information of samples glued with different resins under different humidity and temperature conditions;
2. Compare the shear strength change of resins under different humidity and temperature conditions;
3. Evaluate the strength reduction of different resins under different humidity and temperature conditions.

5.2 Materials and Methods

5.2.1 Materials

Phenol, a 99% aqueous solution (USP), is obtained from Fisher Scientific Co., Ltd (Hampton, NH). Paraformaldehyde, a 96% extra pure powder is purchased from Fisher Scientific Co., Ltd (Hampton, NH). Isocyanate, a polymeric MDI with 33% -NCO functional group, is obtained from Huntsman Corporation (The Woodlands, TX). It is a

dark yellow liquid with a viscosity of 226 mPa·s at 25°C. Sodium hydroxide, 97% pure pellets, is purchased from Fisher Scientific Co., Ltd. Acetone, >= 99.5% liquid, is purchased from Fisher Scientific Co., Ltd.

Southern pine was purchased from East Mississippi Lumber Company (Starkville, MS). Polyurethane (PU) resin, product name LOCTITE PL premium polyurethane adhesive, was purchased from Lowes store (Starkville, MS). Phenol resorcinol formaldehyde (PRF) resin, product name Cascophen (TM) LT-5210Q, was supplied by Hexion Co., Ltd (Columbus, OH).

5.2.2 Methods

Dimensions of 1422mm* 38mm*5mm southern pine lumbers will be glued and pressed using black brothers laminating press (Black bros. Shreveport, LA) under room temperature and 1.90 MPa (Freas and Selbo 1954) for 16 hour with different resins.

To ensure the load can be evenly distributed on the laminated panels, a metal plate with the length of 182.88 cm and width of 4 in were placed on the top of wood sample. Five loading plates with a diameter of 6 in were evenly distributed in an equal length of the laminated sample. The details of the setup were shown in Figure 5.1. The actual pressure (as mentioned above 1.90MPa) can be calculated by the formula described in the technical bulletin No.106 from U.S. Department of Agriculture (Freas and Selbo 1954). In this experiment, FL= 100 feet pounds which can be read from the wrech (71.12 cm long).

$$FL = WR\frac{\pi(fD+K)}{\pi(D-fk)} \quad (5.1)$$

Where: F= force applied to lever (pounds); L= length of lever arm (cm); W=total load (pounds); R= radius of the screw (8.46 mm); D= diameter of the screw (49.3 mm); K= pitch of the thread (2.46 mm); f= coefficient of friction (0.2).

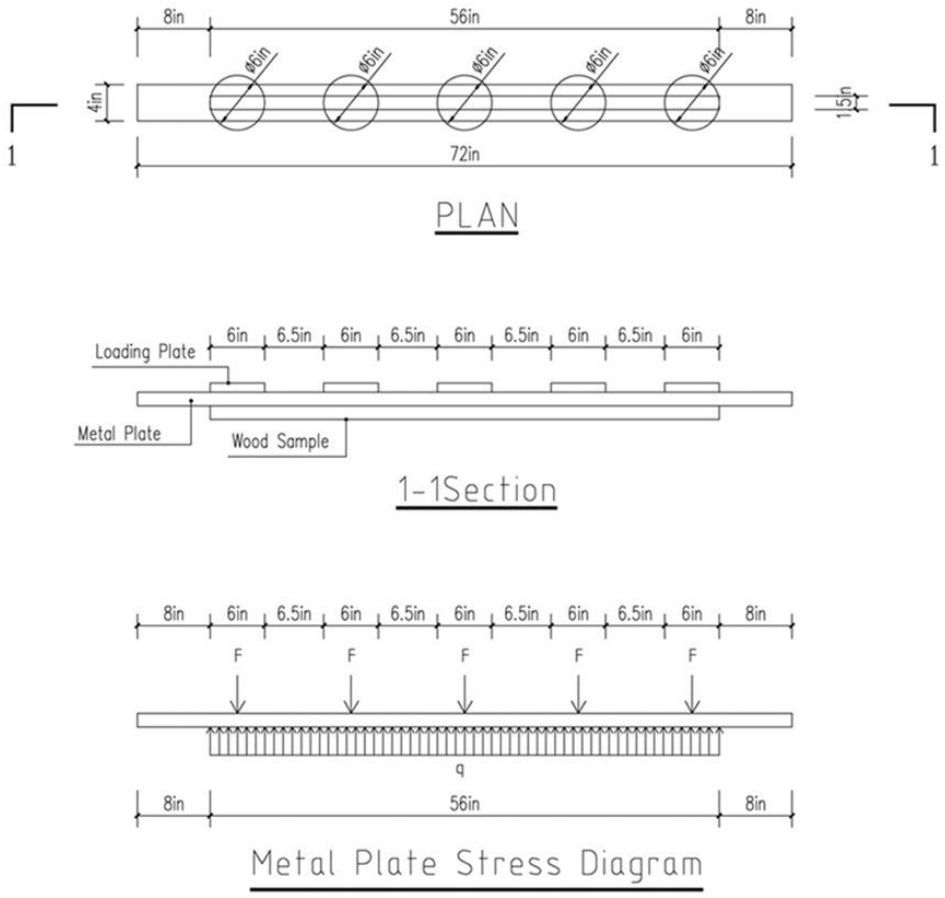

Figure 5.1 Sample manufacturing setup

Then they will be conditioned to 12% moisture content (MC) for 24 hours before compression test. PF and MDI resins with optimized parameters which have been described in former chapters were mixed using laboratory blender (Stir-Pak General Laboratory Mixer, Cole-Parmer, Vernon Hills, IL) with 500 rpm.

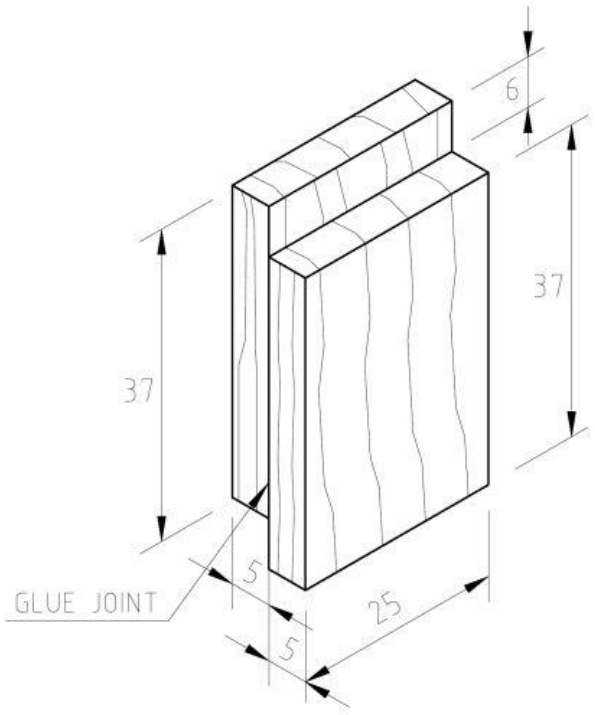

Figure 5.2 Specimen preparation

Table 5.1 Types of adhesives used for preparing specimens

Sample designation	Type of adhesive
A	Frozen dried PF in acetone / MDI
B	PF/MDI
C	Pure PF
D	PRF
E	PU
F (Control)	Solid wood

Table 5.2 Shear strength testing sample preparation conditions

Resins	Standard	Humidity	Temperature	Humidity-temperature
A	RH: 60 ± 5% at 22 ± 2◦C	+35◦C and RH of 95% for 2 days, and then at +35◦C and RH of 20% for 5 days. Two cycles.	−20◦C for 16 h, and then at 50◦C for 8 h. Ten cycles.	50 °C, 95% RH for 12 hours, then -20°C, 20% RH for 12 hours. Two cycles.
B				
C				
D				
E				
F				

The temperature and humidity condition treatments were conducted in a controlled temperature and humidity environmental chamber (Lunaire, TPS Inc., White Deer, PA, USA).

Three batches of experiment with six replicates for each resin and condition combinations were conducted to prepare the test specimens for comparisons. In all of the experiments, solid wood samples were also prepared under same conditions as the control.

Means, coefficients of variation (COV) and fixed strength reduction of the tested data obtained were calculated with SAS® 9.4 software (Cary, NC). The results will be evaluated using a 95% confidence interval, which reflects a significance level of 0.05 ($P<0.05$).

5.3 Results and Discussion

5.3.1 Overall strength (MPa) comparison

From Table 5.3, it shows that there are statistically significant differences between different resins (F: 149.57, P:<0.0001) and different conditions (F: 295.67, P:<0.0001). But there is no significant difference between three batches (F: 0.52, P: 0.5932).

Table 5.3 ANOVA for the comparison among resins, conditions and batches

Source	d.f.	Sum of squares	Mean squares	F	P
Model	10	3385.309473	338.530947	163.59	<.0001
Resin	5	1547.586391	309.517278	149.57	<.0001
Condition	3	1835.559312	611.853104	295.67	<.0001
Batch	2	2.163770	1.081885	0.52	0.5932
Error	421	871.207534	2.069377		
Total	431	4256.517007			

d.f., degrees of freedom.

Table 5.4 summarizes mean values and coefficients of variation (COV) of the shear strength of the tested specimens. It shows very clearly that the strength of each resin decreased under humidity, temperature and their combined conditions as compared to standard conditions. These conditions have had limited effect on the control samples. None of the specimens were delaminated after condition treatment. The COVs are mostly under 30% which was consistent with 14% to 21% for phenol-resorcinol formaldehyde adhesive bonded specimens as required in standard of ASTM D905. Details of how the

condition affected the strength of the resins were talked about in the rest part of this chapter.

Table 5.4 Overall mean strength of different resins under different conditions

Resins & Conditions	Standard	Humidity	Temperature	Humidity-temperature
A	7.31(16.75)	6.28 (12.72)	4.57 (22.56)	2.53 (32.86)
B	8.22 (20.08)	5.52 (18.72)	4.59 (16.90)	2.39 (21.71)
C	7.38 (14.07)	5.21 (17.42)	4.32 (15.11)	2.44 (18.65)
D	9.97 (24.73)	5.68 (21.51)	4.57 (21.71)	2.75 (28.76)
E	10.32 (29.18)	7.39 (13.72)	5.33 (31.61)	3.02 (21.72)
F	12.81 (19.20)	9.99 (9.51)	9.94 (13.52)	8.69 (12.05)

Note: Value in parentheses is coefficient of variation. A: Frozen dried PF in acetone / MDI; B: PF/MDI; C: Pure PF; D: PRF; E: PU; F: Solid wood.

From Table 5.4 and Figure 5.3, it shows that the mean strengths of the resins shared similar trend of change. Under standard condition, all of the resins including the solid control showed the highest strength with a range of 7.31 to 12.81 MPa while they all have had the lowest strength under the combination treatment condition of humidity and temperature with a range of 2.53 to 8.69 MPa.

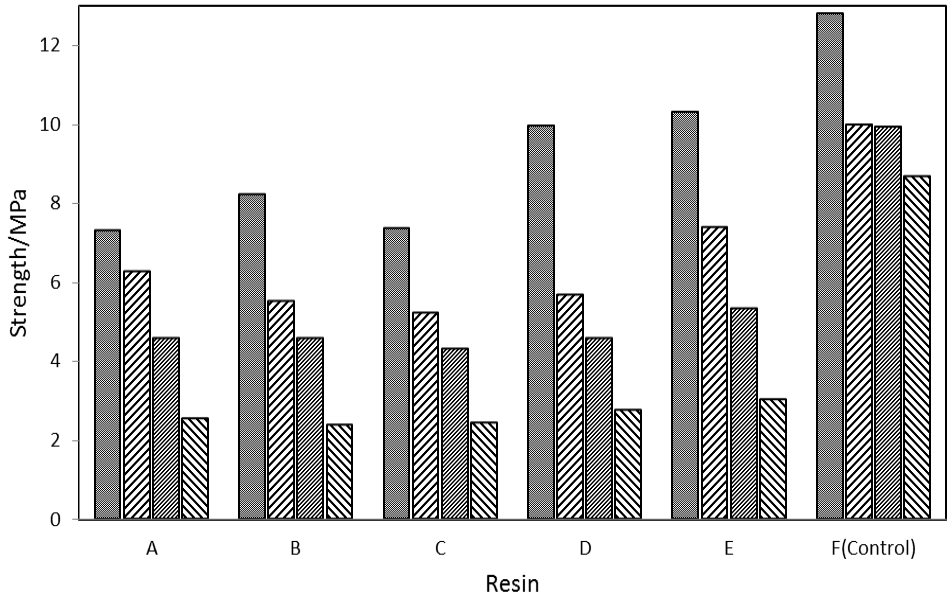

Figure 5.3 Mean strength comparison of different resins under different conditions

Note: Charts with different filling patterns from left to right: standard condition, humidity condition, temperature condition, humidity-temperature condition. A: Frozen dried PF in acetone / MDI; B: PF/MDI; C: Pure PF; D: PRF; E: PU; F: Solid wood.

The mean strengths of the resins under humidity condition were slightly higher than those under temperature condition, which indicates under this accelerated aging experiment design, temperature has higher impact on the change of resins' strength. However, the priority of this study is determining the difference of strength of different resins under different conditions. Whether or not the temperature has higher influence on the reduction of mean strength than humidity is not the interest of the research. There is no big difference in mean strength of solid wood control between humidity and temperature conditions. The reason for the decreasing of shear strength among laminated samples might be due to the variations in the temperature and relative humidity can cause the dimensional changes in the bond line (Wang et al. 1995). Dimensional changes could also decrease the strength of the wood by inducing damage (Price 1976; Geimer 1985).

5.3.2 Mean strength comparison of different resins under same condition

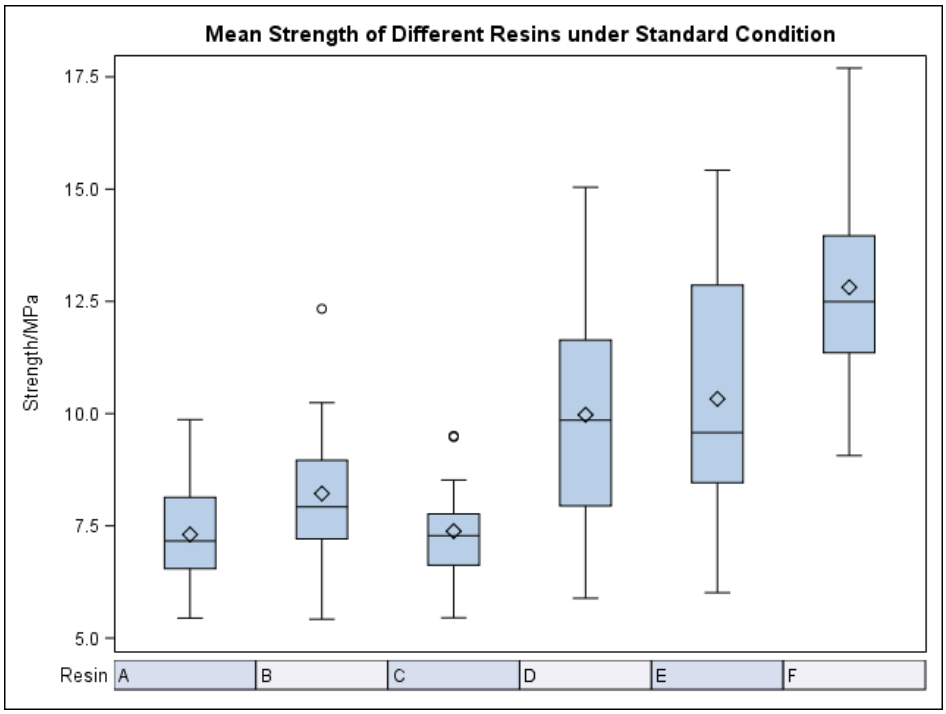

Figure 5.4 Mean strength of different resins under standard condition

Note: A: Frozen dried PF in acetone / MDI; B: PF/MDI; C: Pure PF; D: PRF; E: PU; F: Solid wood.

Under standard condition, solid wood had the highest shear strength with a mean of 12.81 MPa followed by PU resin with a mean shear strength of 10.32MPa which was slightly higher than that of PRF resin with a mean of 9.97 MPa. The mean strengths of frozen dried PF in acetone / MDI and pure PF resins were 7.31 and 7.38 MPa, respectively which were lower than that of PF/MDI resin with a mean strength of 8.22 MPa. However, there was no significant difference between hybrid systems and PF resins. Commercial resins had better performance under standard condition than laboratory made resins.

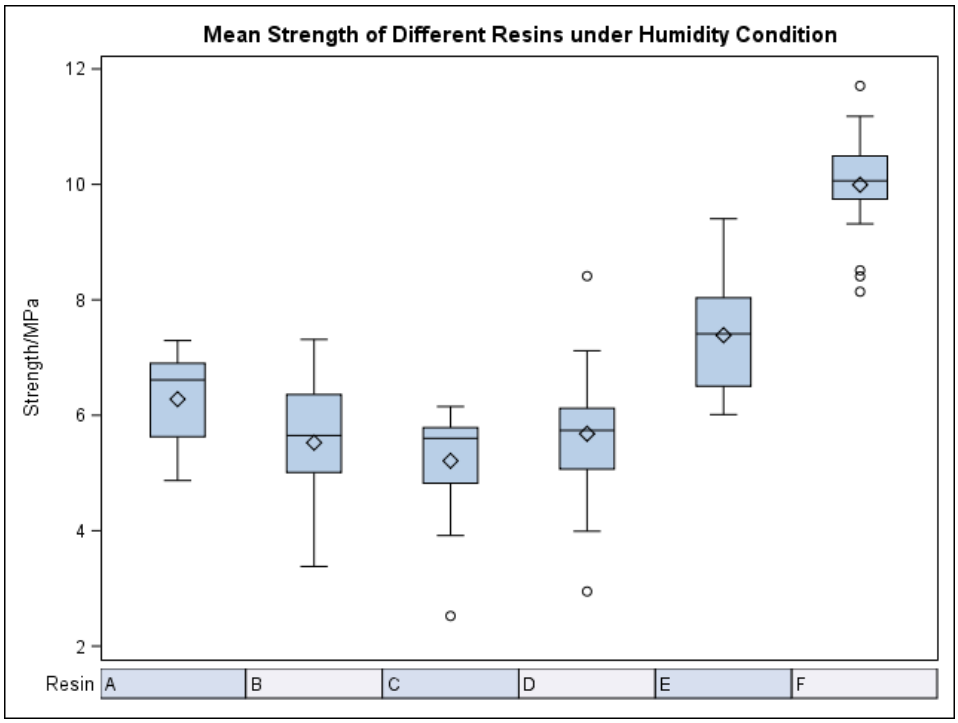

Figure 5.5 Mean strength of different resins under humidity condition.

Note: A: Frozen dried PF in acetone / MDI; B: PF/MDI; C: Pure PF; D: PRF; E: PU; F: Solid wood.

From Figure 5.5, the mean strength of different resins under humidity condition has a very obvious change that the strength of frozen dried PF with acetone/MDI was not the lowest anymore. The strength of it was 6.28 MPa which was higher than that of PF/MDI, pure PF and PRF resins with the mean strength of 5.52, 5.21 and 5.68, respectively. The strength of PU resin and solid wood control were significantly higher than other four resins.

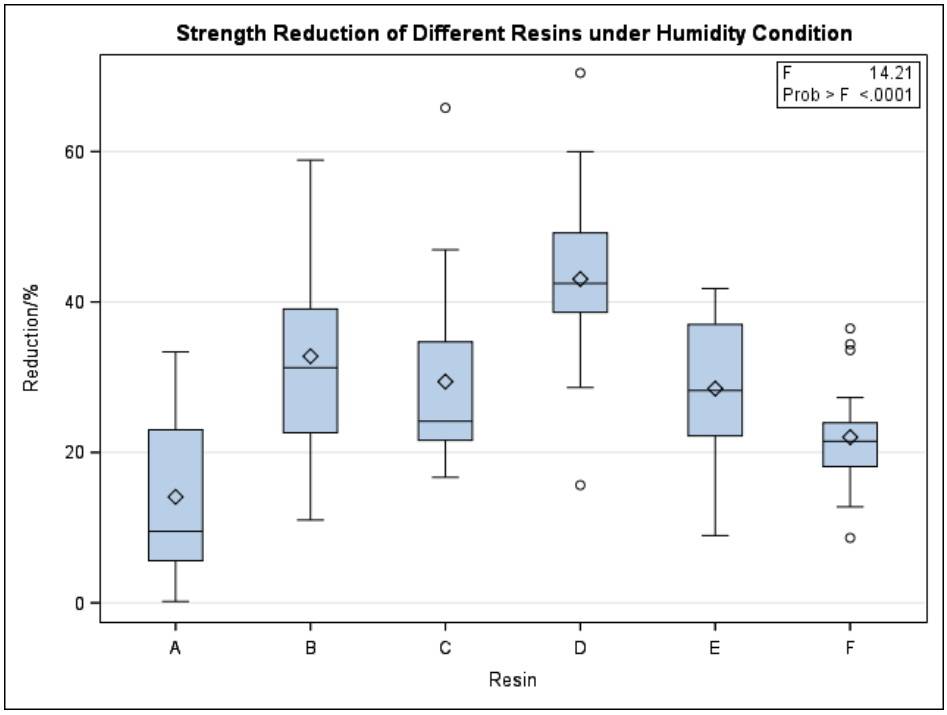

Figure 5.6 Mean strength reduction percentage compared to standard condition of resins under humidity condition

Note: A: Frozen dried PF in acetone / MDI; B: PF/MDI; C: Pure PF; D: PRF; E: PU; F: Solid wood.

The reduction of shear strength of different resins under humidity condition compared to standard condition shows much clearer in Figure 5.6. In spite of solid wood which has 22.01% reduction of mean strength with outliers in both sides, frozen dried PF with acetone/MDI has the lowest reduction of 14.09%. The strength reductions of PF/MDI, pure PF, PRF and PU resins are 32.85%, 29.40%, 43.03% and 28.39% respectively.

Table 5.5 Overall mean strength reduction (%) of different resins under humidity condition

Resins	Mean
A (Frozen dried PF in acetone / MDI)	14.09 D
B (PF/MDI)	32.78 B
C (Pure PF)	29.42 B
D (PRF)	43.06 A
E (PU)	28.48 BC
F (Solid wood)	22.02 C

From Table 5.5, it shows that compared to standard condition, under humidity condition, the shear strength reduction of frozen dried PF with acetone/MDI is significantly smaller than that of any other resins including the solid wood control. The shear strength reductions of PRF resin is significant higher than any other resins including the solid wood control. The shear strength reductions of PF/MDI, pure PF and PU resin have no significant difference.

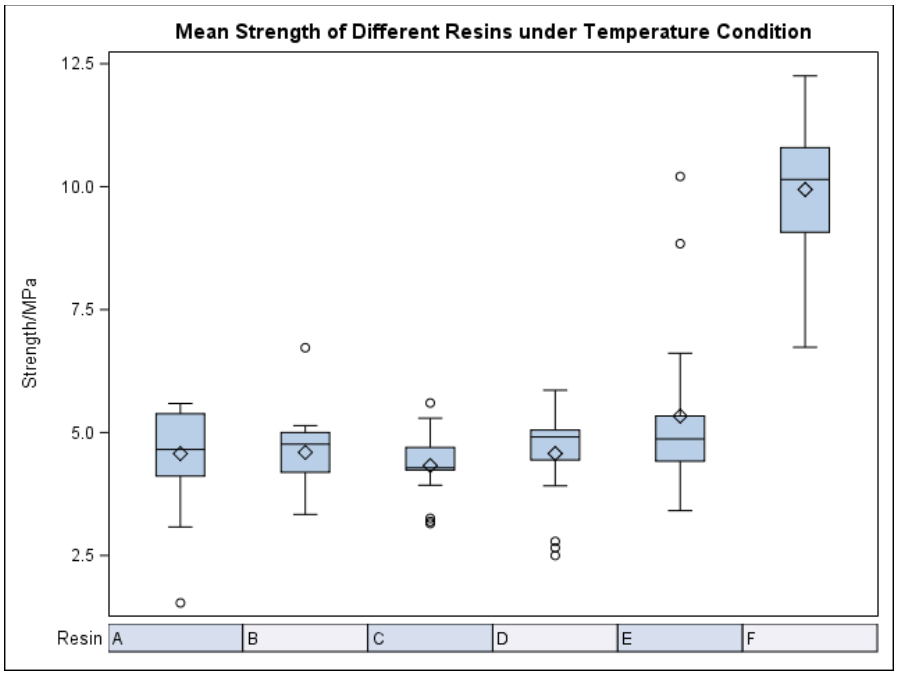

Figure 5.7 Mean strength of different resins under temperature condition

Note: A: Frozen dried PF in acetone / MDI; B: PF/MDI; C: Pure PF; D: PRF; E: PU; F: Solid wood.

As shown in Figure 5.7, the mean shear strength of different resins under temperature condition acted differently under humidity condition. Under temperature condition, the shear strength of solid wood still was around 9.94 MPa which had very minor change compared to that under humidity conditions. The means of frozen dried PF with acetone/MDI, PF/MDI, pure PF, PRF and PU resins were 4.57, 4.59, 4.32, 4.57 and 5.33 MPa, respectively. Among these five resins, no one had shown significant higher strength than any others.

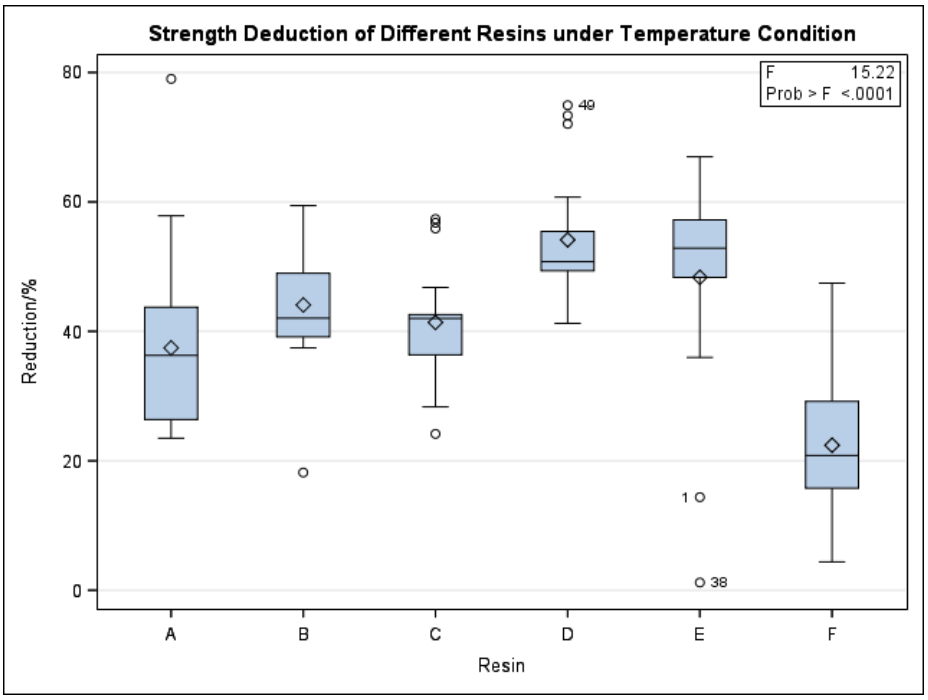

Figure 5.8 Mean strength reduction percentage compared to standard condition of resins under temperature condition

Note: A: Frozen dried PF in acetone / MDI; B: PF/MDI; C: Pure PF; D: PRF; E: PU; F: Solid wood.

From Figure 5.8, compared to the strength of resins under standard condition, the strength reduction of resins under temperature condition had similar trend with those under humidity condition in spite of the solid wood control having the lowest reduction. Other than that, the reduction of frozen dried PF with acetone/MDI was still lower than other four resins including two commercial ones. However, according to Table 5.6, the reduction of solid wood was significantly smaller than that of five resins and there was no significant difference in strength reduction of 5 different resins.

Table 5.6 Overall mean strength reduction (%) of different resins under temperature condition

Resins	Mean
A (Frozen dried PF in acetone / MDI)	37.44 C
B (PF/MDI)	44.08 BC
C (Pure PF)	41.38 BC
D (PRF)	54.14 A
E (PU)	48.35 AB
F (Solid wood)	22.41 D

As shown in Figure 5.9, under humidity- temperature condition, in spite of solid wood, the mean strengths of frozen dried PF with acetone/MDI, PF/MDI, pure PF, PRF and PU resins were 2.53, 2.39, 2.44, 2.75 and 3.02 MPa, respectively which had no significant difference from one to another and were relatively lower than those under other conditions. From Figure 5.10, the strength reduction of frozen dried PF with acetone/MDI, PF/MDI, pure PF, PRF and PU resins were 65.34%, 70.86%, 66.95%, 72.38% and 70.76% and there was no significant difference of strength reduction among different resins (Table 5.7) in which frozen dried PF with acetone/MDI still had the lowest reduction except the reduction of solid wood.

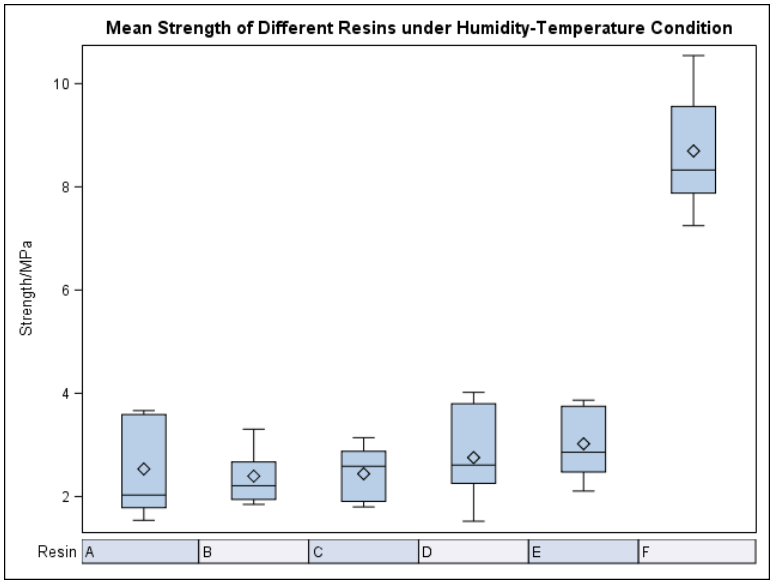

Figure 5.9 Mean strength of different resins under humidity-temperature condition

Note: A: Frozen dried PF in acetone / MDI; B: PF/MDI; C: Pure PF; D: PRF; E: PU; F: Solid wood.

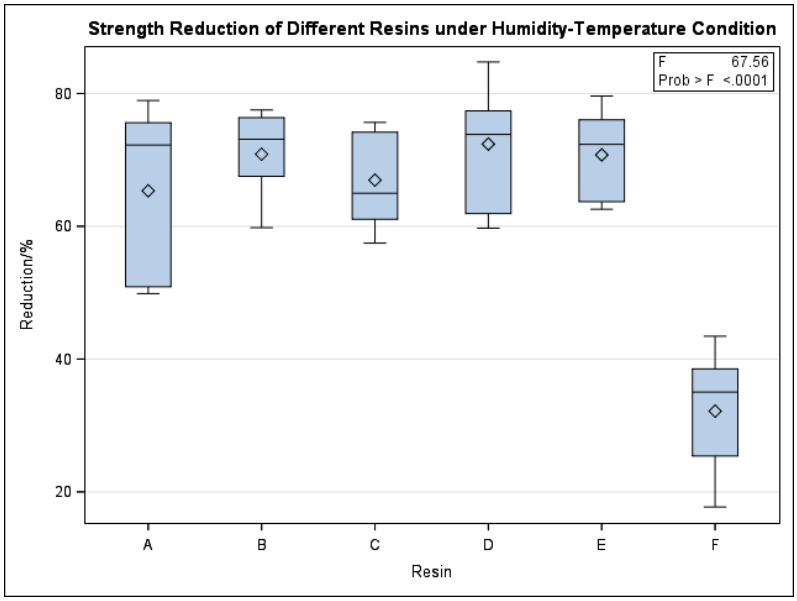

Figure 5.10 Mean strength reduction percentage compared to standard condition of resins under humidity-temperature condition

Note: A: Frozen dried PF in acetone / MDI; B: PF/MDI; C: Pure PF; D: PRF; E: PU; F: Solid wood.

Table 5.7 Overall mean strength reduction (%) of different resins under humidity-temperature condition

Resins	Mean
A (Frozen dried PF in acetone / MDI)	65.34 C
B (PF/MDI)	70.86 AB
C (Pure PF)	66.95 BC
D (PRF)	72.38 A
E (PU)	70.76 AB
F (Solid wood)	32.16 D

The fact that isocyanate groups is very reactive particularly with hydroxyl groups of PF resin even in the presence of excess quantites of water had been reported 1992 (Pizzi and Walton 1992). In other words, the polymeric MDI (MDI) has to react with PF first even moisture exisiting in PF. However, the MDI will still react with hydroxyl groups from water after the priority reaction. This result has also been confirmed in industrial reuslts of using mixed MDI and PF resins for exterior application on plywood (Pizzi et al. 1993). This is also consitent with the fact that in variable humidity environment, frozen dried PF resin with acetone/MDI has the lowest strength reduction. It can be explained that the forzen dried PF can make get rid of the influence of reaction between PDI and water. In order to ekiminate the poor mobility due to lack of water, acetone plays the role of promoting frozen dried PF resin and MDI mixture to penetrate into wood as described in Chapter 3. Free isocyanate groups released after manufacuting

process finished can then react with hydroxyl groups from wood itself and moisture from the environment (humidity condition) to form complex and cross-linked bonds to enhance the bonding in a wood-resin-wood structure.

5.4 Conclusions

Although the shear strength of frozen dried PF with acetone/MDI was not as high as being expected, the strength reduction of it was the lowest in humidity, temperature and humidity-temperature conditions. Especially under just humidity condition, its shear strength reduction was significantly lower than that of any other resins and the solid wood control. This result was consistent with former research which confirmed that this hybrid resin was suitable for exterior environment application. The function of acetone was to improve the mobility of frozen dried PF resin when mixed with MDI and promoted it to penetrate deeper into wood. At the same time, free isocyanate groups reacted with hydroxyl group continuously to create cross-linked bonds between wood substrate and resin and thus to reduce the strength decreasing in different humidity environment. However, it still needs further exploring to improve the shear strength of this hybrid resin in standard atmosphere.

5.5 References

Wang, X. M., Riedl, B., Christiansen, A. W., & Geimer, R. L. (1995). The effects of temperature and humidity on phenol-formaldehyde resin bonding. Wood science and Technology, 29(4), 253-266.

Zheng, J. (2002). Studies of PF resole/isocyanate hybrid adhesives (Doctoral dissertation, Virginia Polytechnic Institute and State University).

Deppe, H. J. (1977). Technical progress in using isocyanate as an adhesive in particleboard manufacture. In Proceedings Washington State University Symposium on Particleboard.

Deppe, H. J., & Ernst, K. (1971). Isocyanate als Spanplattenbindemittel. European Journal of Wood and Wood Products, 29(2), 45-50.

Hse, C. Y. (1978). Development of a resin system for gluing southern hardwood flakeboards. USDA Forest Service General Technical Report WO.

Pizzi, A., Von Leyser, E., & Westermeyer, C. (1995). U.S. Patent No. 5,407,980. Washington, DC: U.S. Patent and Trademark Office.

Batubenga, D. B., Pizzi, A., Stephanou, A., Krause, R., & Cheesman, P. (1995). Isocyanate/phenolics wood adhesives by catalytic acceleration of copolymerization. Holzforschung-International Journal of the Biology, Chemistry, Physics and Technology of Wood, 49(1), 84-86.

Pizzi, A., Valenzuela, J., & Westermeyer, C. (1993). Non-emulsifiable, water-based, mixed diisocyanate adhesive systems for exterior plywood. Part II. Theory application and industrial results. Holzforschung-International Journal of the Biology, Chemistry, Physics and Technology of Wood, 47(1), 68-71.

Freas, A. D., & Selbo, M. L. (1954). Fabrication and design of glued laminated wood structural members (No. 156538). United States Department of Agriculture, Economic Research Service.

ASTM D905-08(2013) Standard Test Method for Strength Properties of Adhesive Bonds in Shear by Compression Loading, ASTM International, West Conshohocken, PA, 2013.

Freas, A. D., & Selbo, M. L. (1954). Fabrication and design of glued laminated wood structural members (No. 156538). United States Department of Agriculture, Economic Research Service.

Iwata, R., & Inagaki, N. (2006). Durable adhesives for large laminated timber. Journal of adhesion science and technology, 20(7), 633-646.

Price, E. W. (1976). Determining tensile properties of sweetgum veneer flakes.

Geimer, R. L., Mahoney, R. J., Loehnertz, S. P., & Meyer, R. W. (1985). Influence of processing-induced damage on strength of flakes and flakeboards. Forest Products Labor.

Pizzi, A., & Walton, T. (1992). Non-emulsifiable, water-based, mixed diisocyanate adhesive systems for exterior plywood-part I. Novel reaction mechanisms and their chemical evidence.

Pizzi, A., Valenzuela, J., & Westermeyer, C. (1993). Non-emulsifiable, water-based, mixed diisocyanate adhesive systems for exterior plywood. Part II. Theory application and industrial results. Holzforschung-International Journal of the Biology, Chemistry, Physics and Technology of Wood, 47(1), 68-71.

CHAPTER VI

SUMMARY AND FUTURE RESEARCH

At the beginning of this paper, three main factors: formaldehyde to phenol (F/P), sodium hydroxide to phenol (S/P) and isocyanate group to hydroxyl group (-NCO/-OH) molar ratios were studied in a series of experiment to determine the best formula to prepare high performance hybrid resins. It confirmed that all these three factors affected the strength of PF resin and hybrid resin significantly. Considering both dry and wet shear strength, the formula NO.8 ((F/P=2.0, S/P=0.4)) with –NCO to –OH ratio of 1.25 was chosen for further study and characterization.

Low, medium and high molecular weights of PF resins based on the best formula were synthesized and then mixed together with MDI resin for bonding southern pine. It shows that the highest molecular weight of PF resin made the reaction of isocyanate and phenolic resin more completely. Co-polymer with highest molecular weight of PF resin showed the best thermal property too. An increasing in molecular weight of PF resin also indicated more crosslinking in the co-polymer system.

With the purpose of eliminating the influence of water in the PF resin, frozen dried method was applied to remove the water. To improve the mobility of mixture of frozen dried PF resins and MDI, acetone was used to disperse the hybrid co-polymer. The effect of acetone on the curing behavior of hybrid resin was studied by differential

scanning calorimetry (DSC), confocal laser scanning microscope (CLSM) and other techniques.

From DSC analysis results, the best mass ratio for using acetone to promote the curing process of optimized hybrid resin was 0.6:1 with the largest heat release and the highest peak temperature.

By analysis and calculation of kinetics parameters of the curing reaction, it has been noted that the energy of activation is 25.28 KJ/mol and the pre-exponential factor is A=5.95*104/ Km·min. The reaction order was 0.77. Three temperatures that were important for hybrid resin curing were 289.06 K (15.85°C), 381.26 K (108.11°C) and 419.10 K (145.95°C), respectively. It illustrates the best curing technique for the optimized hybrid resin with acetone was from the best beginning temperature at 15.85°C and the resin was gradually heated to 108.11°C as the major curing period before the temperature was increased to 145.95°C and kept for a period of time to make sure the resin was fully cured.

When acetone was introduced into frozen dried hybrid resin system, it promoted the curing reaction between phenolic and isocyanate resin. The gel time of hybrid resin with acetone decreased sharply compared to that of pure phenolic resin and original hybrid resin. The glue line was much wider than the one without acetone with an average of 677μm penetration depth. From AFM analysis, hybrid resin improved the toughness of phenolic resin. And dissolving frozen dried hybrid resin into acetone helped it to be better applied on wood surface for ensuring less variation of the strength. The image surface area difference of frozen dried hybrid resin with acetone which is 50.4 % is significantly lower than that of frozen-dried hybrid resin which is 97.3%.

At last, lap shear samples were prepared using room temperature curing commercial polyurethane (PU), phenol-resorcinol-formaldehyde resin (PRF) and laboratory made hybrid resins based on PF and MDI to compare the shear strength difference of resins under different application conditions. The strength reduction of frozen dried PF with acetone/MDI was the lowest in humidity, temperature and humidity-temperature conditions. Especially under just humidity condition, its shear strength reduction was significantly lower than that of any other resins including the solid wood control. .

However there are still further studies should be done to:

1. Further optimize the design of the hybrid resin in terms of curing time, curing temperature and composite strength;
2. Explore the fundamentals of manufacturing and harvesting nanotubes based on hybrid resin concept;
3. Model hybrid resin curing process based on the synthesis parameters and the curing mechanism, using Kissinger equation;
4. Develop a nondestructive evaluation model to determine adhesive strength using AFM technique.

APPENDIX A

HEAT FLOW (mW) OF HYBRID RESIN/ACETONE WITH DIFFERENT MASS RATIOS UNDER DIFFERENT TEMPERATURE

Temperature(°C)	Heat Flow (mW)				
	Ratio 0.2:1	Ratio 0.4 :1	Ratio 0.6:1	Ratio 0.8:1	Ratio 1:1
25	23.3	22.8	23.8	24.1	24.4
50	23	22.3	23.7	23.6	24.1
75	21.9	22.2	22.8	23.1	23.7
100	20.7	21	22.3	22.2	23.1
125	20	20.3	22	21	21.6
150	20.9	21.2	22.3	22.3	23
175	21.7	22	22.6	23	23.3
200	22	22.3	23	22.8	23.7
225	21.4	22.1	23.15	23	23.9
250	22.2	22.6	23.6	23.9	24.3